AFRL-RY-HS-TR-2010-0013

Similarity of the Outer Region of the Turbulent Boundary

David W. Weyburne

AFRL/RYHC
80 Scott Drive
Hanscom AFB, MA 01731-2909

9 February 2009

In-House Technical Report

APPROVED FOR PUBLIC RELEASE; DISTRIBUTION UNLIMITED

AIR FORCE RESEARCH LABORATORY
Sensors Directorate
Electromagnetics Technology Division
Hanscom AFB MA 01731-2909

NOTICE AND SIGNATURE PAGE

Using Government drawings, specifications, or other data included in this document for any purpose other than Government procurement does not in any way obligate the U.S. Government. The fact that the Government formulated or supplied the drawings, specifications, or other data does not license the holder or any other person or corporation; or convey any rights or permission to manufacture, use, or sell any patented invention that may relate to them.

This report was cleared for public release by the Electronic Systems Center Public Affairs Office for the Air Force Research Laboratory Electromagnetic Technology Division and is available to the general public, including foreign nationals. Copies may be obtained from the Defense Technical Information Center (DTIC) (http://www.dtic.mil).

AFRL-RY-HS-TR-2010- 0013 HAS BEEN REVIEWED AND IS APPROVED FOR PUBLICATION IN ACCORDANCE WITH ASSIGNED DISTRIBUTION STATEMENT.

David Weyburne

DAVID WEYBURNE
Contract Monitor

David F. Bliss

DAVID F. BLISS, Acting Chief
Optoelectronic Technology Branch

Robert V. McGahan

DR. ROBERT V. McGAHAN
Technical Communications Advisor
Electromagnetics Technology Division

This report is published in the interest of scientific and technical information exchange, and its publication does not constitute the Government's approval or disapproval of its ideas or findings.

REPORT DOCUMENTATION PAGE

Form Approved
OMB No. 0704-0188

1. REPORT DATE *(DD-MM-YYYY)* 09-02-2009	**2. REPORT TYPE** Technical Report	**3. DATES COVERED** *(From - To)* 1 Dec 2006 – 1 Dec 2008

4. TITLE AND SUBTITLE Similarity of the Outer Region of the Turbulent Boundary Layer	**5a. CONTRACT NUMBER** In-House
	5b. GRANT NUMBER
	5c. PROGRAM ELEMENT NUMBER 624916
6. AUTHOR(S) David W. Weyburne	**5d. PROJECT NUMBER** 4916
	5e. TASK NUMBER HC
	5f. WORK UNIT NUMBER 01
7. PERFORMING ORGANIZATION NAME(S) AND ADDRESS(ES) AFRL/RYHC 80 Scott Drive Hanscom AFB, MA 01731-2909	**8. PERFORMING ORGANIZATION REPORT NUMBER**
9. SPONSORING / MONITORING AGENCY NAME(S) AND ADDRESS(ES) Electromagnetics Technology Division Sensors Directoratorate Source Code: 437890 Air Force Research Laboratory 80 Scott Drive Hanscom AFB, MA 01731-2909	**10. SPONSOR/MONITOR'S ACRONYM(S)** AFRL/RYHC
	11. SPONSOR/MONITOR'S REPORT NUMBER(S) AFRL-RY-HS-TR-2010-0013

12. DISTRIBUTION / AVAILABILITY STATEMENT

DISTRIBUTION A: APPROVED FOR PUBLIC RELEASE: DISTRIBUTION UNLIMITED

13. SUPPLEMENTARY NOTES

The U.S. Government is joint author of this work and has the right to use, modify, reproduce, release, perform, display, or disclose the work. Cleared for Public Release by 66ABW-2010-0163, dated 17 February 2010.

14. ABSTRACT

New similarity criteria are obtained for the velocity profile and the Reynolds stress terms by a stream function approach using the transformed x-momentum balance equation and the transformed Reynolds stress transport equation. The similarity criteria are similar to earlier results but are developed without a priori assumptions as to the velocity or Reynolds stress term scaling variables. Using the criteria, eleven experimental datasets for turbulent flow on a wedge are found. Scaling results indicate that the displacement thickness, the momentum thickness, the ninety-nine percent thickness, and the Rota-Clauser thickness all work as the outer region similarity thickness scale. The experimental and theoretical evidence indicates the free stream velocity works well as the velocity scaling parameter. For the Reynolds stress scaling, experimental evidence is for the most part ambiguous. However, recent DNS results clearly indicate that the friction velocity squared is the proper scaling but this result is seemingly at odds with the new theoretical criteria. Resolution of the conflict is made by the observation that similarity-like behavior of the velocity profile and the Reynolds stress terms are only obtained for the flow datasets where the ratio of the free stream velocity to the friction velocity is almost constant.

15. SUBJECT TERMS

Fluid Boundary Layers, Turbulent Flow, Velocity Profiles, Reynolds Stress, Similarity

16. SECURITY CLASSIFICATION OF:			**17. LIMITATION OF ABSTRACT**	**18. NUMBER OF PAGES**	**19a. NAME OF RESPONSIBLE PERSON** David W. Weyburne
a. REPORT Unclassified	**b. ABSTRACT** Unclassified	**c. THIS PAGE** Unclassified	SAR	91	**19b. TELEPHONE NUMBER** n/a

Standard Form 298 (Rev. 8-98)
Prescribed by ANSI Std. Z39.18

Contents

List of Figures

List of Tables

Acknowledgement

The author would like to acknowledge the support of the Electromagnetics Technology Division of the Sensors Directorate of the Air Force Research Laboratory. In addition, the author would like to thank a number of authors who contributed their experimental datasets including David DeGraaff and John Eaton, George Khujadze and Martin Oberlack, Jens Österlund, Per Egil Skåre and Per-Åge Krogstad, K. Elsberry, J. Loeffler, M. D. Zhou, and I. Wygnanski, A. Samuel and P. Joubert, and Randall Smith and Alexander Smits.

Summary New similarity criteria are obtained for the velocity profile and the Reynolds stress terms by a stream function approach using the transformed x-momentum balance equation and the transformed Reynolds stress transport equation. The similarity criteria are similar to earlier results but are developed without *a priori* assumptions as to the velocity or Reynolds stress term scaling variables. Using the criteria, eleven experimental turbulent boundary layer datasets displaying similarity-like behavior in the outer region of the boundary layer are found. Scaling results indicate that the displacement thickness, the momentum thickness, the ninety-nine percent thickness, and the Rotta-Clauser thickness all work as the outer region similarity thickness scale. The experimental and theoretical evidence indicates the free stream velocity works well as the velocity scaling parameter. For the Reynolds stress scaling, experimental evidence is for the most part ambiguous. However, recent DNS results clearly indicate that the friction velocity squared is the proper scaling but this result is seemingly at odds with the new theoretical criteria. Resolution of the conflict is made by the observation that similarity-like behavior of the velocity profile and the Reynolds stress terms are only obtained for the flow datasets where the ratio of the free stream velocity to the friction velocity is almost constant.

1. Introduction

The question of similarity of the turbulent boundary layer has been around almost as long as the studies of modern fluid flow itself. Similarity solutions of the flow governing equations are well known for laminar flow. Turbulent flow similarity is more problematic. Since the equations for very few turbulent flows admit to exact similarity solutions, the community has long sought to establish their possible existence by looking for "scaling laws", which basically consist of trying to guess the scaling variables and then plotting experimental velocity profiles using the guessed scaling. Rather than searching blindly, it is desirable to have some theoretical guidance that would help design and/or search for the conditions leading to the experimental discovery of the similarity scaling laws for the turbulent boundary layer. This guidance would be of the form of determining what theory can tell us about the functional behavior of the length, velocity, and Reynolds stress scaling variables along the length of the wedge.

The search for similarity scaling behavior for the turbulent boundary layer began with the experimental and theoretical work of Clauser [1]. Using the friction velocity u_τ as the velocity scaling variable for the turbulent boundary layer, Clauser predicted that equilibrium (similar) boundary layers are only obtained for the nonzero pressure gradient case when

$$\beta_\tau = -\frac{\delta_1}{\rho u_\tau^2}\frac{dp_e}{dx} \qquad (1)$$

is a constant. In this equation δ_1 is the displacement thickness, ρ is the density, p_e is the pressure at the boundary layer edge, and x-direction is along the flow direction. Based on Eq. 1 criteria, Clauser was able to generate similarity-like behavior for certain turbulent flows but found, in general, that the experimental equilibrium similarity condition is relatively rare and difficult to generate.

Rotta [2] and Townsend [3] subsequently developed some additional theoretical conditions for turbulent boundary layer similarity. Like Clauser, Rotta made specific assumptions about the velocity scaling ($=u_\tau$) and the Reynolds stress scaling ($=u_\tau^2$). More recently, Castillo and George [4], using a momentum balance approach, found that the free stream velocity u_e must be the velocity scaling variable for flows with a pressure gradient. Furthermore, they found that similarity exists only when the parameter

$$\Lambda = -\frac{\delta \, du_e/dx}{u_e \, d\delta/dx} \qquad (2)$$

is a constant. In this equation δ is the thickness scaling variable. This provides a very specific test for discovering similarity in a set of experimental profiles, *i.e.* along the length of the plate we must have $\delta \propto u_e^{-1/\Lambda}$ with $\Lambda =$ constant. Taking δ equal to the ninety-nine percent thickness δ_{99}, Castillo and George showed that rather than being rare, most nonzero pressure gradient turbulent boundary layer flows with constant upstream conditions were in equilibrium by this measure. In fact, they showed that only three values of this pressure parameter were needed to characterize all equilibrium turbulent boundary layers. One was for the adverse pressure gradient (APG) flow with $\Lambda = 0.22$, one for the favorable pressure gradient (FPG) flow with $\Lambda = -1.92$, and one for the zero pressure gradient (ZPG) flow with $\Lambda = 0$. In a later publication, Cal, Johansson, and Castillo [5] backed off from this strong stance indicating other values for Λ are possible. Indeed, Maciel, Rossignol, and Lemay [6] presented a modified Castillo and George formulation and, after looking at a range of experimental datasets, concluded that universal similar profiles for the ZPG, APG, and FPG boundary layers do not exist. While they concede the existence of similarity-like behavior in certain sets of experimental profiles, they contend that most turbulent boundary layers found in the real world are almost never in a state of equilibrium.

One possible explanation for this conundrum as to whether similarity-like behavior is rare or common in the turbulent boundary layer is that the Eq. 2 criterion is not complete. It may be there are some additional criteria not yet considered that further limit the allowable behavior of the length and velocity scaling along the plate. This prompted us to take another look at similarity criteria of the turbulent boundary layer flow on a wedge. We are particularly interested in pointing out the scaling criteria that are based only on theoretical considerations rather than some specific assumptions of the flow behavior. Using a stream function approach, the x-momentum balance equation and the Reynolds stress transport equation are transformed and a set of parameters like Eqs. 1 and 2 are developed. These new parameters must be constant for similarity and result in a set of requirements as to the functional behavior of the boundary layer thickness scaling variable, the velocity scaling variable, and the Reynolds stress term scaling variable along the length of the wedge.

There are two major differences between our approach and what has appeared in the past. The first difference is that we include the Reynolds stress transport equation with the normally used x-momentum balance equation. We note that Townsend [3] used the x-momentum balance equation together with the kinetic energy balance equation but Townsend's subsequent conclusions are derivable from the x-momentum balance equation alone. The transport equation for the Reynolds stress we use herein is an exact equation derived from the momentum equation by multiplying by the fluctuating velocity component and the result Reynolds-averaged (see, for example, White [7]). The inclusion of the Reynolds stress transport equation with the normally used x-momentum balance equation allowed us to determine that the length scale must be linearly proportional to the distance along the wedge and that velocity scale must be a power function of the distance along the wedge. These results have already been obtained in the past but in every previous effort it was necessary to make certain assumptions about the x-behavior of the velocity scaling variable or the Reynolds stress terms. Our new derivation avoids making any *a priori* assumptions as to the velocity or Reynolds stress terms scaling variables.

The second major difference between this effort and earlier work is that scaling guidance results are obtained for all pressure gradient variations including the zero-pressure gradient case. This is in contrast to the criteria given by Eqs. 1 and 2, for example, which must be zero for the ZPG case. These two criteria therefore provide no guidance as to the behavior of the similarity thickness parameter δ for the ZPG case.

The new criteria are used to discover eleven APG, FPG, and ZPG experimental datasets having similarity in the outer region of the turbulent boundary layer. Four different length scales and three different velocity scales were examined for the velocity profile scaling including the traditional Rotta-Clauser scaling. The scaling results are different than those obtained in previous studies. The Reynolds stress terms appear to scale with inner layer scaling variables. We point out that an important property of each of the datasets for which we found similarity-like behavior is that the ratio of the free stream velocity to friction velocity is almost constant as required by Rotta [2]. This turns out to be critical in explaining the experimental results in light of the new theoretical guidance.

2. Exact Equations

To develop the theoretical guidance for discovering scaling laws, we start with the *x*-momentum balance equation. For a 2-D incompressible turbulent boundary layer that is steady state on the mean, the Reynolds-averaged stream-direction component (*x*-direction) of the momentum balance along a wedge is given by

$$u\frac{\partial u}{\partial x} + v\frac{\partial u}{\partial y} + \frac{\partial}{\partial x}\left\{\overline{\tilde{u}\tilde{u}}\right\} + \frac{\partial}{\partial y}\left\{\overline{\tilde{u}\tilde{v}}\right\} = -\frac{1}{\rho}\frac{\partial P}{\partial x} + \nu\frac{\partial^2 u}{\partial y^2} \quad , \tag{3}$$

where the bar above a variable is the Reynolds average operator and the tilde operator designates the instantaneous velocity. Next, we introduce the Reynolds stress transport equation given by

$$u\frac{\partial\overline{\tilde{u}\tilde{v}}}{\partial x} + v\frac{\partial\overline{\tilde{u}\tilde{v}}}{\partial y} - 2\overline{\tilde{u}\tilde{v}}\frac{\partial u}{\partial y} - \nu\frac{\partial^2\overline{\tilde{u}\tilde{v}}}{\partial y^2} + \frac{\partial}{\partial y}\overline{\left(\tilde{u}\tilde{v}\tilde{v} + \frac{\tilde{P}\tilde{u}}{\rho}\right)} + 2\nu\overline{\frac{\partial\tilde{u}}{\partial y}\frac{\partial\tilde{v}}{\partial x}} - \overline{\frac{\tilde{P}}{\rho}\left(\frac{\partial\tilde{u}}{\partial y} + \frac{\partial\tilde{v}}{\partial x}\right)} = 0 \ . \tag{4}$$

Solutions to these equations are presently not possible for turbulent flows since the functional form of many of terms are not known. Nevertheless, it is still possible to learn some important information about the boundary layer behavior by proceeding with a similarity scaling analysis.

3. Scaling Variable Transformation

To investigate similarity scaling we start by transforming the momentum equations using candidate similar scaling variables for the length and velocity given by δ and u_s, respectively, which are functions of x but not y. We begin by introducing the independent variables

$$\xi = x \quad , \quad \eta = \frac{y}{\delta} \quad .$$

Furthermore, we define a stream function, $\psi(x,y)$, in terms of a dimensionless function $f(\xi,\eta)$ as

$$\frac{\psi(x,y)}{\delta\, u_s} = f(\xi,\eta) \quad .$$

The stream function satisfies the conditions

$$u = \frac{\partial\psi(x,y)}{\partial y}, \qquad v = -\frac{\partial\psi(x,y)}{\partial x} \quad .$$

This means that

$$u = u_s f' \quad , \qquad v = -\frac{d\{\delta u_s\}}{dx} f + u_s\frac{d\delta}{dx}\eta f' - \delta u_s\frac{\partial f}{\partial\xi} \quad ,$$

where the prime indicates differentiation with respect to η.

The above variable switch can be used to transform the two equations. The x-momentum balance equation, Eq. 3, reduces to

$$u_s \frac{du_s}{dx} f'^2 - u_s \frac{du_s}{dx} ff'' - \frac{u_s^2}{\delta}\frac{d\delta}{dx} ff'' + u_s^2 f' \frac{\partial f'}{\partial \xi} - u_s^2 f'' \frac{\partial f}{\partial \xi} + \tag{5}$$

$$-\frac{uu(x)}{\delta}\frac{d\delta}{dx}\eta g_{11}' + \frac{duu(x)}{dx} g_{11} + \frac{uv(x)}{\delta} g_{12}' \quad = \quad -\frac{1}{\rho}\frac{\partial P}{\partial x} + \nu \frac{u_s}{\delta^2} f''' \quad ,$$

where we have assumed that the Reynolds stress terms can be separated into the product of an x-dependent functional and a η-dependent functional as

$$\frac{\overline{\tilde{u}\tilde{v}}}{uv(x)} \quad = \quad g_{12}(\xi,\eta), \quad \frac{\overline{\tilde{u}\tilde{u}}}{uu(x)} \quad = \quad g_{11}(\xi,\eta) \ . \tag{6}$$

The Reynolds stress transport equation, Eq. (4), reduces to

$$-uv(x)\frac{du_s}{dx} f g_{12}' - uv(x)\frac{u_s}{\delta}\frac{d\delta}{dx} f g_{12}' + u_s \frac{\partial uv(x)}{\partial x} f' g_{12} - uv(x) u_s \frac{\partial f}{\partial \xi} g_{12}' + \tag{7}$$

$$2\frac{u_s uv(x)}{\delta} g_{12} f'' + \nu \frac{uv(x)}{\delta^2} g_{12}'' + \{3 \ additional \ terms\} \quad = \quad 0 \quad ,$$

where the three additional terms are not written out expressly because they cannot be written in terms of $\overline{\tilde{u}\tilde{v}}$. This is not to say that these terms can be neglected. In fact the opposite is true; the three additional terms in Eq. 7 include the numerically significant energy dissipation rate and the velocity-pressure gradient terms. However, for the purposes of obtaining similarity scaling information for δ, u_s, and the Reynolds stress terms, these three additional terms do not contribute anything useful.

4. Similarity Scaling

Eqs. 5 and 7 are exact equations. The first step to obtain similar scaling factors is to assume that the f and g's are only a function of η. This means that all of the $\partial f/\partial \xi$, $\partial f'/\partial \xi$, *etc.* terms in the transformed equations are assumed equal to zero. The next step is to insure that all of the x-dependent variable groupings appearing in Eq. 5 have the same functional dependence. This must also be true for Eq. 7. Equivalently, we can divide the equations through by one of the variable groupings and check for constancy of the resulting parameters. For the x-momentum equation we will divide through by $(u_s/\delta)d\{\delta u_s\}/dx$ and for the Reynolds stress transport equation we will divide through by $uv(x)u_s/\delta$. The transformed x-component of the momentum balance, Eq. 5, becomes

$$\frac{\lambda}{\lambda+1} f'^2 - ff'' - \tau_1 \eta g_{11}' + \tau_2 g_{11} + \tau_3 g_{12}' \quad = \quad -\frac{\delta}{\rho u_s \, d\{\delta u_s\}/dx}\frac{\partial P}{\partial x} + \frac{1}{\alpha} f''' \tag{8}$$

and the transformed Reynolds stress transport balance, Eq. 7, becomes

$$-\kappa f g_{12}' - \varepsilon \eta f' g_{12}' + \tau_4 f' g_{12} + 2 g_{12} f'' + \chi g_{12}'' + \{3 \ additional \ terms\} = 0 \quad , \tag{9}$$

where

$$\alpha = \frac{\delta^2}{\nu}\frac{du_s}{dx} + \frac{\delta u_s}{\nu}\frac{d\delta}{dx} \quad , \quad \lambda = \frac{\delta}{u_s}\frac{du_s/dx}{d\delta/dx} \quad , \tag{10}$$

$$\chi = \frac{\nu}{\delta u_s} \quad , \quad \varepsilon = \frac{d\delta}{dx} \quad , \quad \text{and} \quad \kappa = \frac{\delta}{u_s}\frac{du_s}{dx} \quad ,$$

and where the τ_i are given by

$$\tau_1 = \frac{uu(x)}{u_s^2(\lambda+1)} \quad , \quad \tau_2 = \frac{duu(x)/dx}{u_s\, du_s/dx + \left(u_s^2/\delta\right) d\delta/dx} \quad , \tag{11}$$

$$\tau_3 = \frac{uv(x)}{\delta u_s\, du_s/dx + u_s^2\, d\delta/dx} \quad , \quad \text{and} \quad \tau_4 = \frac{\delta}{uv(x)}\frac{duv(x)}{dx} \quad .$$

Eq. 8, without the stress terms, is the Falkner and Skan [8] equation. The λ parameter is the negative of the Castillo and George [4] equilibrium similarity parameter Λ (Eq. 2) if one takes u_e as the similarity velocity scale. The α parameter is the same as the Falkner and Skan α parameter from Schlichting [9].

Thus far we have left the pressure terms unassigned. The pressure for the case of a nonzero wedge angle includes an invisid flow contribution. Therefore we can define the total pressure as

$$P(x,\eta) = p(x,\eta) + p_e(x) \quad , \tag{12}$$

where $p_e(x)$ is the pressure at the boundary layer edge and $p(x,\eta)=0$ for η above the boundary layer edge. It is universally assumed that $p_e(x)$ is given by the Euler equation so that

$$-\frac{1}{\rho}\frac{\partial p_e}{\partial x} = u_e\frac{du_e}{dx} \quad . \tag{13}$$

If we substitute Eq. 12 into Eq. 5 and use Eq. 13, we obtain one more similarity criterion in addition to those in Eqs. 10 and 11. Thus, for a nonzero wedge angle we also must have the ratio

$$\frac{u_e\dfrac{du_e}{dx}}{u_s\dfrac{du_s}{dx} + \dfrac{u_s^2}{\delta}\dfrac{d\delta}{dx}} = \frac{u_e\, du_e/dx}{u_s\, du_s/dx}\frac{\lambda}{\lambda+1} \tag{14}$$

equal to a nonzero constant for similarity. The general solution to Eq. 14 equal to a nonzero constant is given by $u_s = \sqrt{a + b\, u_e^2}$ where a and b are constants. With only a slight loss of generality (taking a=0), we see that for similarity, this reduces to $u_s \propto u_e$ in accordance with the result of Castillo and George [4].

5. Similarity Scenarios

Next, we consider two possibilities for similarity. We concentrate on similarity scenarios applicable to the outer region of the turbulent boundary layer. The first is similarity of the outer region in which the viscosity terms can be neglected. Secondly, there is the ZPG case that is best handled separately.

5.1 Similarity of the Outer Region with a Pressure Gradient

First we consider the case of turbulent flow with a nonzero pressure gradient such that $u_s \propto u_e$. In the outer region of a turbulent boundary layer on a wedge we will assume that the viscous forces are negligible. This means that the viscous terms in Eqs. 8 and 9 are equal to zero (eliminating α and χ). Therefore, the functional form that u_s and δ may take is now governed by λ, ε, and κ from Eq. 10. It can be shown mathematically that having these three parameters be constant restricts the functional forms that δ may take to a linear function of the type $\delta = a_1(x - x_0)$ and $u_s \propto u_e$ to a power law function of the type $u_e = a_2(x - x_0)^m$, such that a_1, a_2, m, and x_0 are constants. For the Reynolds stress terms we must have $uu(x) \propto (x - x_0)^{2m}$ and $uv(x) \propto (x - x_0)^{2m}$.

A second possibility is to have $\delta =$ constant and $u_s \propto u_e$ be an exponential function of the type $u_e = be^{x/c}$, such that b and c are constants. We include this possibility because, as we will see below, there is one experimental realization of this condition in the data of Herring and Norbury [10].

5.2 Similarity of the Outer Region of a Flat Plate

For similarity for this case we will examine two possible scenarios; one in which u_s=constant and one in which $u_s \neq$constant with respect to *x*. Consider first the case where u_s=constant. If the velocity u_s is constant, then the scaled momentum equations simplify somewhat. Only α, χ, ε, and the four τ parameters are nonzero for the flat plate case. For similarity in just the outer region (neglecting α and χ) with u_s=constant, the ε term from the *y*-momentum equation provides guidance as to the functional form that δ may take. The general solution for similarity is that δ must be a linear function of *x*. For the Reynolds stress terms we must have $uu(x) =$ constant and $uv(x) =$ constant.

For the outer region of the turbulent boundary layer on a flat plate with $u_s \neq$constant, the functional form for δ, u_s, and the Reynolds stress terms will be governed by the conditions outlined in Section 5.1 above. However, for this case it is not necessary that $u_s \propto u_e$.

6. Experimental

The above theoretical results are new in the sense that the similarity requirement for linear behavior of the length scaling parameter is obtained without first making an assumption about the velocity scaling parameter. This will be discussed more thoroughly in the Discussion section below. We point this out because, while the theoretical results are new, others have already obtained experimental similarity scaling results in the outer region of the turbulent boundary layer in which the length scale is a linear function of the distance along the wedge. Maciel, Rossignol, and Lemay [6] point out a number of examples from the literature.

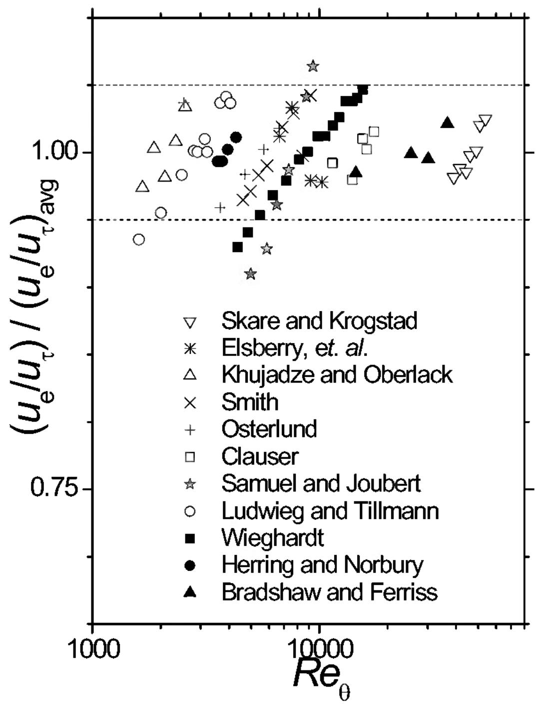

Fig. 1: The ratio u_e/u_τ normalized by the average value versus the Reynolds number for the eleven datasets considered herein.

When looking at the available data, it became apparent that there is an important consideration that has been missing from recent developments. What has been lacking in previous reports from the last few years (*e.g.* Refs. 4 and 6) is that for the available experimental data we examined, simultaneous similarity of the velocity profiles and the Reynolds stress terms are only obtained for the case where the ratio u_e/u_τ is almost constant. To emphasize this point, in Fig. 1 we show the normalized u_e/u_τ ratio for the two APG datasets, Elsberry, *et. al.* [11] and Skåre and Krogstad [12], and one ZPG data set, Khujadze and Oberlack [13], which show simultaneous similarity in the velocity profiles and the Reynolds stress terms. Also included in the plot are the ZPG results for Wieghardt and Tillmann [14], Smith [15], and Österlund [16], the FPG results of Ludwieg and Tillmann [17] and Herring and Norbury [10], and the APG results for Bradshaw and Ferriss [18] and Samuel and Joubert [19] for which only velocity profile data is available. The datasets used herein are summarized in Table 1 (located after the Reference's). The dashed lines in Fig. 1 represent the 5% high/low lines. As is plainly demonstrated, u_e/u_τ is almost constant. Notice that in most cases, the ratio values are monotonically increasing with Reynolds number. Thus, it is necessary to emphasize the "almost" constant aspect. The importance of having the ratio u_e/u_τ almost constant will become evident below.

Using the criteria from Section 5 along with looking for $u_e/u_\tau \cong$ constant, we searched for and found eleven experimental datasets which show similarity-like behavior. For these datasets we found the length parameters δ_1, the Rotta-Clauser thickness Δ, the momentum thickness δ_2, and δ_{99} are all linear functions of the type $a_1(x-x_0)$, a_1 and x_0 constants, with the exception of Herring and Norbury [10] for which δ_1, Δ, δ_2, and δ_{99} are constant (see Appendix A). This means that these four thickness variables satisfy the ε equal a constant requirement and are therefore possible candidates for the similarity thickness δ.

To determine which of these possibilities worked best, we turned to the experimental data. For the length scaling, we found only small differences between plots using δ_1, Δ, δ_2, or δ_{99} as the length scale combined with various velocity candidate scaling (see

Appendix B). All worked fairly well. Given the probable error bars, we do not believe the differences are significant. Therefore, based on the experimental results for the velocity profile plots, we conclude that the outer region similarity thickness scale could be δ_1, Δ, δ_2, or δ_{99}. Since the displacement thickness δ_1 has the smallest error bar and is a well-defined integral parameter, we will initially adopt δ_1 as the similarity thickness scale δ.

The investigated possibilities for u_s scaling include u_e, u_τ, and the empirical velocity proposed by Zagarola and Smits [21] given by $u_{ZS} = u_e \delta_1 / \delta$ (see Appendex B). For the APG and FPG cases, Eq. 14 indicates that we must have $u_s \propto u_e$ for the outer region of a turbulent boundary layer. However, since the ratio u_τ / u_e is almost constant for the eleven datasets, then u_τ is still a possibility. After plotting and comparing, we found a clear advantage for u_e over u_τ and u_{ZS} for producing similarity-like collapse of the velocity profile for the eleven datasets. For illustrative purposes, we plot the APG data of Skåre and Krogstad [12] in Figs. 2a, 2b, and 2c and the ZPG data of Wieghardt and Tillmann [14] in Figs. 3a, 3b, and 3c using the three velocity scalings. These plots as well as others (see Appendex B) have convinced the author that that u_e is superior to u_τ and u_{ZS} (with $\delta = \Delta$, δ_2, or δ_{99}) as the outer region velocity profile scaling variable for all cases including the ZPG cases.

Experimentally it is evident that u_e is the outer region similarity variable u_s but does it satisfy the theoretical guidance? Using the same x_0 value from the thickness fit, we found the fit $u_e \cong a_2 \left(x - x_0\right)^m$ works well for six of the seven non-ZPG cases. For the ZPG cases, u_e=constant. Simple mathematics can be used to show that for ten of the datasets, the above similarity criteria requiring λ, ε, and κ to be a constant are satisfied for $u_s \propto u_e$ and any choice of the linear thickness parameters δ_1, Δ, δ_2, or δ_{99}. Herring and Norbury [10] is the one exception where we found that u_e fits to an exponential for this case and that δ_1 is a constant. Thus this dataset also satisfies the above similarity criteria (see Section 5.2). Therefore, all eleven datasets satisfy the similarity criteria thereby confirming that the velocity scale u_e is an acceptable velocity scale that can result in similarity-like behavior of the velocity profile of the outer region of the turbulent boundary layer.

To illustrate the similarity-like behavior we have plotted multiple datasets of the velocity profiles in Figs. 4 – 6 using the δ_1 and u_e as the scaling variables. In Fig. 4 we plot three ZPG sets and the mild APG set. In Fig. 5 we plot the mild APG and FPG cases as well as one ZPG set for reference. Finally, in Fig. 6 we plot the moderate and strong APG cases as well as one ZPG case for reference. It is evident that the similarity-like collapse of the data using u_e as the similarity velocity scale u_s and δ_1 as the similarity thickness scale δ is very good. The figures also indicate that the profile shape is changing with the strength of the pressure gradient contrary to Castillo and George's conjecture.

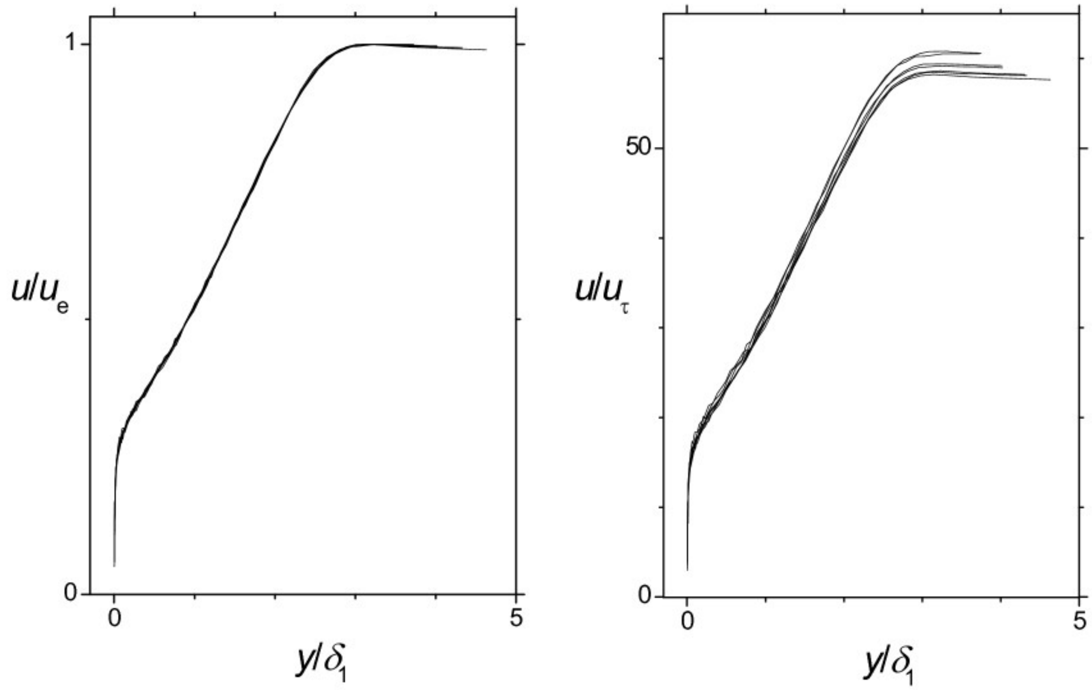

Fig. 2a, 2b, and 2c: Skåre and Krogstad [12] seven APG velocity profiles scaled with u_e, u_τ, and u_{ZS}.

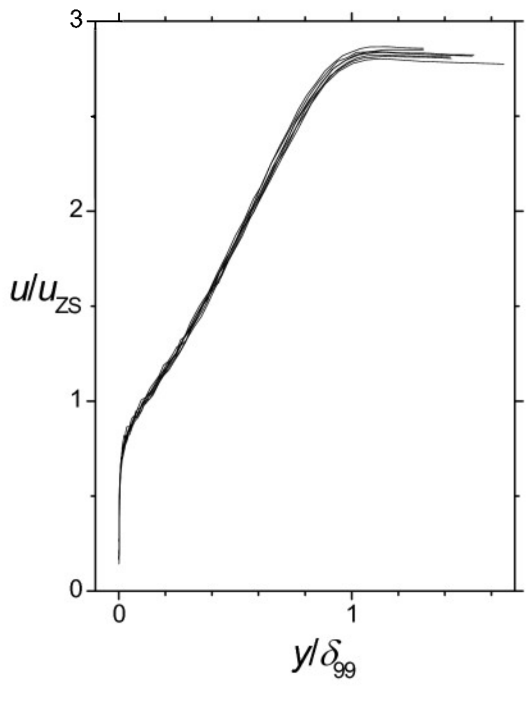

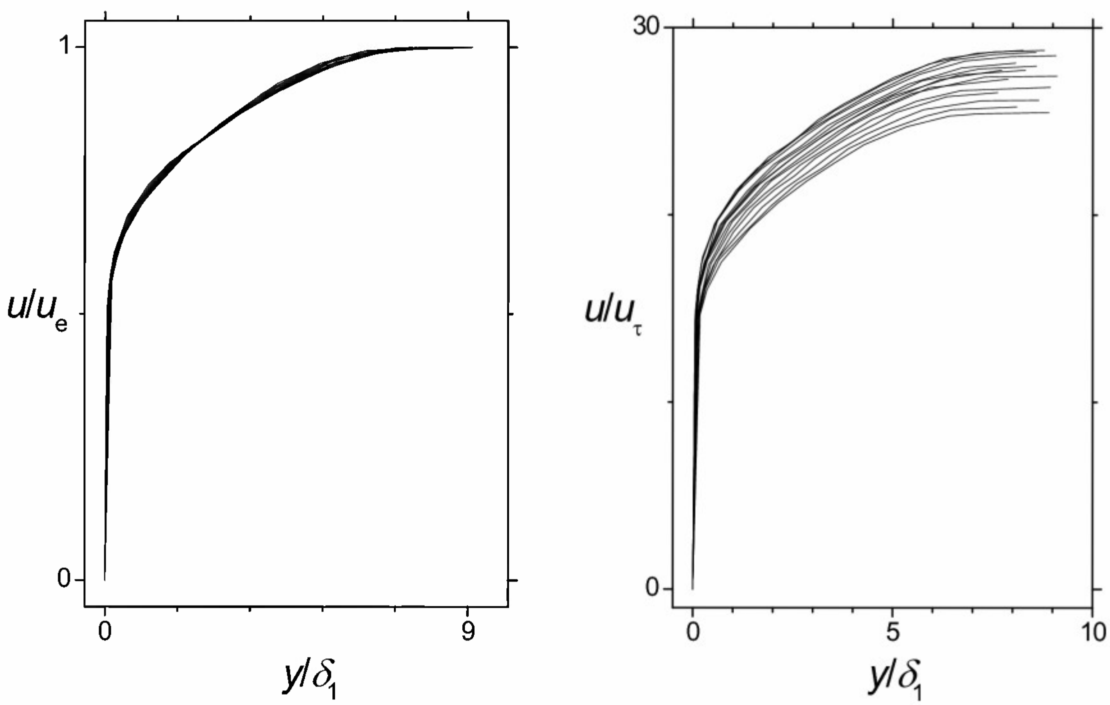

Fig. 3a , 3b, and 3c: Wieghardt and Tillmann [14] fifteen ZPG velocity profiles scaled with u_e , u_τ , and u_{ZS} .

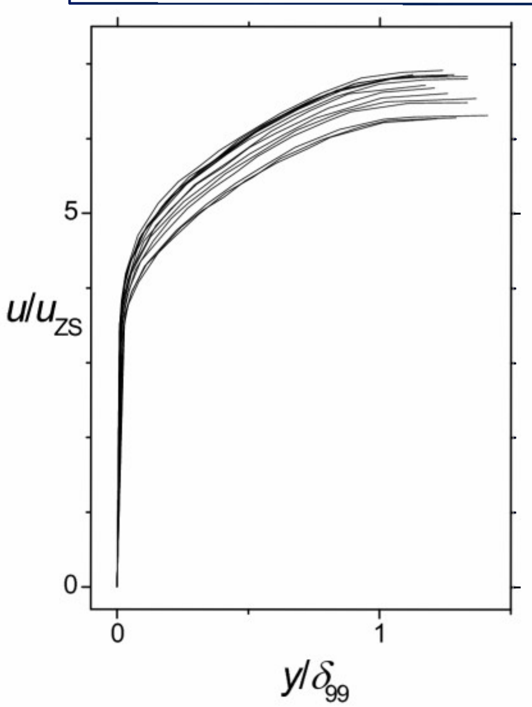

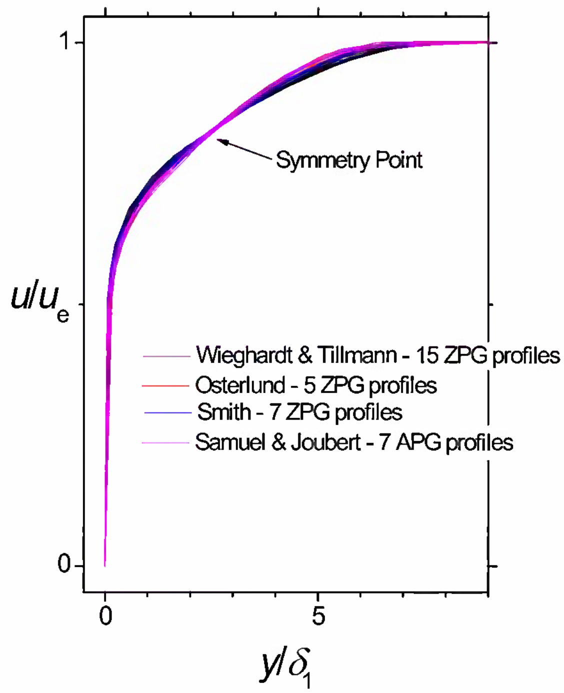

Fig. 4: ZPG and mild APG velocity profiles from various sources.

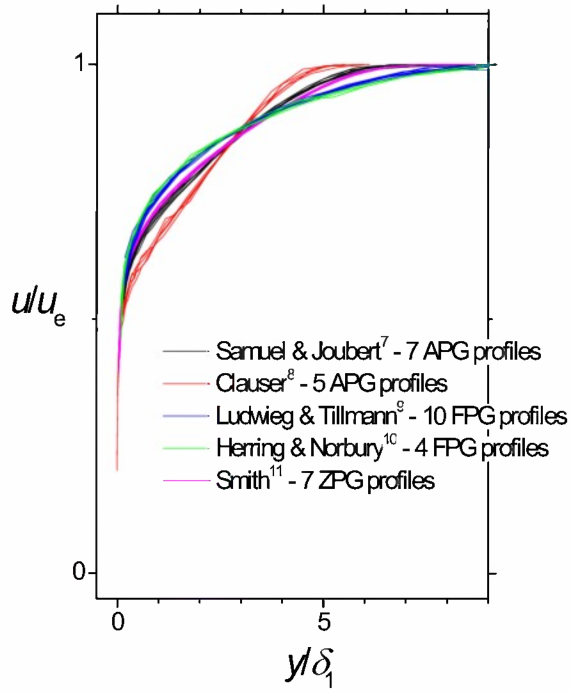

Fig. 5: Mild APG, mild FPG, and ZPG velocity profiles from various sources.

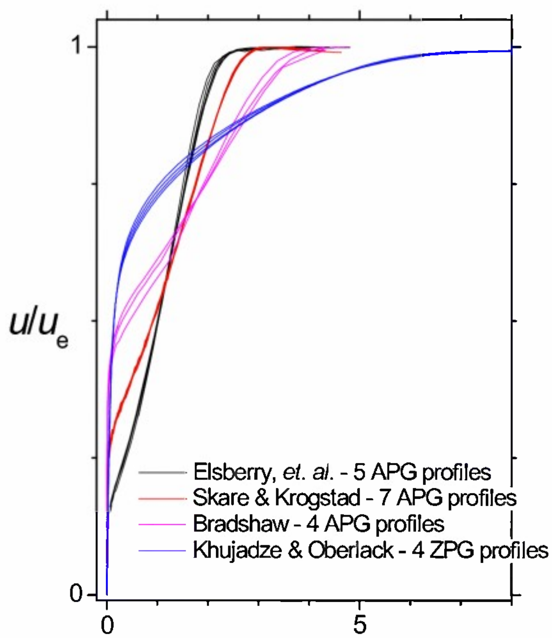

Fig. 6: Moderate APG, strong APG, and ZPG Velocity profiles from various sources.

Next we looked at the Reynolds stress term $\overline{\tilde{u}\tilde{v}}$. As in the velocity profile case, we found the length parameters δ_1, Δ, δ_2, and δ_{99} all worked fairly well as the thickness scaling parameter (see Appendic C). The one exception was the DNS results of Khujadze and Oberlack [13] for which the parameters δ_1 and δ_2 had a small but noticeable advantage over Δ and δ_{99}. Since the displacement thickness δ_1 also worked well for the velocity profile plots, has the smallest error bar, and is a well-defined integral parameter, in what follows we will adopt δ_1 as the similarity thickness scale δ.

For the outer region similarity $uv(x)$ scaling, we looked at various possibilities including $uv(x)=u_e^2$, $uv(x)=u_\tau^2$, and $uv(x)=u_0^2$, u_0 a constant, as well as the mixed cases such as $uv(x)=u_e u_\tau$, *etc.* (see Appendix C). Using the Skåre and Krogstad [12] data, we found the fits $u_e \cong a_2\left(x-x_0\right)^m$ and $u_\tau \cong a_3\left(x-x_0\right)^n$ work well using the same x_0 value from the thickness fit. (The Elsberry, *et. al.* [11] u_τ data was too scattered to make a proper fit). We have already established that $u_s = u_e$ from the velocity profile considerations. Thus, the similarity requirements that τ_3 and τ_4 from Eq. 11 be constant with respect to x are satisfied if one takes any choice of the linear thickness parameters δ_1, Δ, δ_2, and δ_{99} in combination with either u_e^2 or, if $m=n$, u_τ^2 for the Reynolds stress scaling parameter. For the Skåre and Krogstad fits, we found that $m \neq n$ thus seemingly excluding u_τ^2. For the non-zero pressure gradient cases, the velocity scaling involving u_0, including the mixed scaling $uv(x)=u_e u_0$ advocated by Elsberry, *et al.* [11], does not satisfy the similarity requirements from above and is therefore also excluded.

The theoretical considerations would therefore favor u_e^2 for the scaling of $\overline{\tilde{u}\tilde{v}}$. However, when we plotted and compared $\overline{\tilde{u}\tilde{v}}$ scaled with either u_e^2 or u_τ^2 for the Skåre and Krogstad [12] and Elsberry, *et. al.* [11] datasets, we found there was little difference between either of these velocity scales in regards to the peak location and the peak value of the Reynolds shear stress for the two data sets. Although the scaling in some cases seems to favor one choice or another, the differences are relatively small and we believe would wash out when one considers the probable error bars on the various velocity scaling's. Therefore, based on the limited experimental data, we conclude that the linear thickness scaling parameter is δ_1 and that the scaling parameter for $\overline{\tilde{u}\tilde{v}}$ could be either $uv(x)=u_e^2$, $uv(x)=u_\tau^2$, or even $uv(x)=u_e u_\tau$.

To determine which of these choices might be correct, we looked at the ZPG case. Since we have already established that $u_s = u_e$, the similarity requirement that τ_3 and τ_4 from Eq. 11 be constant means that for the ZPG case, $\overline{\tilde{u}\tilde{v}}$ = constant. This again would seem to favor $uv(x)=u_e^2$ since u_e is necessarily a constant for the ZPG case. However, for the one high quality ZPG experimental dataset available to the authors, that being the Direct Numerical Simulation results of Khujadze and Oberlack [13], we found a clear advantage for u_τ^2 scaling compared to u_e^2. The results for the two scalings are shown

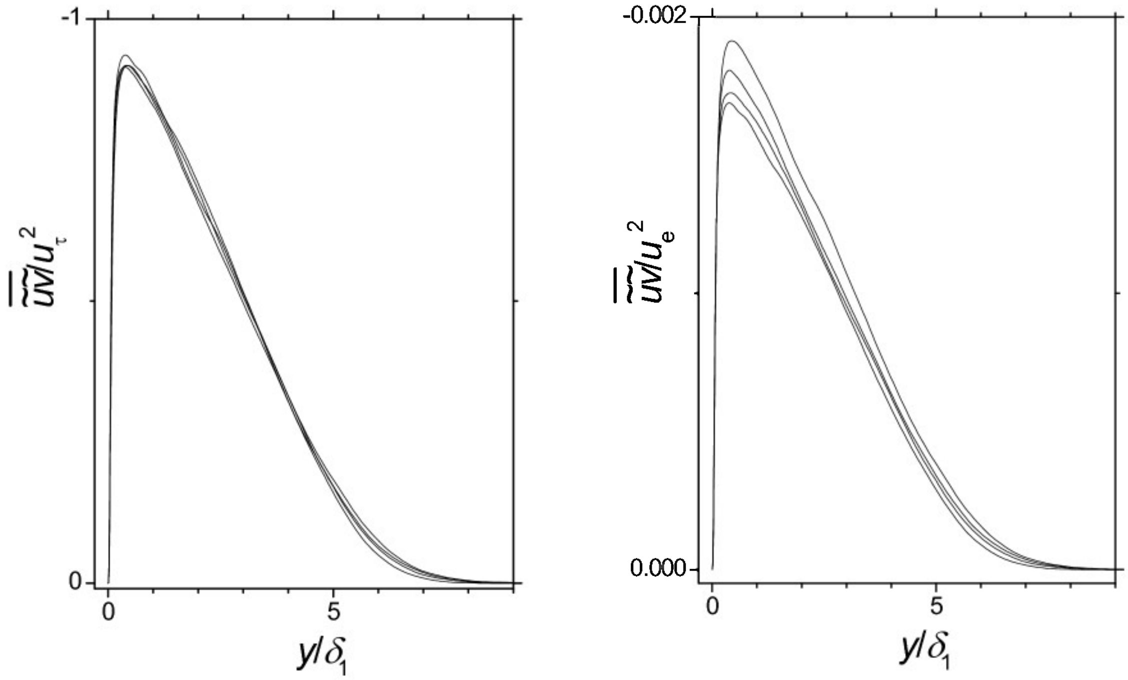

Fig. 7a and 7b: Khujadze and Oberlack [13] data plotted with two different y-axis scales.

in Fig. 7a and 7b. Thus, while the similarity requirement that τ_3 and τ_4 be constant would seem to favor $uv(x) = u_e^2$, the DNS results point to $uv(x) = u_\tau^2$ as the proper one with respect to x (for the DNS data we found $u_\tau \cong 0.1733(x+254)^{-0.22}$ for $150 \le x \le 300$) for the Reynolds stress scaling. For the ZPG case it is generally true that u_τ is not a constant. Thus for the $uv(x) = u_\tau^2$ choice it would appear that it is not possible to have $\overline{\tilde{u}\tilde{v}} =$ constant as required. The theoretical guidance and the experimental results seem to be at odds. The resolution to this conflict comes from the fact that for the data being investigated, the ratio u_e/u_τ is almost constant thus making τ_3 and τ_4 (almost) constant. This same almost constant ratio also makes $uv(x) = u_\tau^2$ work for the APG cases discussed above since again we have the case that τ_3 and τ_4 are (almost) constant. Therefore, even though the experimental evidence is for the most part ambiguous, we believe the DNS results are correct and that $uv(x) = u_\tau^2$ is the correct scaling for the outer region of the turbulent boundary layer.

Finally we looked at the Reynolds stress term $\overline{\tilde{u}\tilde{u}}$ case (see Appendix D). The results are very similar to the $\overline{\tilde{u}\tilde{v}}$ case. We found the length parameters δ_1, Δ, δ_2, and δ_{99} all worked well as the thickness scaling parameter. Furthermore, the experimental results showed only small differences between $uu(x) = u_e^2$, $uu(x) = u_\tau^2$, or $uu(x) = u_e u_\tau$. Based on the Elsberry, *et. al.* [11] and Skåre and Krogstad [12] datasets, we conclude that the linear thickness scaling parameter could be either δ_1, Δ, δ_2, or δ_{99} and that the scaling parameter for $\overline{\tilde{u}\tilde{u}}$ could be either $uu(x) = u_e^2$, $uu(x) = u_\tau^2$, or $uu(x) = u_e u_\tau$.

We again turned to the ZPG case to determine which of these choices might be correct. Since we have already established that $u_s = u_e$, the similarity requirement that τ_1 and τ_2 be constant means that for the ZPG case, $\overline{\tilde{u}\tilde{u}}$ = constant. Looking at the Khujadze and Oberlack [13] DNS data, we found the u_τ^2 or $u_\tau u_e$ scaling is better than u_e^2 scalings in terms of peak scaling of $\overline{\tilde{u}\tilde{u}}$ as shown in Fig. 8a, 8b, and 8c. We therefore conclude that the $\overline{\tilde{u}\tilde{u}}$ case could scale as either $uu(x) = u_\tau^2$ or $uu(x) = u_e u_\tau$. Both satisfy the similarity requirements as long as we have the ratio u_e/u_τ almost constant. We note that the mixed scaling case has been advocated by DeGraaff and Eaton [22].

In summary, the new theoretical guidance combined with experimental comparisons therefore allows us to make the following conjecture: For the outer region of the turbulent boundary layer, similarity-like behavior can be expected if: 1) the thickness scales as δ_1 and is a linear function of the distance along the wedge, 2) the velocity scales as free stream velocity u_e and is a power law function of the distance along the wedge, 3) the Reynolds stress scalings are taken as $uv(x) = u_\tau^2$ and $uu(x) = u_\tau^2$ or $uu(x) = u_e u_\tau$, and 4) the ratio u_e/u_τ is almost constant.

7. Discussion

The purpose of the above theoretical analysis was to determine what theory could tell us about functional scaling behavior of δ, u_s, and the Reynolds stress terms along the free stream direction of the wedge for the outer region of the turbulent boundary layer. This can then be used to provide the experimentalist with theoretical guidance for discovering, and/or designing experiments to discover similarity in the outer region of the turbulent boundary layer. Comparing the above theoretical results with previous results in the literature is informative. As already mentioned in the Introduction, Clauser [1], Rotta [2], and Townsend [3] made similar momentum balance deliberations. However, Clauser and Rotta incorporated specific assumptions as to the identity of the scaling velocity and the Reynolds stress term scalings while Townsend made the assumption that the Reynolds stress terms are proportional to the velocity scaling variable squared, *i.e.* he assumed $uv(x) = uu(x) = u_s^2$. The more recent work of Castillo and George [4] and Maciel, Rossignol, and Lemay [6] avoided making any specific assumptions for the length or velocity scaling variables or the Reynolds stress terms. The above analysis follows this same tack.

One of the major differences between previous efforts and the new theoretical construct was the use of the Reynolds stress transport equation in addition to the normally used x-momentum balance equation. We note that Townsend [3] used the x-momentum balance equation together with the kinetic energy balance equation but Townsend's subsequent conclusions are derivable from the x-momentum balance equation alone. The inclusion of the Reynolds stress transport equation as used herein with the normally used

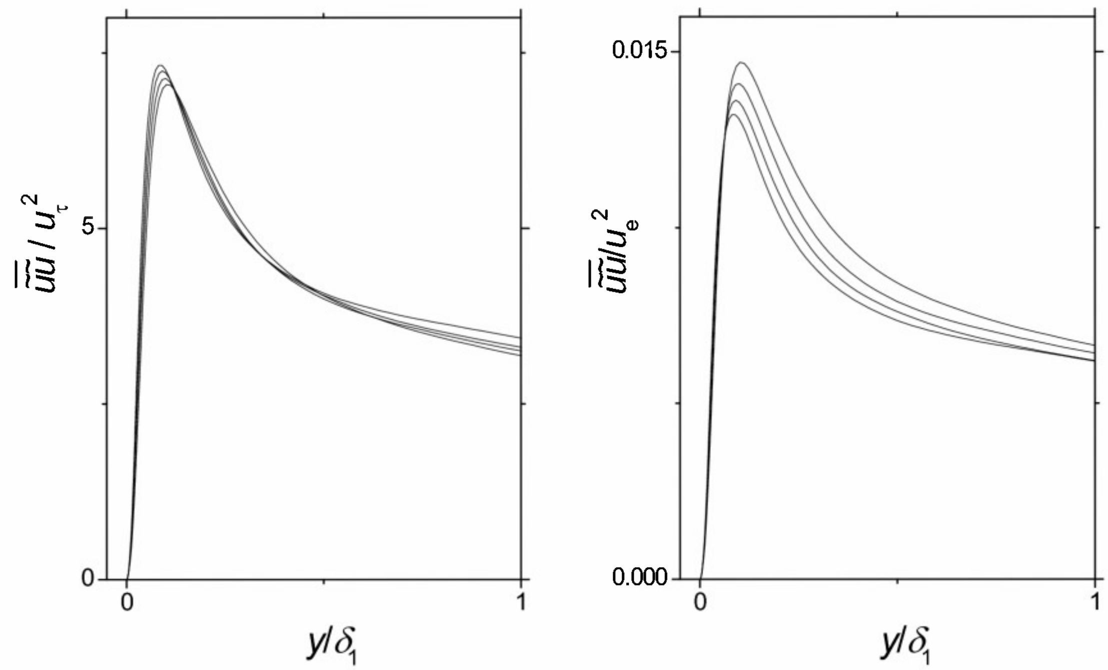

Fig. 8a, 8b, and 8c: Four Reynolds shear stress $\overline{\tilde{u}\tilde{u}}$ profiles from Khujadze and Oberlack [13].

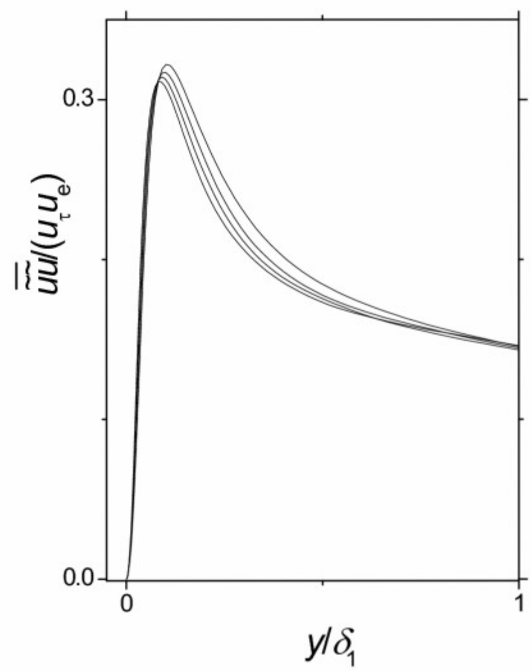

x-momentum balance equation was the key to obtaining the additional criteria χ, ε, and κ (Eq. 10).

Consider the χ parameter. The χ parameter is obtained from the viscous term of the Reynolds stress transport equation. The inclusion of the χ parameter would mean that the only allowable solution is for δ to be linear in x and u_s to go as $1/x$. This corresponds to a converging wedge (sink) flow that, as pointed out by Townsend [3], is also obtained if the α term from Eq. 10 is included. While it is readily accepted that the viscous term (α term) of the x-momentum equation is negligible for the outer region of turbulent boundary layer, there is only limited information on the behavior of χ in the outer region. The DNS results of Spalart [23] indicates that the viscous term of Eq. 4 is indeed negligible compared to the other terms of the Reynolds stress transport equation in the outer region of the turbulent boundary layer. The viscous term was less than 0.2% of the normalized sum of the terms of Eq. 4 in the outer region. Thus, for the outer region of the turbulent boundary layer, both of the viscous terms α and χ can be neglected.

Of the next two terms, ε and κ, it is clear that the ε term is the key term that dictates the behavior of the length scaling variable. The ε term establishes the linear behavior requirement. At first glance this does not appear to be a new result. A number of groups have claimed that the boundary layer thickness scaling variable δ for the turbulent boundary layer flow must be a linear function of x. Rotta [2] made this assertion based on similarity arguments using the reduced x-momentum equation. However, Rotta made an explicit assumption about the x-dependence of the various scaling terms, *i.e.* he assumed that $u_s = u_\tau$ and that $uu(x) = uv(x) = u_\tau^2$. In so far as these assumptions are true (the present author's contend $u_s = u_e$ not $u_s = u_\tau$), then one can see from Eq. 11 that this would require that the similarity length scale δ must be a linear function of x. However, from purely theoretical considerations of the x-momentum equation, there is no justification for these assumptions for the outer region of a turbulent boundary layer. Another group, Maciel, Rossignol, and Lemay [6], make a linear behavior assertion based on the claim that flow equilibrium implies a constant ratio of turbulent and streamwise time scales. However, they offered no theoretical or experimental verification for their assertion, which means that their claimed linear dependence is no different than an assumption. Skåre and Krogstad [12] make the linear behavior assertion based on Townsend's claim. Towsend [3] assumed that $uu(x) = uv(x) = u_s^2$. In so far as this assumption is true (which the present authors believe to be false), then one can see from Eq. 11 that this would require that the similarity length scale δ must be a linear function of x. What differentiates the new results above from these previous efforts is that the linear behavior was obtained without making *a priori* assumptions about the x-behavior of the velocity scaling variable or the Reynolds stress terms.

The other major difference between the above analysis and the earlier work is that results are obtained for the ZPG case. The key to obtaining the usable criteria for the length scale δ for the ZPG case was to 1) the use of the Reynolds stress transport equation to obtain the ε parameter and 2) carefully pick the scaling group to divide the scaled momentum equations by. We used the factors $(u_s/\delta)d\{\delta u_s\}/dx$ for the x-momentum equation and $u_s uv(x)/\delta$ for the Reynolds stress transport equation. In this way, even if u_s is equal to a constant, we do not have a divide-by-zero problem. The result is that we are able to establish that for similarity-like behavior, the length scale δ must be a linear function of the distance along the wedge for all pressure gradient cases including the ZPG case.

Applying the theoretical results to existing experimental data was very informative. We noticed that for the experimental datasets we examined, simultaneous similarity of the velocity profiles and the Reynolds stress terms are only obtained for the Rotta criterion where the ratio u_e/u_τ is almost constant. Although we found only three cases for which simultaneous similarity of the velocity and Reynolds stress exists, we believe there is indirect supporting evidence for this being a general requirement for similarity-like behavior of the outer region of the turbulent boundary layer. This support comes from the fact that of the cases where only velocity profile data was available, we also only found similarity-like behavior of the velocity profile for the case where the ratio u_e/u_τ is almost constant. The reason this is important is that, as pointed out by Townsend [3], it is not possible to have similarity-like behavior in the turbulent boundary layer unless both the velocity profile and the Reynolds stress terms show simultaneous similarity behavior. If $u_s = u_e$ and $uu(x) = uv(x) = u_\tau^2$ as we propose, then simultaneous similarity would explain why the ratio u_e/u_τ needs to be almost constant because it is only under these conditions that the τ_1, τ_2, τ_3, and τ_4 of Eq. 11 will be constant. Having the requirement that the ratio u_e/u_τ be almost constant would explain why Clauser and others have concluded that the appearance of similarity-like behavior in the turbulent boundary layer is relatively rare (the contrary view of Castillo and George [4] will be discussed below). The simple fact is that u_e/u_τ is rarely constant over a significant distance along a wedge and is a condition for which the experimental conditions must be carefully manipulated to in order to obtain the almost constant condition.

Rotta [2] also concluded that u_e/u_τ must be constant for similarity-like behavior of the turbulent boundary layer. This conclusion rests on Rotta's assumption that $u_s = u_\tau$ and that $uu(x) = uv(x) = u_\tau^2$. While these scalings may work for inner layer similarity, we can say that experimental evidence we studied clearly shows that $u_s = u_\tau$ is not the correct scaling for the velocity profile for the outer region of the turbulent boundary layer (see Figs. 2 and 3 for example). Brzek, *et. al.* [24] and Maciel, Rossignol, and Lemay [25] have come to the same conclusion. Thus, even though Clauser [1] and Skåre and Krogstad [12], for example, successfully designed their experiments to show flow equilibrium in the turbulent boundary layer based on keeping u_e/u_τ constant, they succeed not because the Rotta scaling assumptions are correct but because the scaling's advocated herein, $u_s = u_e$ and $uu(x) = uv(x) = u_\tau^2$, are correct and the only time one will see similarity-like behavior under these conditions is when u_e/u_τ is almost constant.

Having the ratio u_e/u_τ almost constant was critical in resolving the apparent conflict between the theoretical similarity criteria and the experimental results. This lead us to make the following conjecture: For the outer region of the turbulent boundary layer, similarity-like behavior can be expected if: 1) the thickness scales as δ_1 and is a linear function of the type $\delta_1 = a_1(x - x_0)$, 2) the velocity scales as the free stream velocity u_e and is a power function of the type $u_e = a_2(x - x_0)^m$, 3) the Reynolds stress scales as $uv(x) = u_\tau^2$ and $uu(x) = u_\tau^2$ or $uu(x) = u_e u_\tau$ and 4) the ratio u_e/u_τ is almost constant. Compare this to the Castillo and George [4] results, for example, where they indicated that the proper outer layer thickness scale is δ_{99}, the velocity scale is the Zagarola–Smits velocity u_{ZS}, and the Reynolds shear stress scaled as $u_e^2\, d\delta/dx$ while the normal stress component scaled as u_e^2.

A second important finding concerning the experiment data is that the linear requirement of the thickness scaling parameter was satisfied by length parameters δ_1, Δ, δ_2, or δ_{99}. All worked reasonably well for the eleven experimental datasets we investigated. In most cases there were no significant observable differences between plots using the four length scales (see Appendix B). The one exception was the DNS results of Khujadze and Oberlack [13] for which the parameters δ_1 and δ_2 had a small but noticeable advantage over Δ and δ_{99}. This result along with the fact that δ_1 has the smallest error bar, is a well defined integral parameter, and shows up in theoretical boundary layer equations (momentum integral equation) led us to choose δ_1 over the other variable candidates. Why δ_1, Δ, or δ_2 have not been tested before as possible length scale parameters is inexplicable.

One important point that must be made in regards to the experimental results and conclusions is that we have noticed that in most cases the profiles plotted using δ_1 and u_e as the scaling variables do not possess true similarity behavior in the sense that the curves collapse directly onto one another. Instead the curves have a symmetry point as denoted in Fig. 4. This symmetry point has the property that if one looks at the section of curves to the left of the symmetry point, the curves all line up with the highest Reynolds number curve having the largest amplitude. To the right of the symmetry point, the order reverses and the lowest Reynolds number profiles have the largest amplitude. This behavior seems to show up in many of the datasets that show similarity-like behavior (see Figs. 4 – 6). We call this behavior similarity-like behavior as opposed to true similarity behavior. It is apparent that for a given set of similarity-like turbulent boundary layer velocity profiles, there will be a particular Reynolds number that will produce a velocity profile that is symmetric about the symmetry point in regards to this behavior. We speculate that this symmetric profile is the case where true similarity collapse would be attained if the experimental conditions could be manipulated to produce this specific value of the ratio u_e/u_τ for a significant distance along the wedge surface. Indeed, consider the Skåre and Krogstad [12] data shown in Fig. 2a that does not show this symmetry point behavior. What is special about this dataset is that the spread of the u_e/u_τ values is among the smallest of the eleven datasets we investigated (see Fig. 1). Clauser [1] and Skåre and Krogstad [12] have pointed out that it is very difficult to generate and maintain a constant u_e/u_τ condition for true similarity behavior. Thus, the symmetry point behavior may be the best one can expect for datasets in which the spread of the u_e/u_τ values is larger than a few percent. Therefore, from an engineering standpoint, the symmetry point type similarity-like behavior described herein is a more reasonable design goal then true similarity behavior.

At this point it is appropriate to comment on the contention by Castillo and George [4] that most turbulent boundary layers are in equilibrium. The claim is based in part on the apparent success of δ_{99} when used with the Zagorola and Smits [21] velocity scale given by $u_e\delta_1/\delta_{99}$. Castillo and George and co-workers have attempted to show that many of the existing, as well as their own, experimental datasets have similarity-like behavior when plotted with this length and velocity scale. We have found that in some cases the supposed success is being realized because of a flaw in the way the plots are being presented. Consider a couple of specific cases as examples. In Castillo and George [4], the authors claim that the δ_{99} and the velocity scale $u_{ZS} = u_e\delta_1/\delta_{99}$ results in similarity collapse of the profile data for Clauser's [1] mild APG case. We reproduce their Fig. 8a here as our Fig. 9a. In Fig. 9b we plot the same exact data using the y-axis scale u/u_{ZS} instead of $(u_e-u)/u_{ZS}$. Contrary to Castillo and George's claim, the Clauser data scaled with δ_{99} and $u_e\delta_1/\delta_{99}$ does not result in similarity-like behavior. Compare this to a subset of Clauser's data plotted in Fig. 5 using δ_1 and u_e which does show similarity-like behavior. Consider another example given by Castillo and Walker [26] in which they claim the δ_{95} and the velocity scale $u_{ZS} = u_e\delta_1/\delta_{95}$ results in similarity collapse of

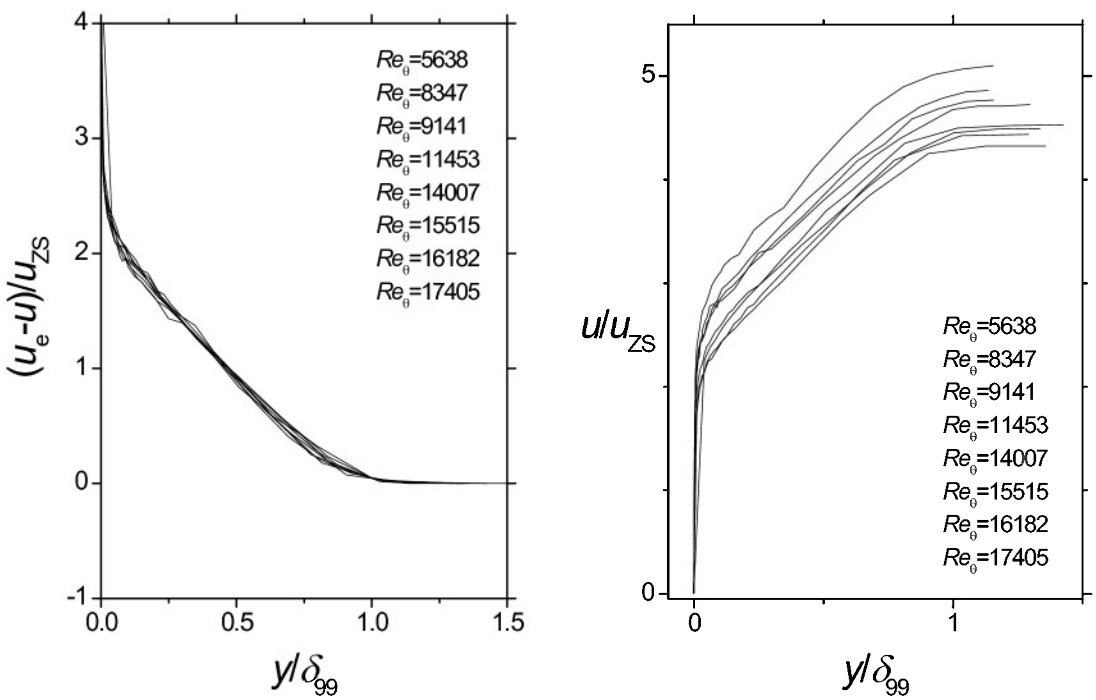

Fig. 9a and 9b: Clauser's mild APG data plotted with two different y-axis scales.

the data for some of Österlund's [16] ZPG datasets. We reproduce their Fig. 3 here as Fig. 10a. In Fig. 10b we plot the same exact data using the *y*-axis scale u/u_{ZS} instead of $(u_e - u)/u_{ZS}$. One would obviously come to a very different opinion as to the correctness of the similarity scaling depending on which figure one was presented. In Fig. 10c, we plot the same data using δ_1 and u_e. The fact that these same datasets (actually subsets of the datasets) show similarity-like behavior when plotted using δ_1 and u_e scaling makes it difficult to directly rule out Castillo and George's [4] contention that most turbulent boundary layers are in equilibrium. However, what we can say is that it will require a careful reexamination of all of their data before they can make this contention. Furthermore, based on our own tests of the eleven datasets considered herein, we can say that the Zagarola and Smits [21] velocity scale pared with δ_{99} as the length scale was noticeably inferior to δ_1 and u_e for producing similarity-like behavior (see Figs. 2, 3, and 10 for example).

We should also comment on the DeGraaff and Eaton [22] mixed scaling for the scaling for $\overline{\tilde{u}\tilde{u}}$. DeGraaff and Eaton [22] and Metzger, *et. al.* [27] contend that $uu(x) = u_e u_\tau$ collapses the data from a number of ZPG cases better than u_τ^2. However, for the datasets we investigated, we found the differences to be small. If one considers the uncertainty of measuring u_τ compared to u_e, which is typically much higher, then the argument for $uu(x) = u_e u_\tau$ over $uu(x) = u_\tau^2$ is tenuous. The DNS data of Khujadze and Oberlack [13] also indicates that the scaling could be either $uu(x) = u_e u_\tau$ or $uu(x) = u_\tau^2$ (see Figs. 8a and 8c). Either selection will satisfy the theoretical requirements above for experiments in which similarity-like behavior is obtained when the ratio u_e/u_τ is almost constant. At this point in time, we do not believe the experimental evidence is sufficient to distinguish between the two choices.

8. Conclusion

The transformed *x*-momentum and Reynolds stress transport equations are used to obtain similarity criteria for both the velocity profile and the Reynolds stress terms. For similarity in the outer turbulent boundary layer region it was shown that the boundary layer thickness must be a linear function of the distance along the wedge and free stream velocity must be a power function of the distance along the wedge. Results were obtained for all pressure gradient variants including the flat plate case. Comparison of experimental data plots was used to conclude that the thickness scales as the displacement thickness, the velocity scales as the free stream velocity, and the Reynolds stresses scale as the square of the friction velocity. Furthermore, similarity-like behavior in the outer region of the turbulent boundary layer is only obtained when the ratio of the free stream velocity to the friction velocity is almost constant.

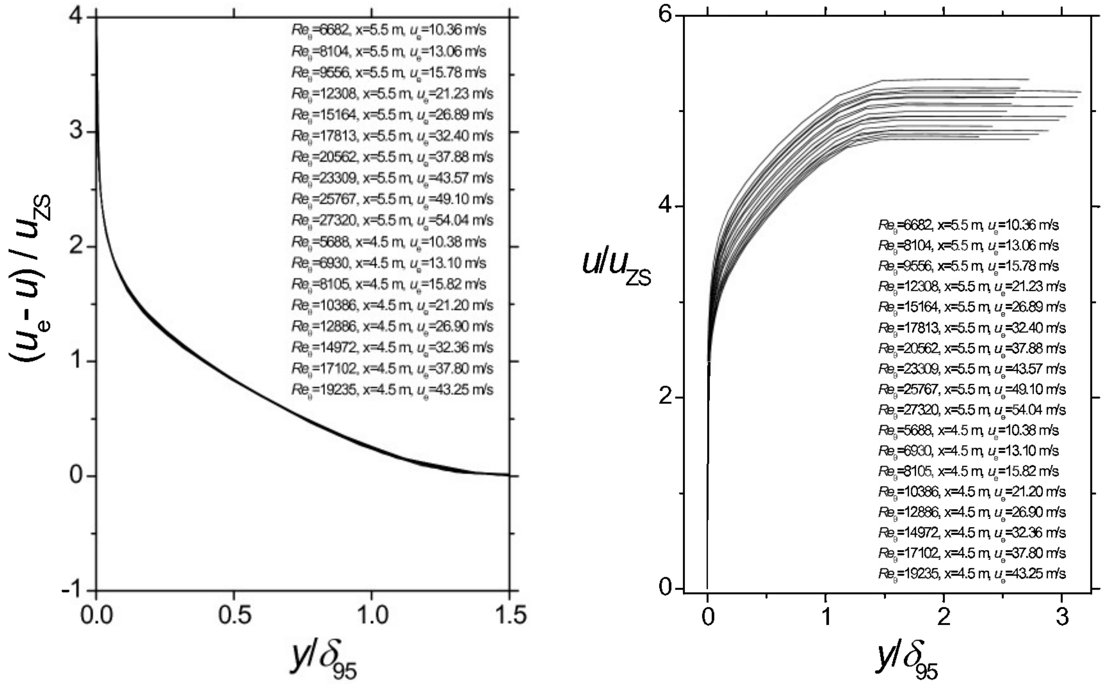

Fig. 10a, 10b, and 10c : Österlund's data plotted with three different y-axis scales.

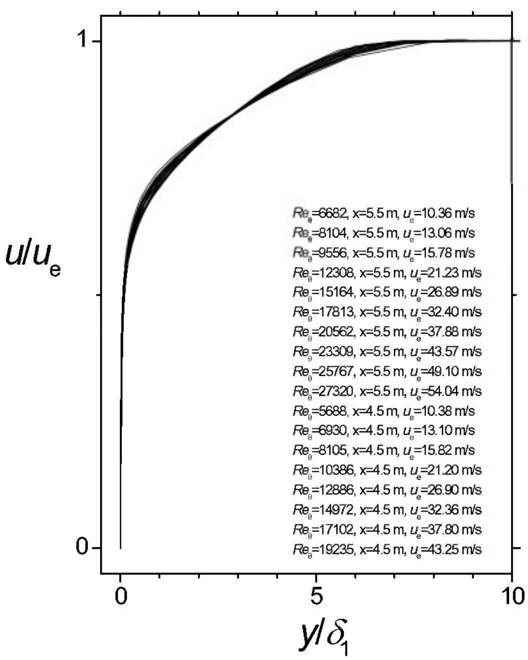

9. References

[1] F. H. Clauser, "The turbulent boundary layer in adverse pressure gradients," J. Aeronaut. Sci. **21**, 91 (1954).

[2] J. Rotta, "Turbulent Boundary Layers in Incompressible Flow," Prog. Aerospace Sci. **2**, 1 (1962).

[3] A. A. Townsend, *The Structure of Turbulent Shear Flow*, 2nd edn. (Cambridge University Press, Cambridge, 1956).

[4] L. Castillo and W. George, "Similarity Analysis for Turbulent Boundary Layer with Pressure Gradient: Outer Flow," AIAA J. **39**, 41 (2001).

[5] R. Cal, G. Johansson, and L. Castillo, "Upstream Condition Effects on Turbulent Boundary Layers Subject to Favorable Pressure Gradients," AIAA J. **44**, 2488 (2006).

[6] Y. Maciel, K.-S. Rossignol, and J. Lemay, "Self-Similarity in the Outer Region of Adverse-Pressure-Gradient Turbulent Boundary Layers," AIAA J. **44**, 2450 (2006).

[7] F. White, *Viscous Fluid Flow*, 2nd edn. (McGraw-Hill, New York, 1991), pp. 406-409.

[8] V. Falkner and S. Skan, "Some Approximate solutions of the boundary layer solutions," Philosophical Magazine **12**, 865 (1931).

[9] H. Schlichting, *Boundary Layer Theory*, 7th edn.(McGraw-Hill, New York, 1979).

[10] H. Herring, and J. Norbury, "Some Experiments on Equilibrium Boundary Layers in Favourable Pressure Gradients," J. Fluid Mech. **27**, 541 (1967).

[11] K. Elsberry, J. Loeffler, M. Zhou, and I. Wygnanski, "An experimental study of a boundary layer that is maintained on the verge of separation," J. Fluid Mech. **423**, 227 (2000).

[12] P.E. Skåre and P.A. Krogstad, "A Turbulent Equilibrium Boundary Layer near Separation," J. Fluid Mech. **272**, 319 (1994).

[13] G. Khujadze and M. Oberlack, "DNS and scaling laws from new symmetry groups of ZPG turbulent boundary layer flow," Theoret. Comput. Fluid Dynamics **18**, 391 (2004).

[14] K. Wieghardt and W. Tillmann, "On the Turbulent Friction for Rising Pressure,' NACA TM 1314 (1951).

[15] R. Smith, "Effect of Reynolds Number on the Structure of Turbulent Boundary Layers," Ph.D. Thesis, Department of Mechanical and Aerospace Engineering, Princeton University, 1994.

[16] J. Österlund, "Experimental studies of zero pressure-gradient turbulent boundary layer flow," PhD thesis, Royal Institute of Technology, KTH, Stockholm, 1999.

[17] H. Ludwieg and W. Tillmann, "Investigations of the Wall Shearing Stress in Turbulent Boundary Layers," NACA TM 1285 (1950).

[18] P. Bradshaw and D. Ferriss, "The Response of a Retarded Equilibrium Turbulent Boundary Layer to the Sudden Removal of Pressure Gradient," NPL Aero. Rept. 1145 (1965).

[19] A. Samuel and P. Joubert, "A Boundary Layer Developing in an Increasingly Adverse Pressure Gradient," J. Fluid Mech. **66**, 481 (1975).

[20] D. Coles and E. Hirst, eds., *Proceedings of Computation of Turbulent Boundary Layers, AFOSR–IFP–Stanford Conference*, Vol. 2, (Thermosciences Div., Dept. of Mechanical Engineering, Stanford Univ. Press, Stanford, CA, 1969).

[21] M. Zagarola and A. Smits, "Mean-flow scaling of turbulent pipe flow," J. Fluid Mech. **373**, 33 (1998).

[22] D. DeGraaff and J. Eaton, ''Reynolds number scaling of the flat plate turbulent boundary layer,'' J. Fluid Mech. **422**, 319 (2000).

[23] P. R. Spalart, "Direct simulation of a turbulent boundary layer up to $R\theta = 1410$," J. Fluid Mech. **187**, 61 (1988).

[24] B. Brzek, O. Turan, C. Anderson, and L. Castillo, "Outer Scaling in Turbulent Boundary Layers," AIAA 2005-4814 (2005).

[25] Y. Maciel, K.-S. Rossignol, and J. Lemay, "A study of a turbulent boundary layer in stalled-airfoil-type flow conditions," Exp. Fluids **41**, 573 (2006).

[26] L. Castillo and D. Walker, "Effect of Upstream Conditions on the Outer Flow of Turbulent Boundary Layers," AIAA J. **40**, 1292 (2002).

[27] M. Metzger, J. Klewicki, K. Bradshaw, and R. Sadr, "Scaling the near-wall axial turbulent stress in the zero pressure gradient boundary layer," Phys. Fluids **13**, 1819 (2001).

Tables

Table 1: Summary of Datasets		
Author	**Stations showing velocity profile similarity**	**Source of dataset**
Clauser [1]	x=18.58, 23.83, 26.92, 29.75, and 32.25	Coles and Hirst [20] Ident 2200
Bradshaw and Ferris [18]	x=1.917, 3.917, 5.417, and 6.917	Coles and Hirst [20] Ident 2600
Skåre and Krogstad [12]	x=4.0, 4.2, 4.4, 4.6, 4.8,5.0, and 5.2	Author
Elsberry, *et. al.* [11]	Case A, $(x-x_0)/\theta_0$ = 239, 264, 295, 325, and 362	Author
Samuel and Joubert [19]	x= 0.855, 1.16, 1.44, 1.76, 2.1, 2.26, and 2.4	Journals of Fluids Engineering Databank Web site, DB96-243/D1/f0141
Ludwieg and Tillmann [17]	x=1.782, 2.282, 2.782, 3.132, 3.332, 3.532, 3.732, 3.932, 4.132, and 4.332	Coles and Hirst [20] Ident 1300
Herring and Norbury [10]	x= 2, 3, 4, and 5	Coles and Hirst [20] Ident 2700
Wieghardt and Tillmann [14]	x=1.087, 1.237, 1.437, 1.637, 1.987, 2.287, 2.587, 2.887, 3.187, 3.487, 3.787, 4.087, 4.387, 4.687, and 4.987	Coles and Hirst [20] Ident 1400
Smith [15]	x= 1.021, 1.161, 1.302, 1.451, 1.721, 2.021, and 2.523	Princeton University Gas Dynamics Lab Web site
Österlund [16]	x=1.5,2.5,3.5, 4.5 and 5.5 ($u_e \cong$ 10.3 m/s) consisting of SW981129A, SW981128A, SW981127H, SW981126C, and SW981112A	Author
Khujadze and Oberlack [13]	Re_θ = 2088, 2333, 2569, and 2807.	Author

Appendix A: Data Fits

The following plots are support data for the Technical Report entitled "Similarity Scaling of the Outer Region of the Turbulent Boundary Layer", by David W. Weyburne. In the Report it was determined that the functional form the thickness scaling constant δ may take is a function of the type $\delta = a_1(x - x_0)$ and that the velocity similarity scaling constant u_s is a power law function of the type $u_s = a_2(x - x_0)^m$, such that a_1, a_2, m, and x_0 are constants. The following plots are compiled to show the data fits for the data sets considered for the paper. We found that in almost all cases, the δ_1, Δ, δ_2, and δ_{99} are all linear functions of the type $a\left(x - x_0\right)$, with the exception of Herring and Norbury [10] for which δ_1, Δ, δ_2, and δ_{99} are constant. Fits were performed to $u_e = a_2(x - x_0)^m$ using the same x_0 from the thickness fitting. For the four ZPG cases, it was found that u_τ could be fitted by $u_\tau = a_2(x - x_0)^m$ using the same x_0 from the thickness fitting. It should be mentioned that in most cases the value of x_0 changed when fitting δ_1, Δ, δ_2 or δ_{99} for the same dataset. However, it was found that the subsequent fits to $u_e = a_2(x - x_0)^m$ could still be effected. Thus there does not seem to a single set of constants a_1, a_2, x_0, and m that satisfy a given dataset for similarity. The plots are provided for visual verification of the claims made in the main body of the Report. They are not identified with Figure numbers but rather as the ensemble of plots as Appendix A.

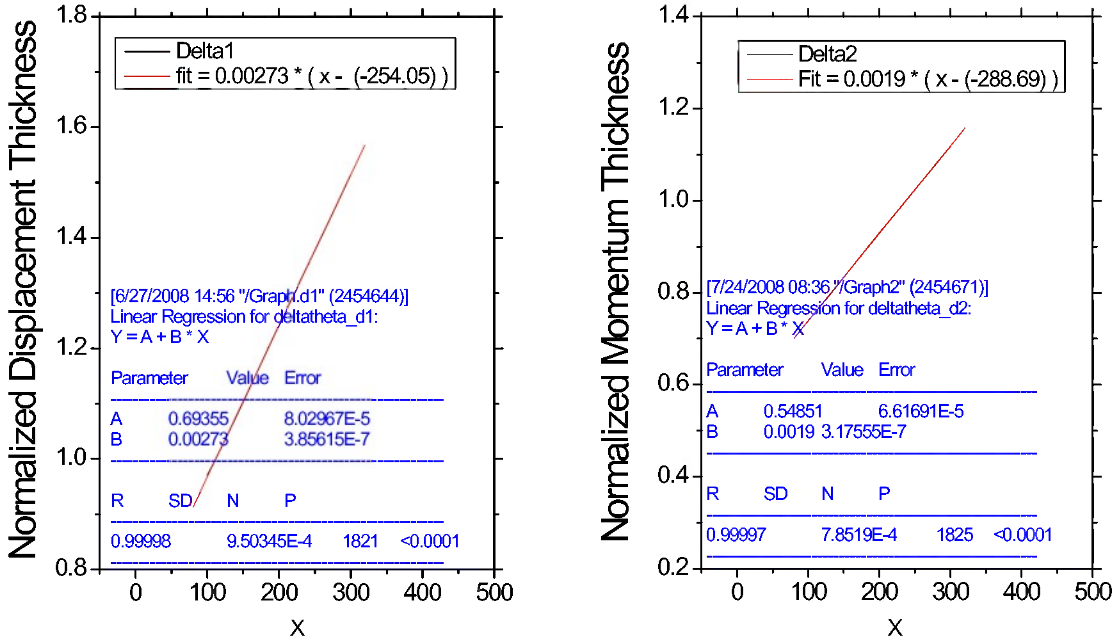

Khujadze and Oberlack [13] fits for Re_θ = 1850, 2088, 2333, 2569, and 2807. Each experimental line (black line) represents over 1800 data points.

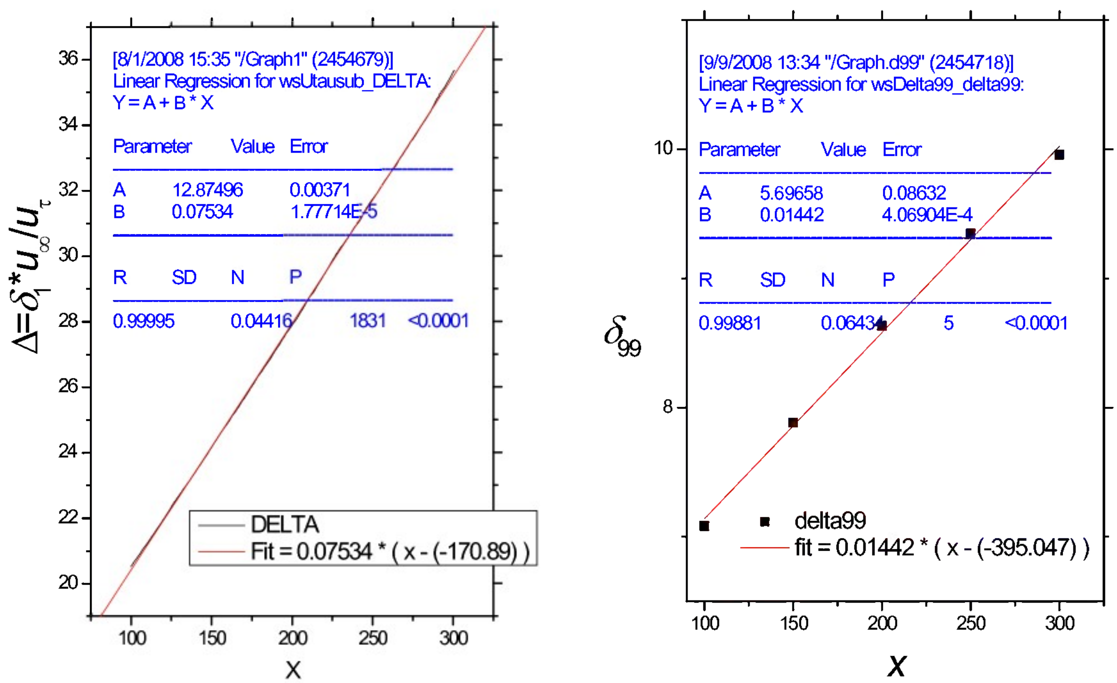

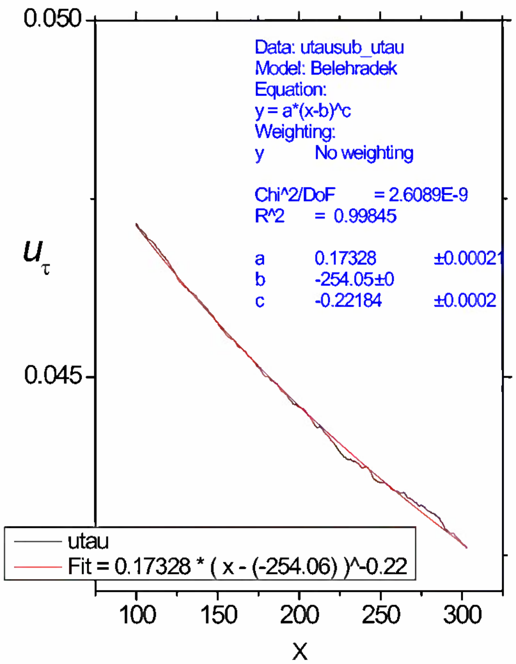

Khujadze and Oberlack [13] fits for Re_θ = 1850, 2088, 2333, 2569, and 2807. Each experimental line (black line) represents over 1800 data points.

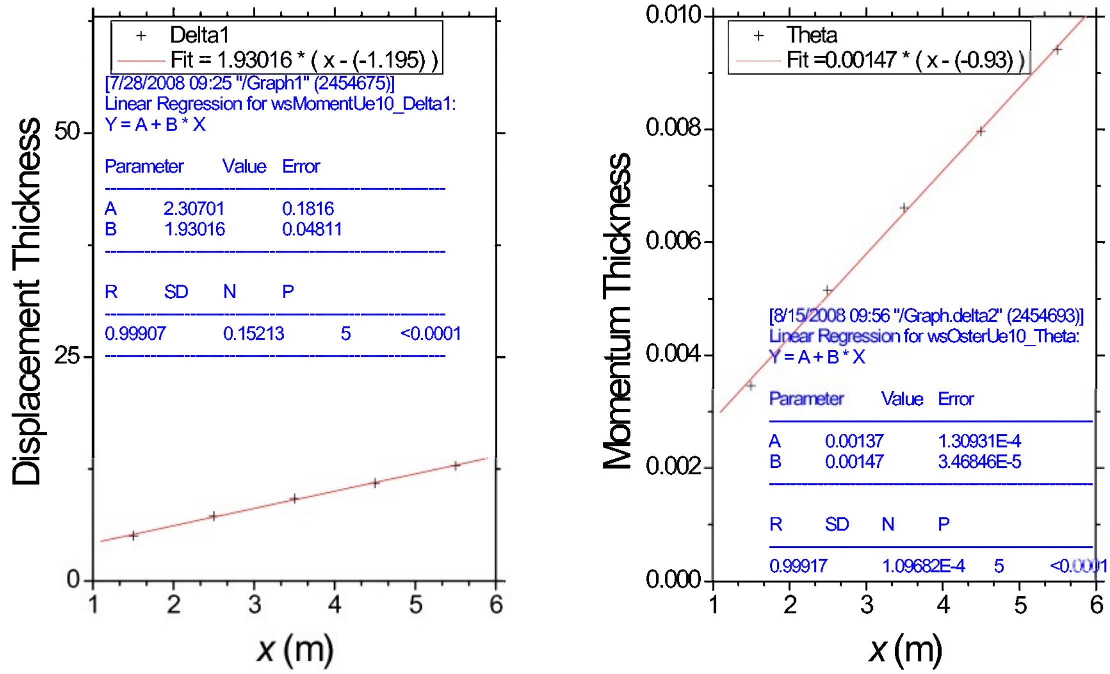

Osterlund [16] fits of data that have $u_e \cong 10.3$ m/s consisting of SW981129A, SW981128A, SW981127H, SW981126C, and SW981112A data sets.

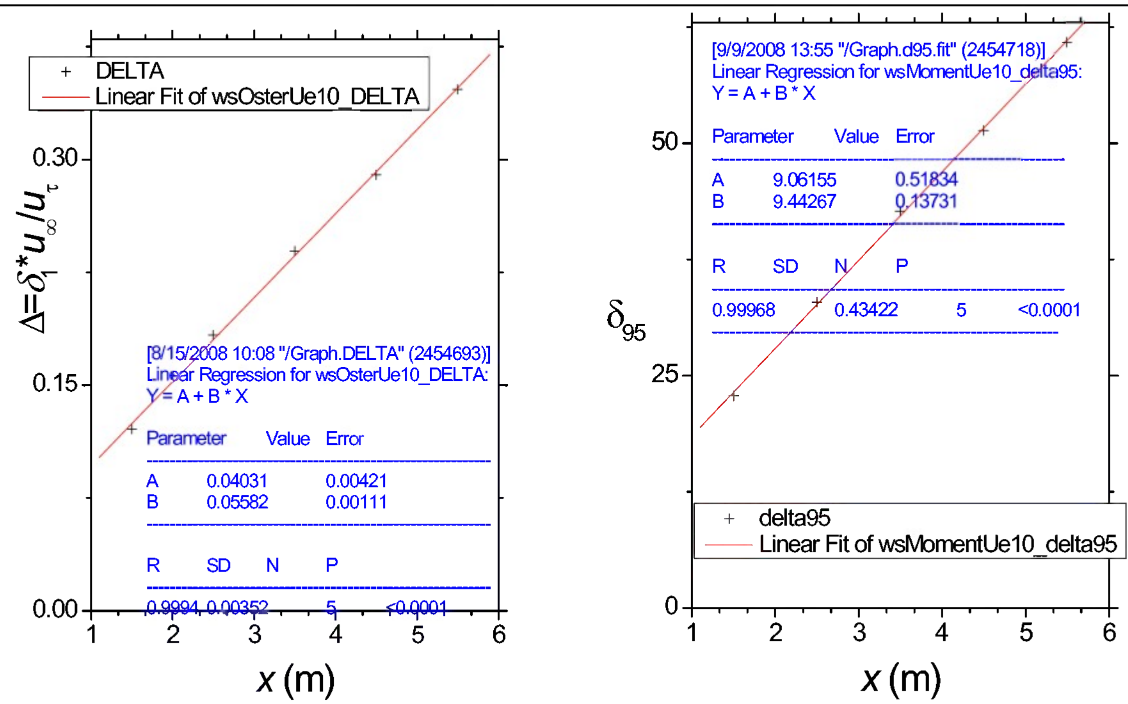

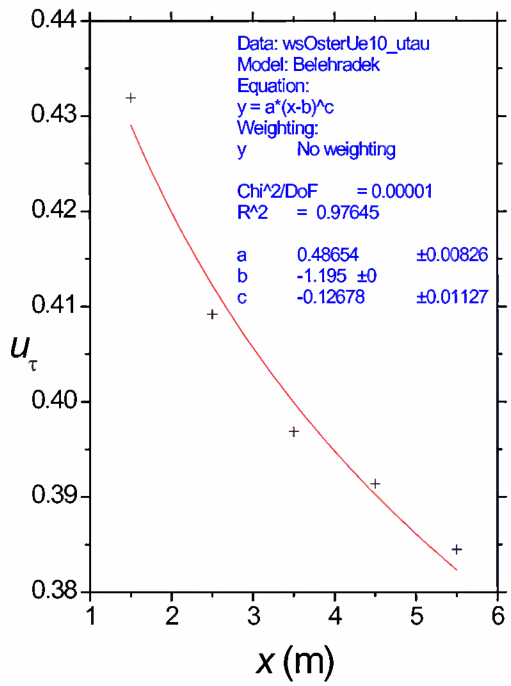

Osterlund [16] fits of data that have $u_e \cong 10.3$ m/s consisting of SW981129A, SW981128A, SW981127H, SW981126C, and SW981112A data sets.

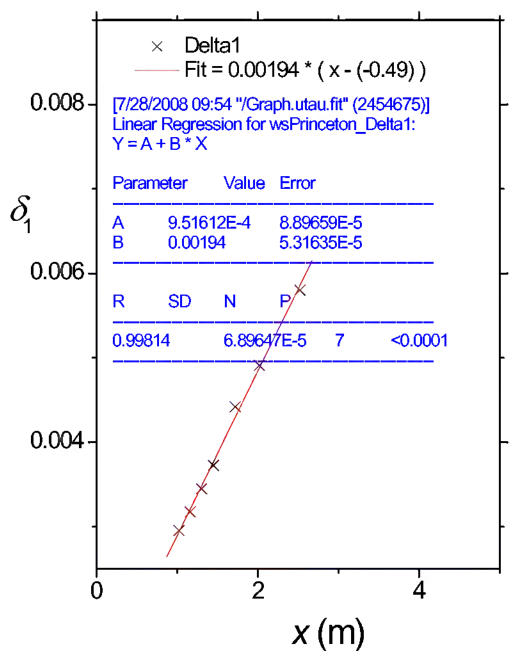

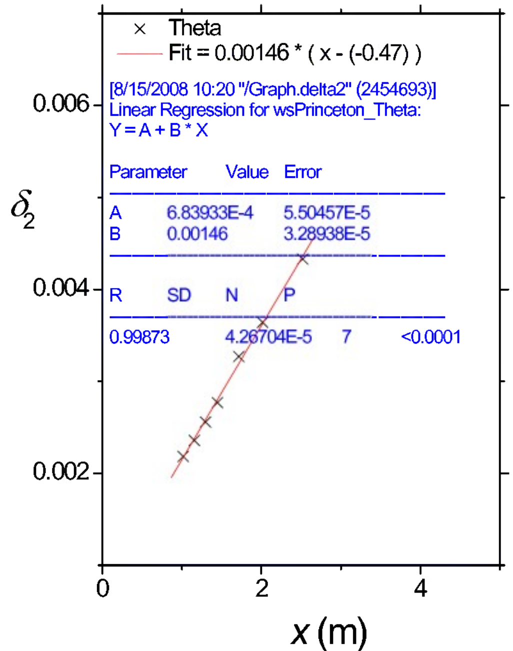

Smith [15] data fits for seven data sets consisting of Re_θ =4601, 4980, 5388, 5888, 6866, 7696, and 9148.

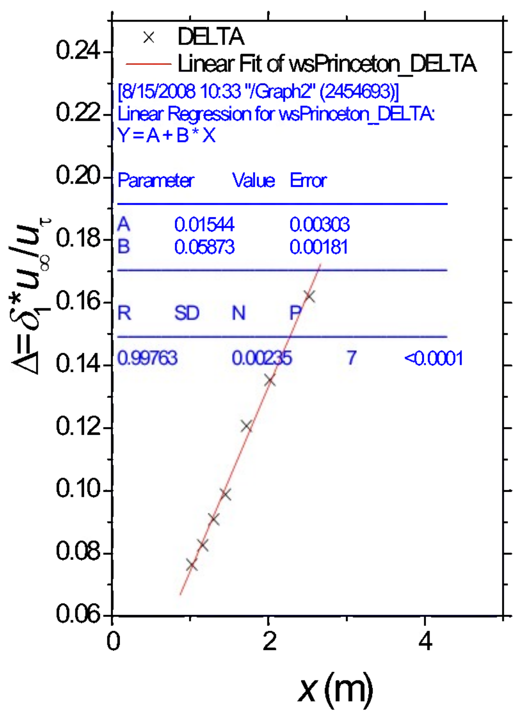

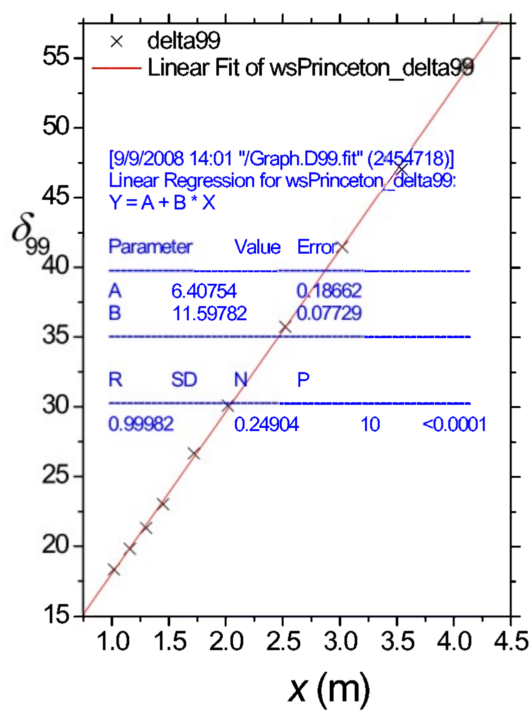

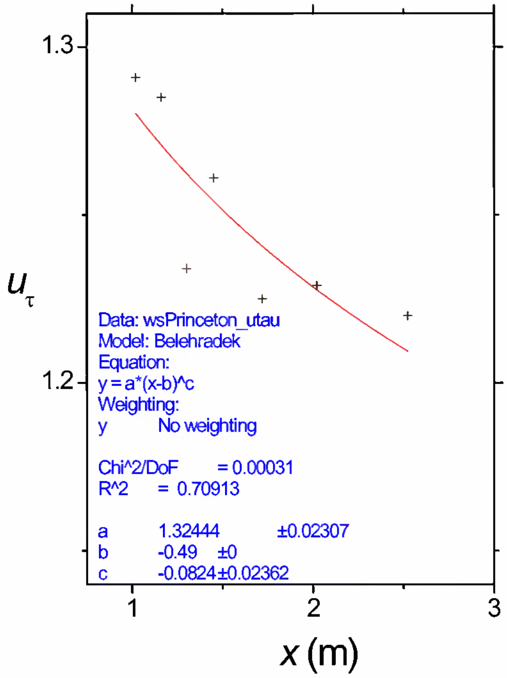

Smith [15] data fits for seven data sets consisting of Re_θ=4601, 4980, 5388, 5888, 6866, 7696, and 9148.

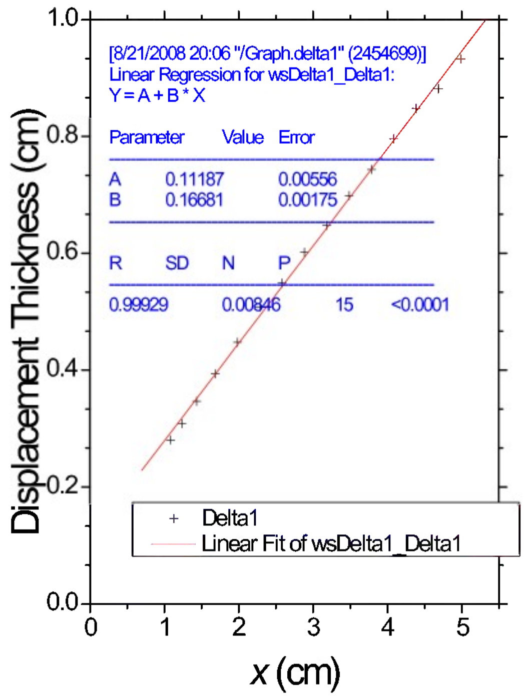

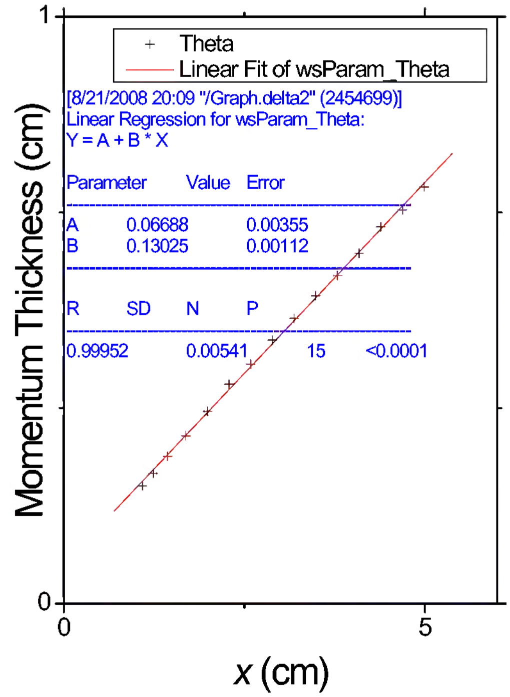

Wieghardt and Tillmann [14] data fits for 15 profiles with Re_θ = 4387, 4858, 5473, 6229, 7170, 8172, 8897, 9815, 10611, 11472, 12223,13043, 14024, 14703, and 15518.

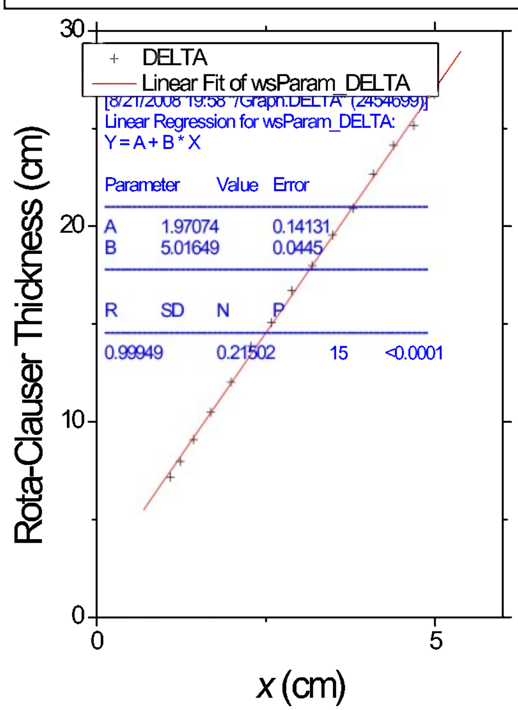

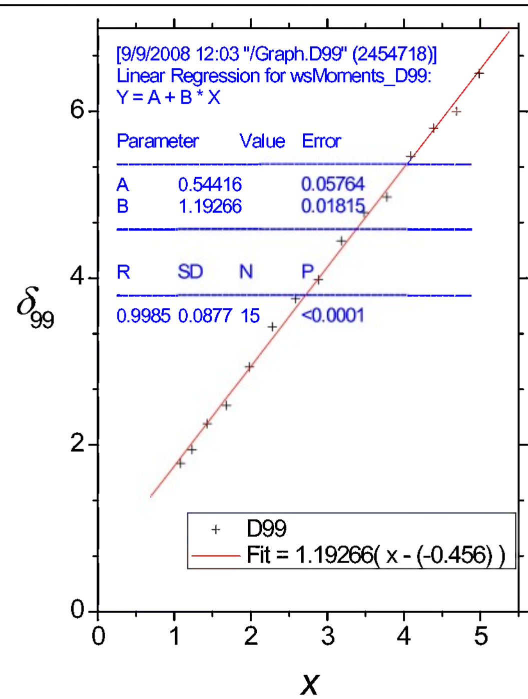

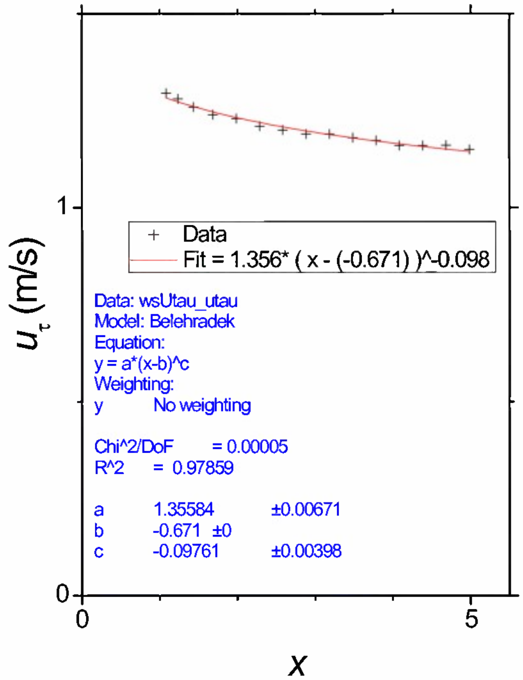

Wieghardt and Tillmann [14] data fits for 15 profiles with Re_θ = 4387, 4858, 5473, 6229, 7170, 8172, 8897, 9815, 10611, 11472, 12223,13043, 14024, 14703, and 15518.

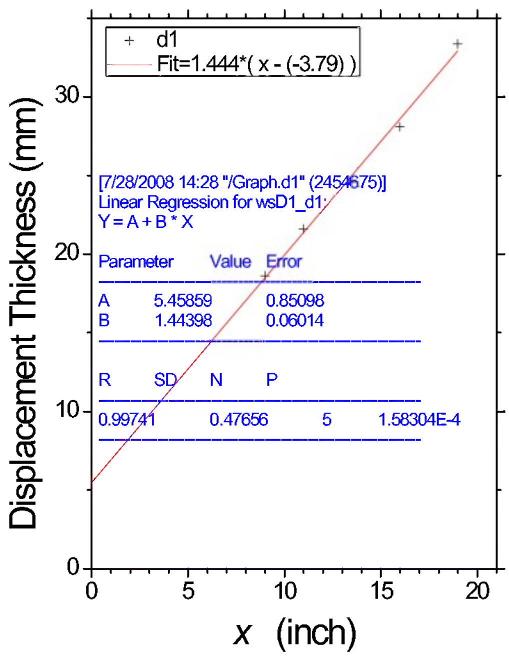

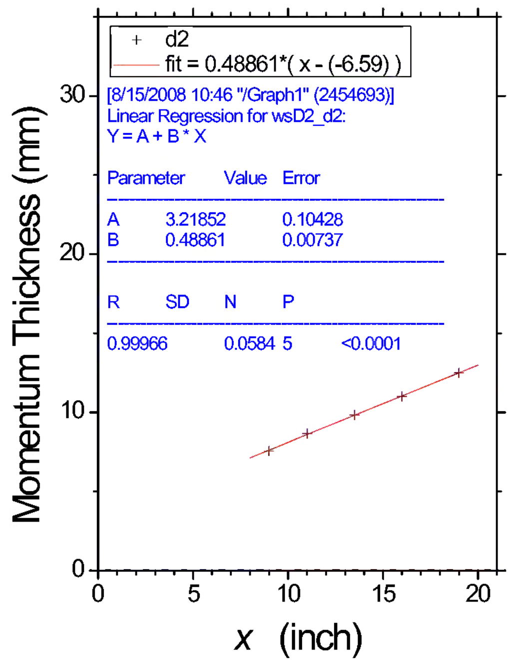

Elsberry, *et. al.* [11] data fits for five data sets designated as CASE A $(x-x_0)/\theta_0$ = 239, 264, 295, 325, and 326 by Elsberry, *et. al.*

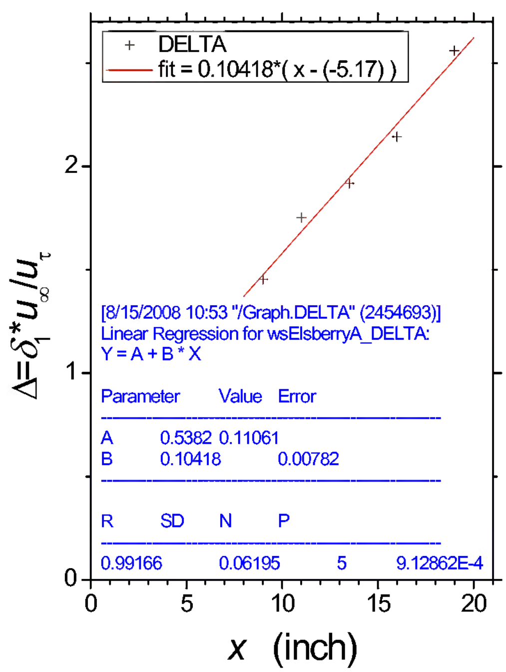

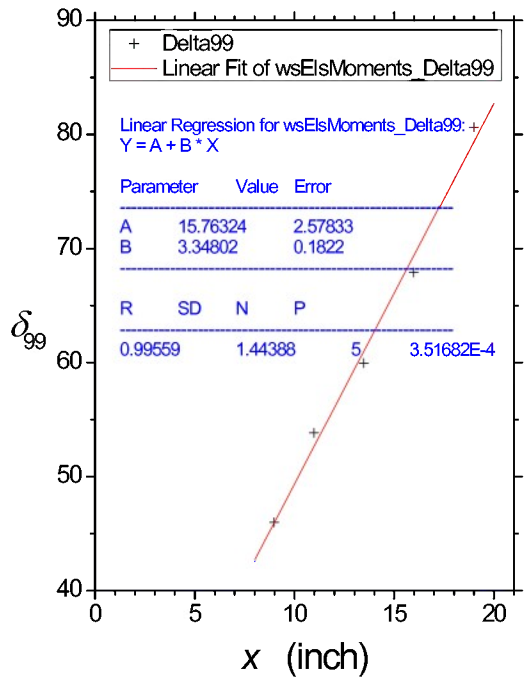

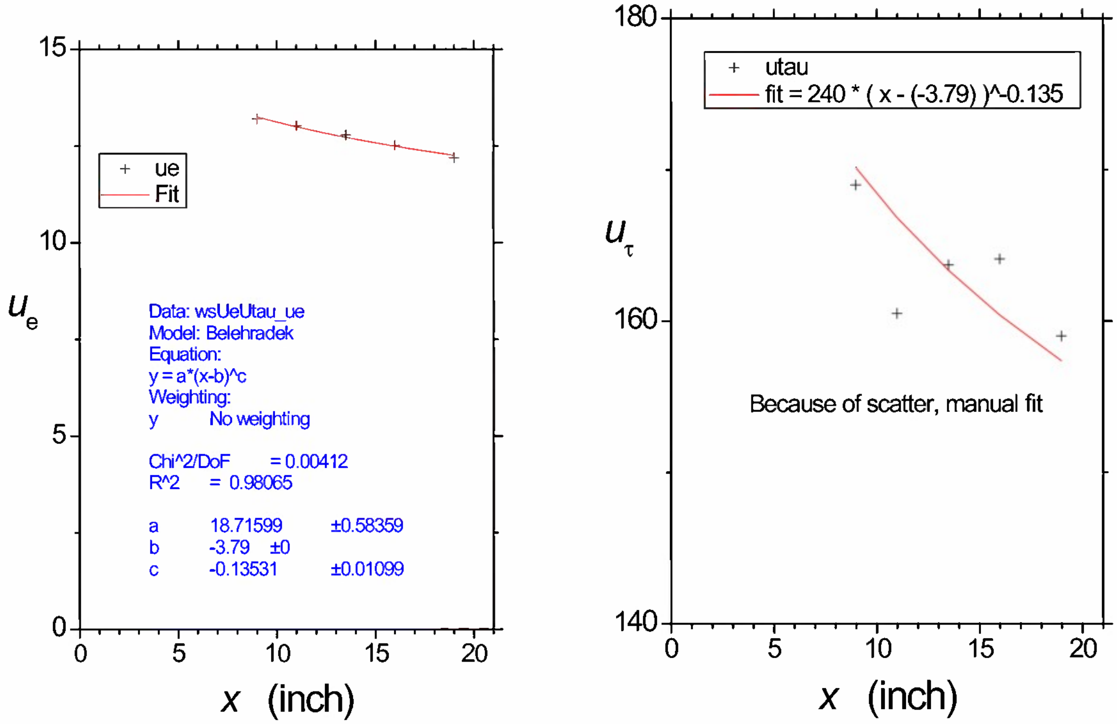

Elsberry, *et. al.* [11] data fits for five data sets designated as CASE A $(x - x_0)/\theta_0$ = 239, 264, 295, 325, and 326 by Elsberry, *et. al.*

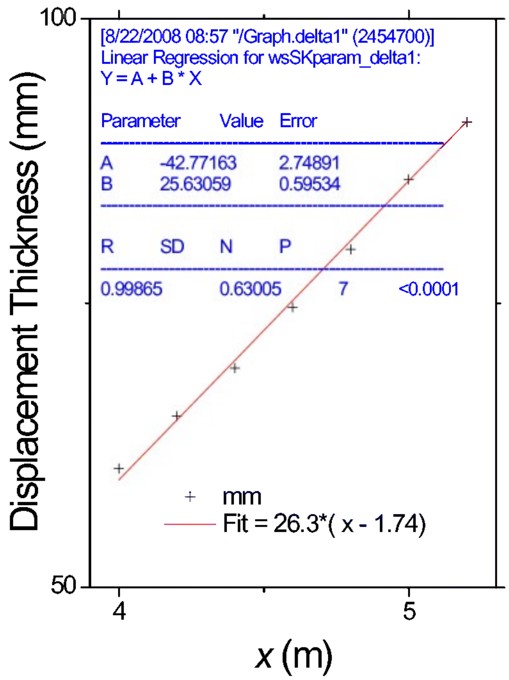

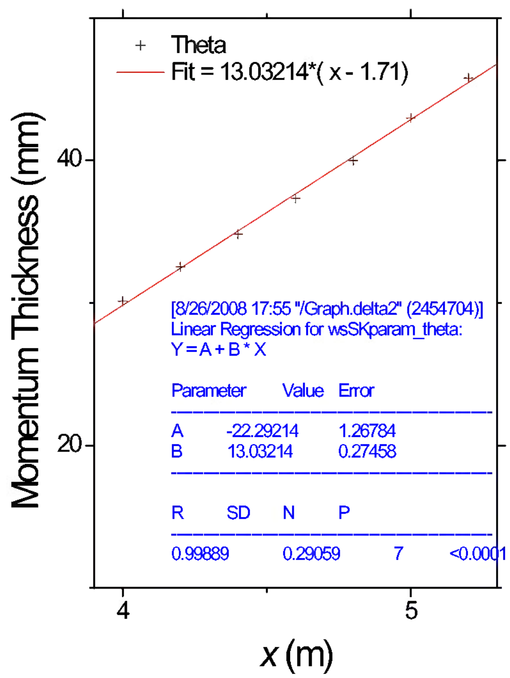

Skåre and Krogstad [12] data fits for seven data sets consisting of data at x=4.0, 4.2, 4.4, 4.6, 4.8, 5.0, and 5.2 m.

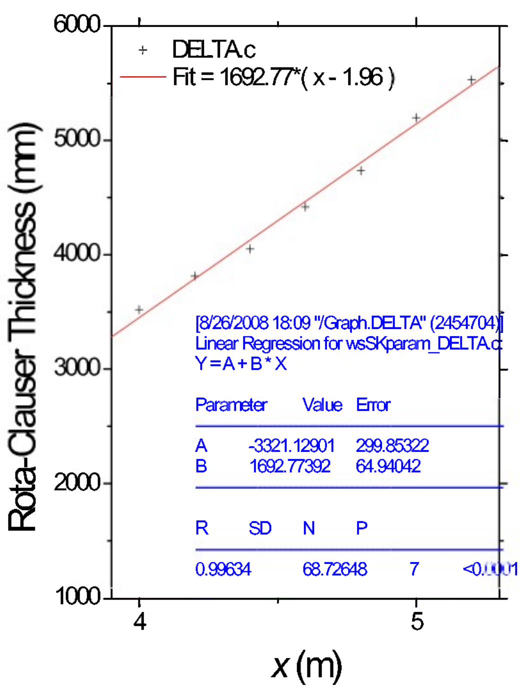

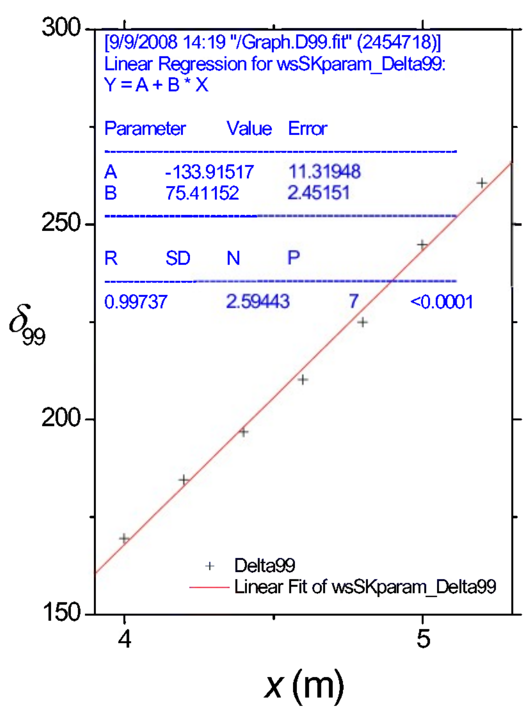

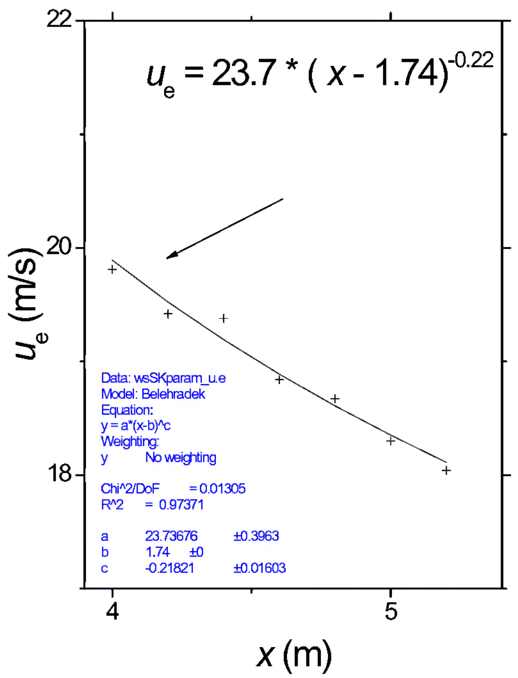

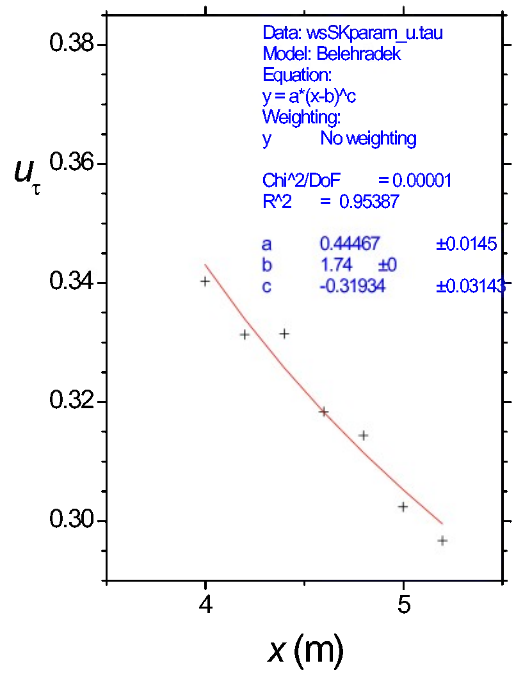

Skåre and Krogstad [12] data fits for seven data sets consisting of data at x=4.0, 4.2, 4.4, 4.6, 4.8, 5.0, and 5.2 m.

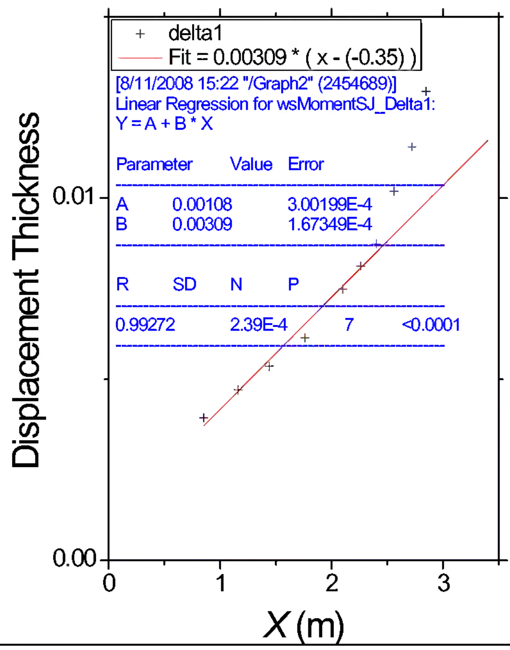

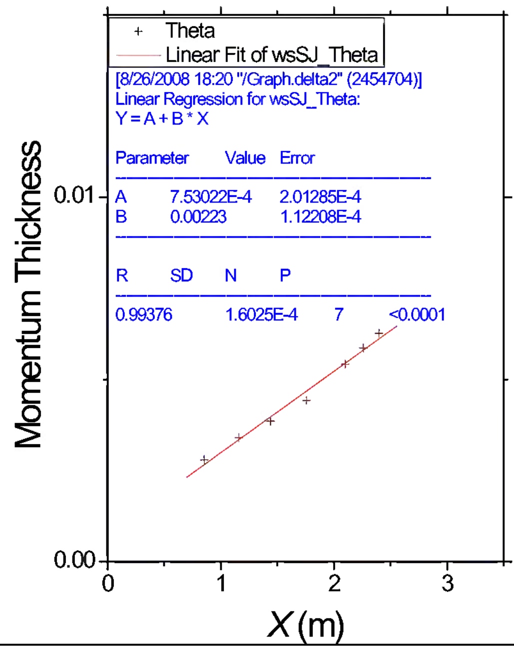

Samuel and Joubert [19] fits to seven profiles taken at x= 0.855, 1.16, 1.44, 1.76, 2.1, 2.26, and 2.4 m. The five other data sets that do not fit to the fitting lines do not show similarity.

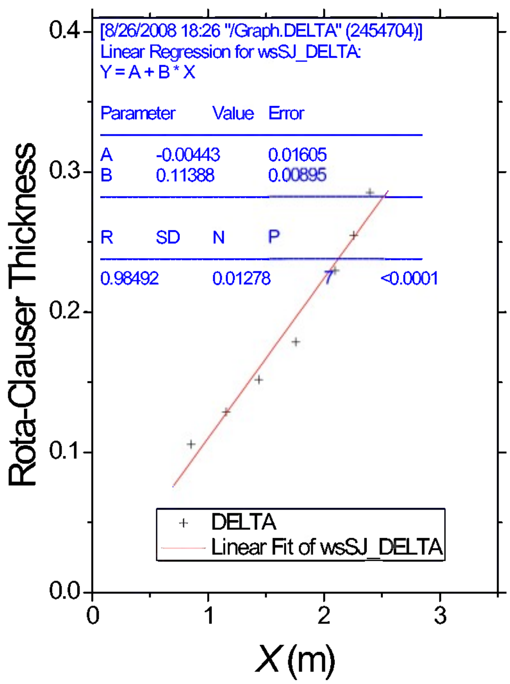

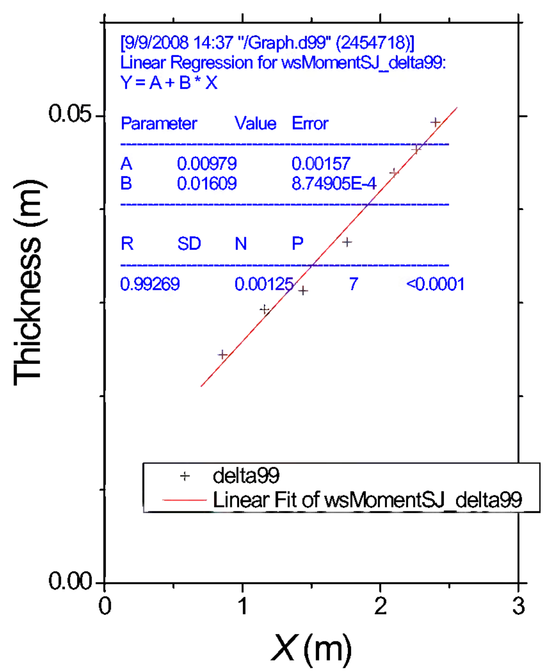

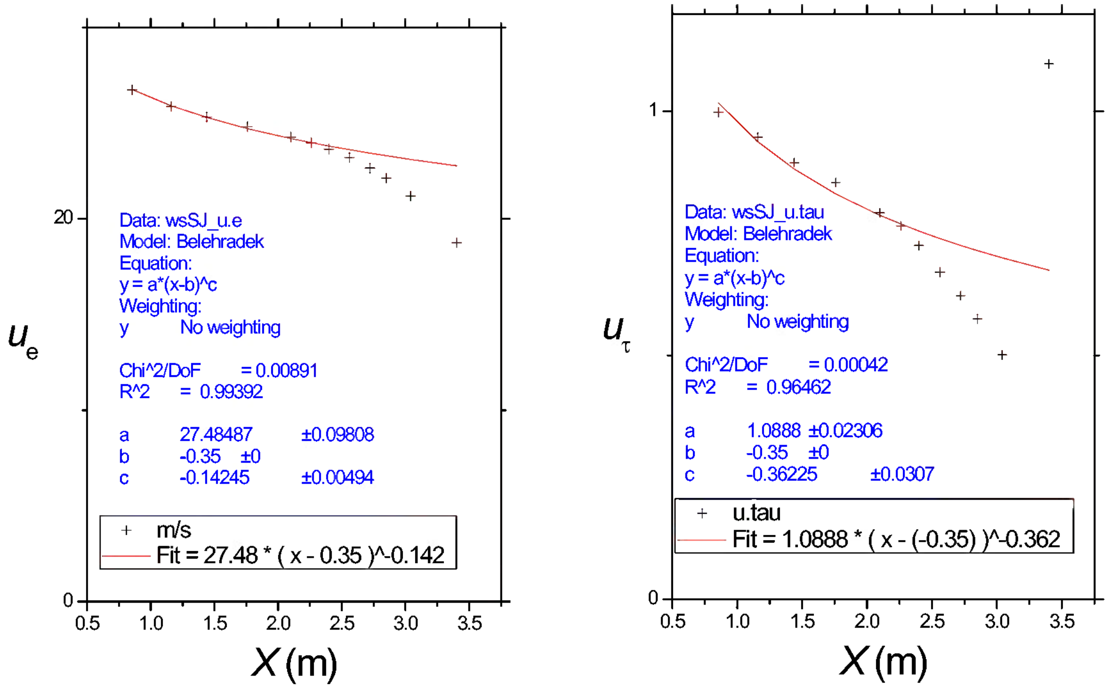

Samuel and Joubert [19] fits to seven profiles taken at x= 0.855, 1.16, 1.44, 1.76, 2.1, 2.26, and 2.4 m. The five other data sets that do not fit to the fitting lines do not show similarity.

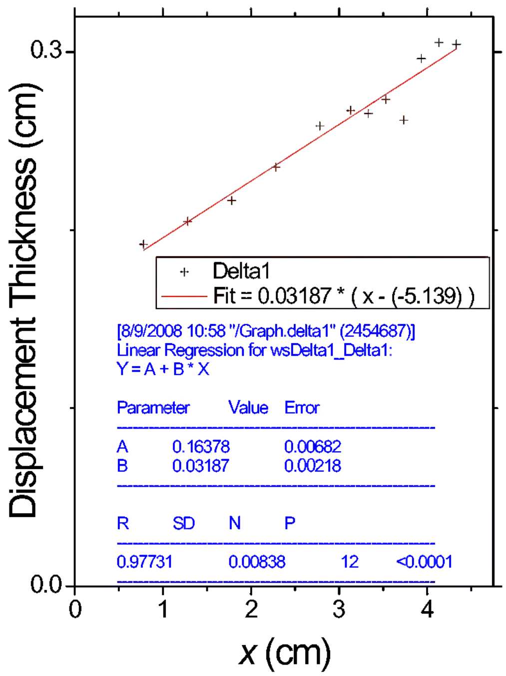

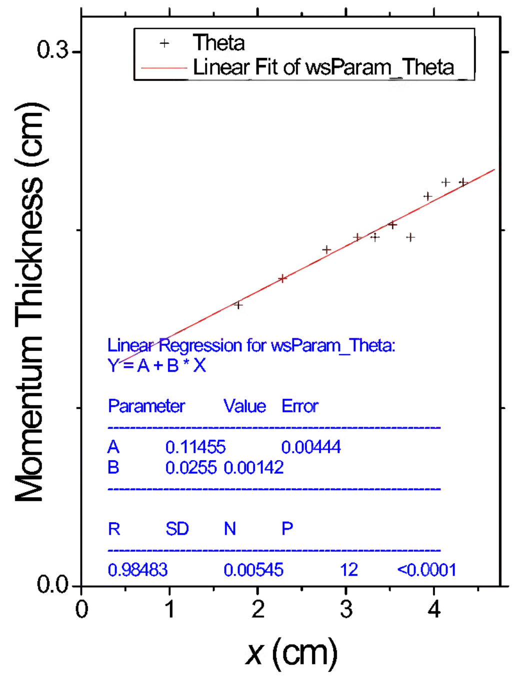

Ludwieg and Tillmann [17] fits to ten profiles taken at Re_{θ} = 1602, 2008, 2480, 2806, 2914, 3119, 3203, 3666, 3888 and 4062.

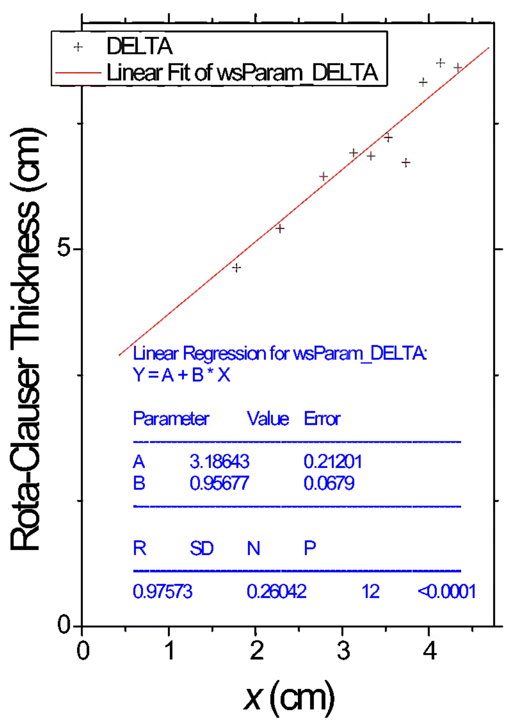

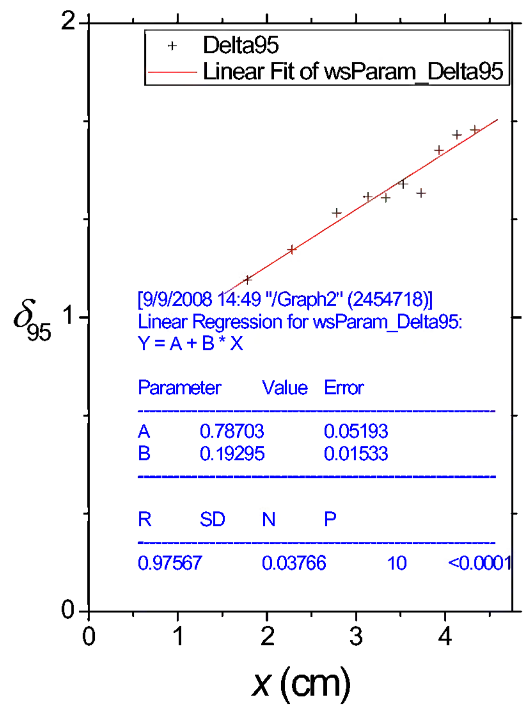

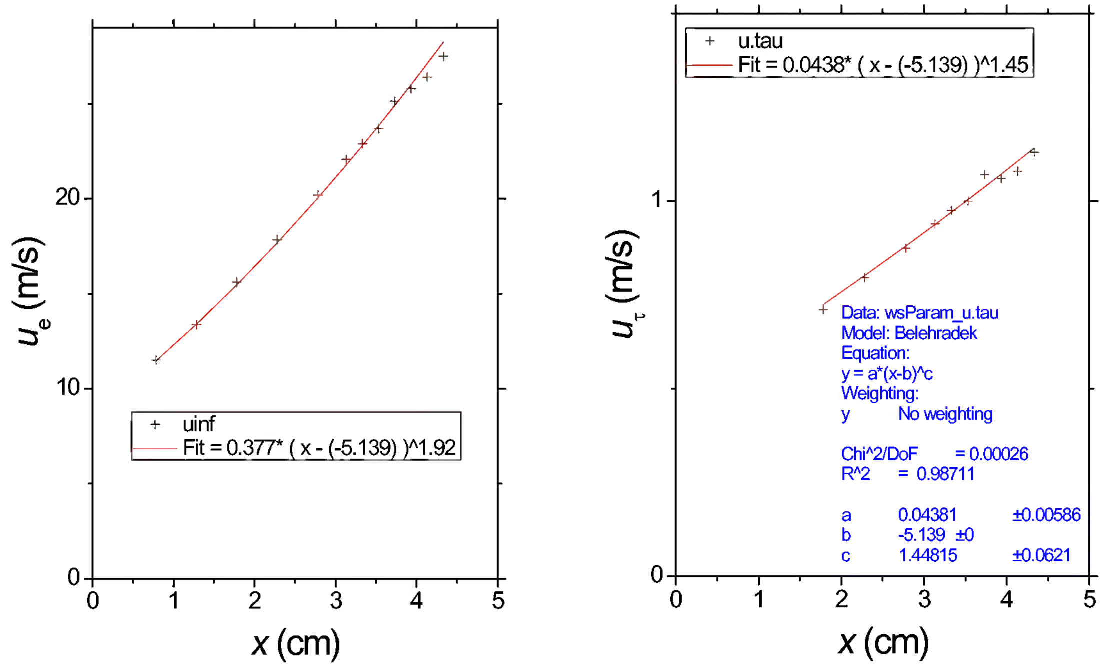

Ludwieg and Tillmann [17] fits to twelve profiles taken at $Re_\theta = 1602, 2008,$ 2480, 2806, 2914, 3119, 3203, 3666, 3888 and 4062.

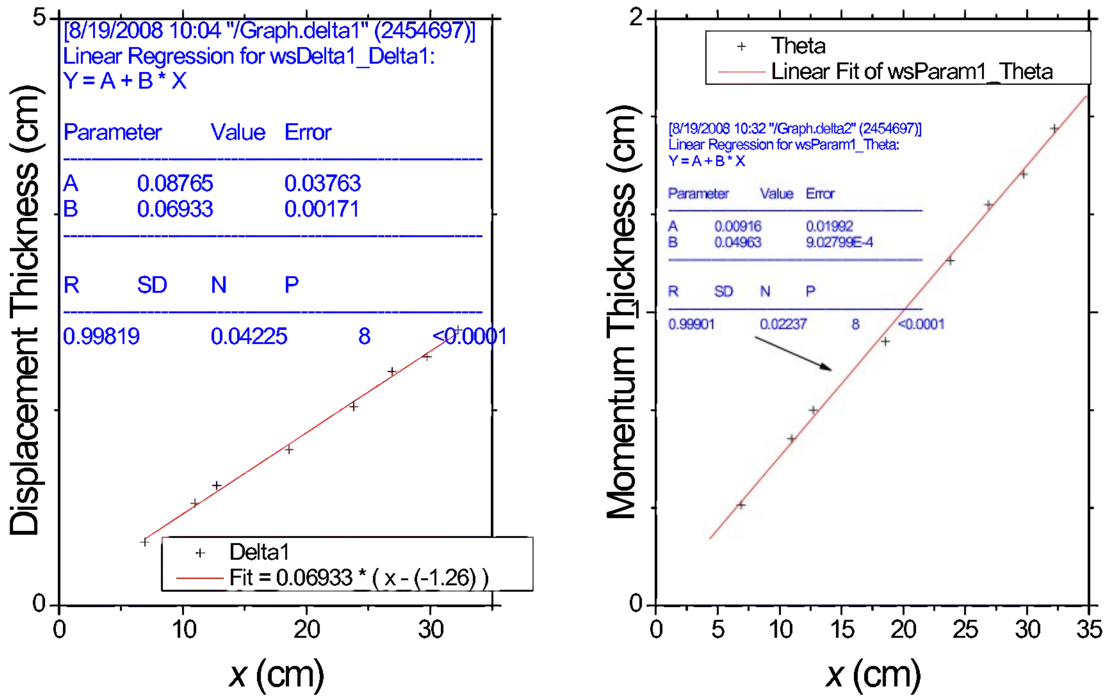

Clauser [1] fits to eight profiles designated Set 1 by Clauser.

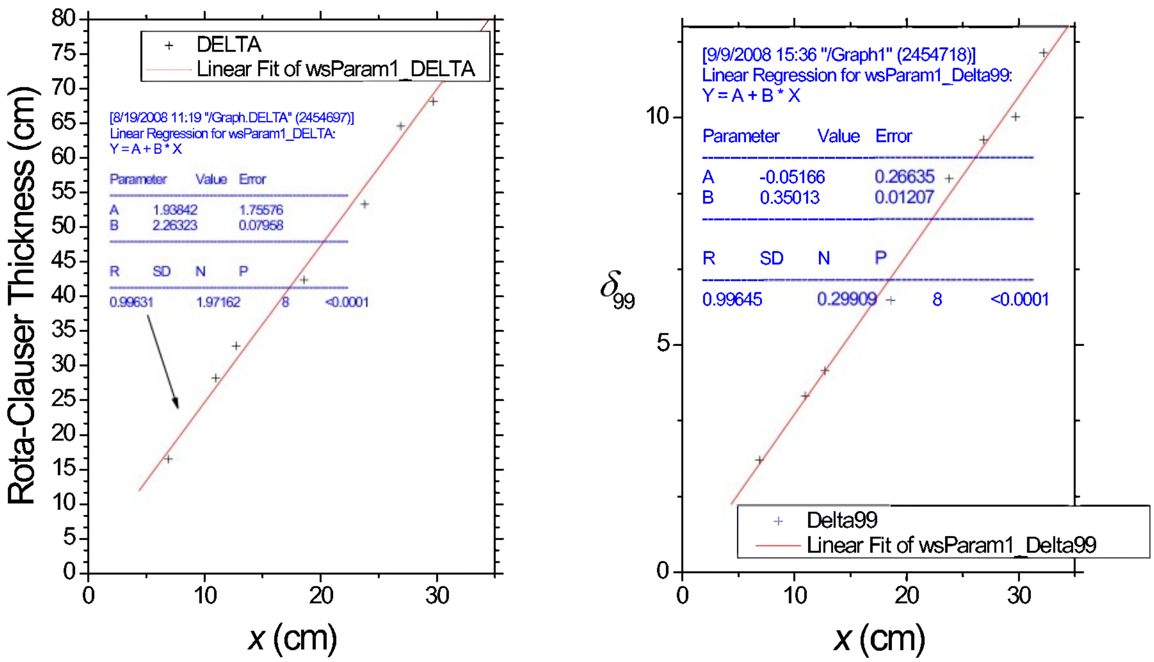

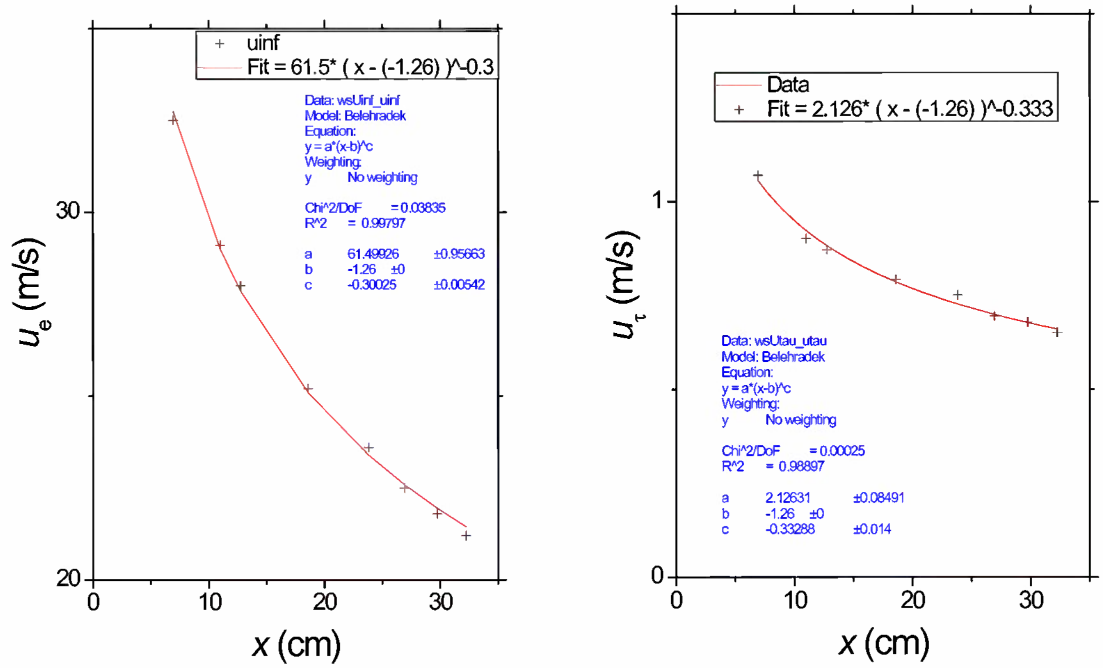

Clauser [1] fits to eight profiles designated Set 1 by Clauser.

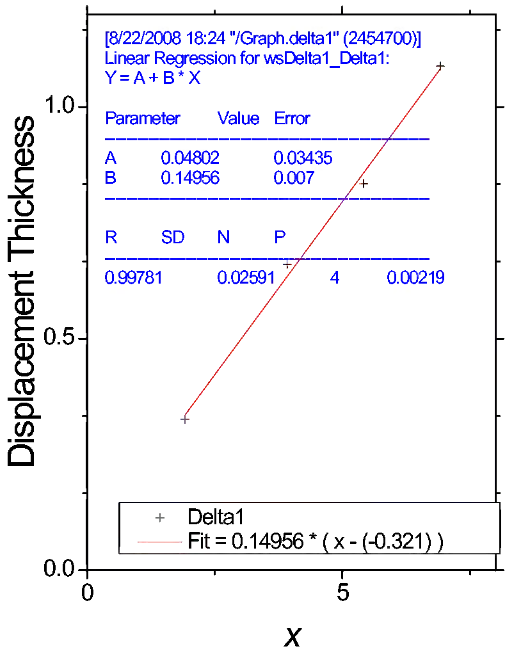

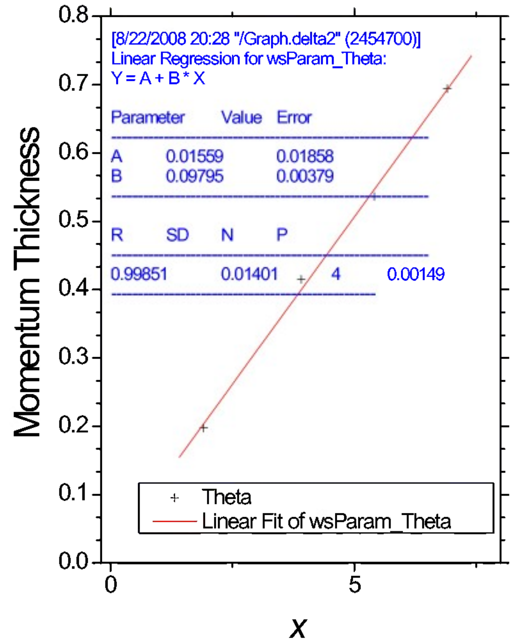

Bradshaw and Ferriss [18] data set; fits to four profiles designated Ident 2600.

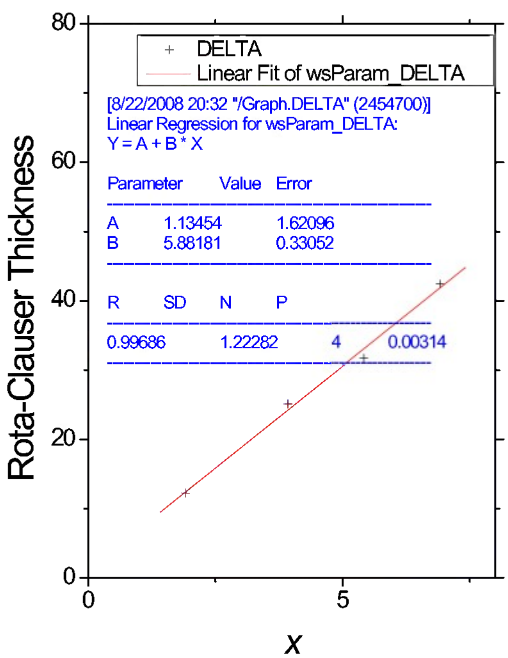

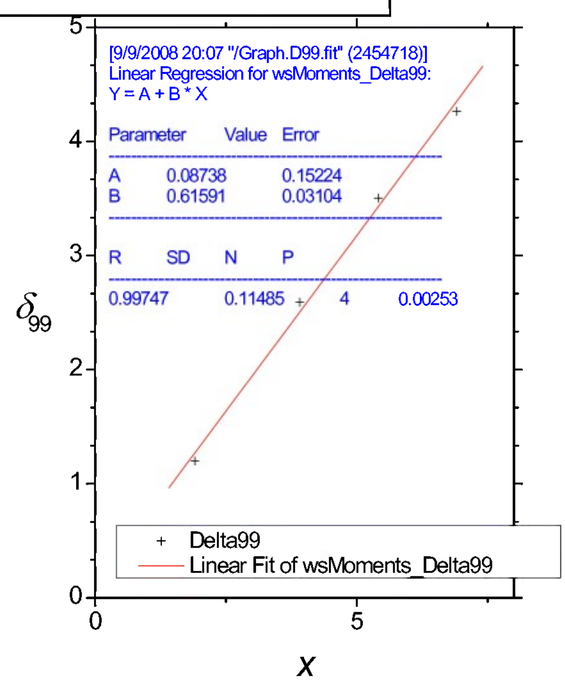

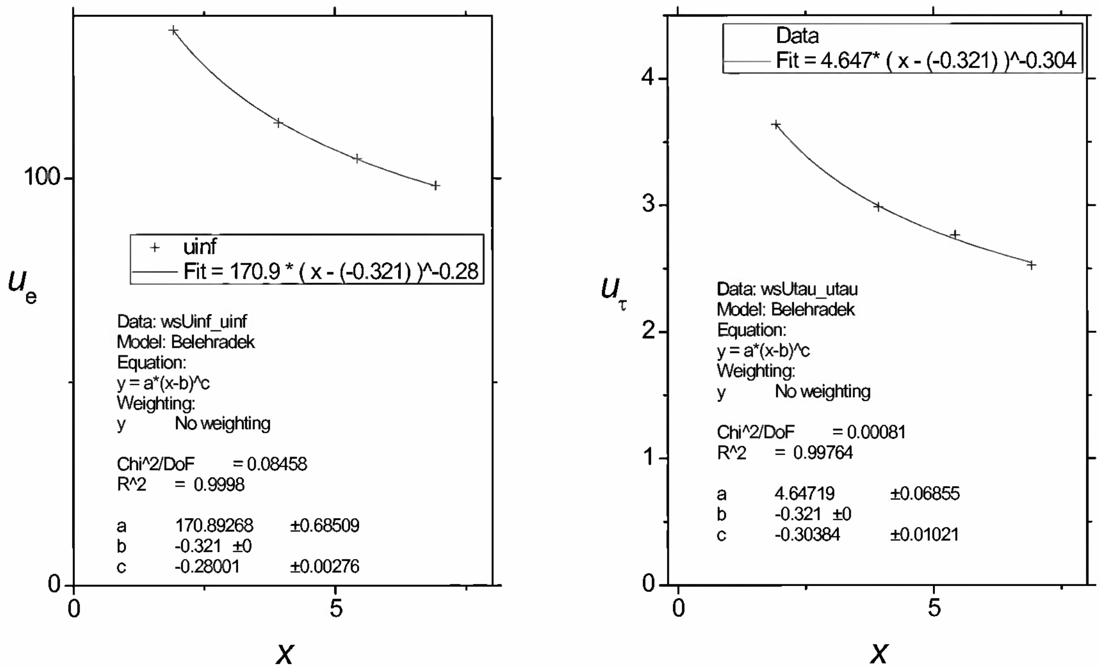

Bradshaw and Ferriss [18] data set; fits to four profiles designated Ident 2600.

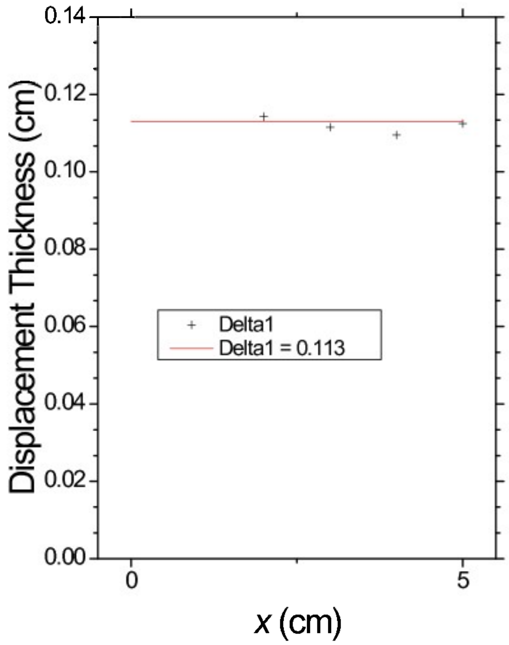

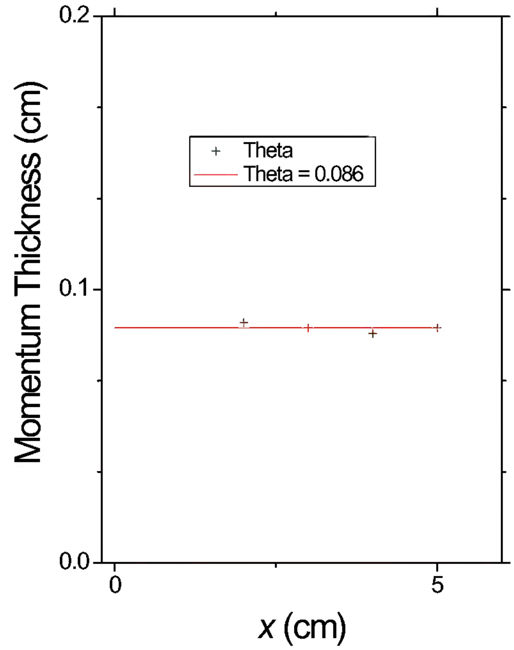

Herring and Norbury [10] data set; fits to four profiles of six designated Ident 2700.

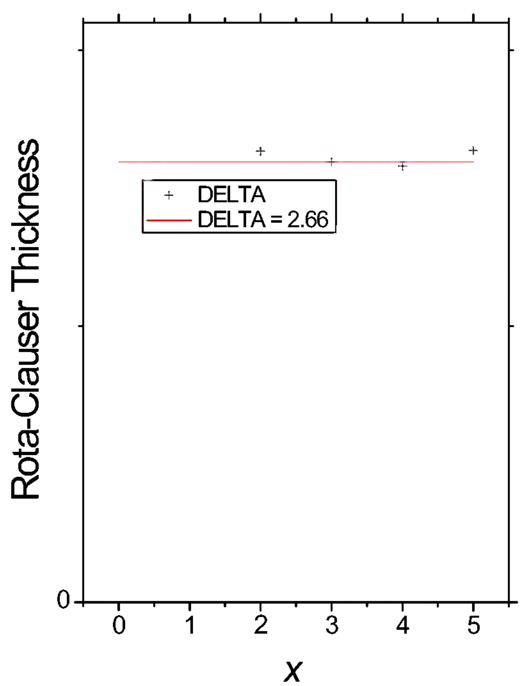

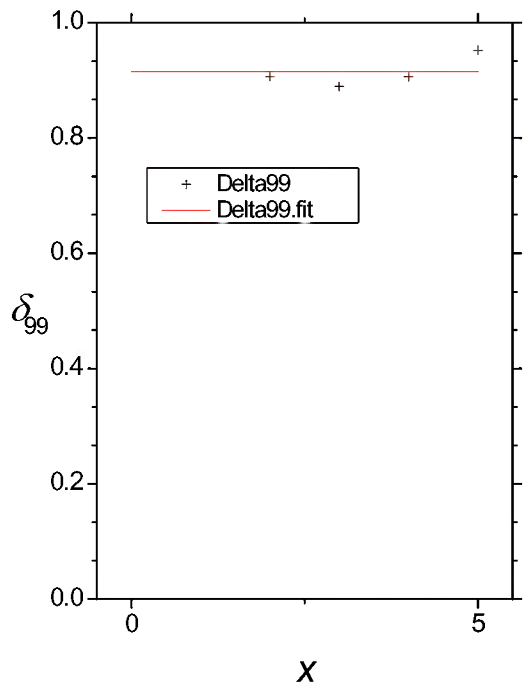

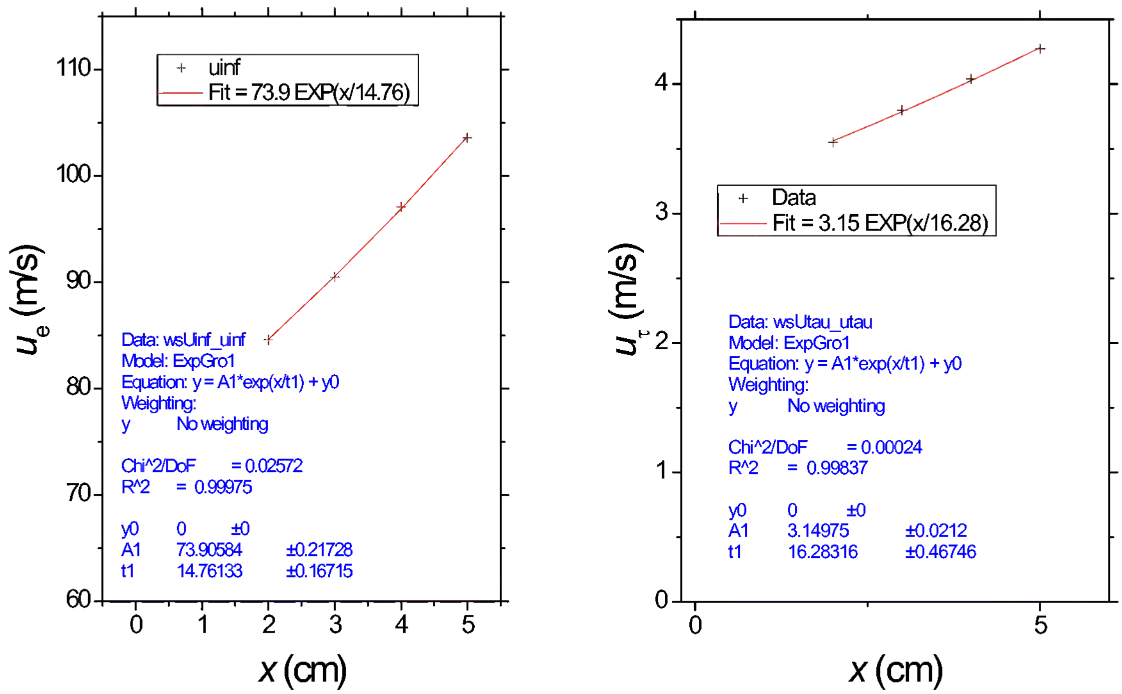

Herring and Norbury [10] data set; fits to four profiles of six designated Ident 2700.

Appendix B: Velocity Profile Scale Comparisons

The following plots are support data for the Technical Report entitled "Similarity Scaling of the Outer Region of the Turbulent Boundary Layer", by David W. Weyburne. The plots are compiled to show the velocity profiles plotted using the length scales δ_1, Δ, δ_2, and δ_{99} for the datasets considered for the paper. The velocity scaling variables tested are u_e, u_τ, and u_{ZS} where u_{ZS} is the Zagarola and Smits velocity. Also note that $u^+ = u(y)/u_\tau$. The plots are provided for visual verification of the claims made in the main body of the Report. They are not identified with Figure numbers but rather as the ensemble of plots as Appendix B.

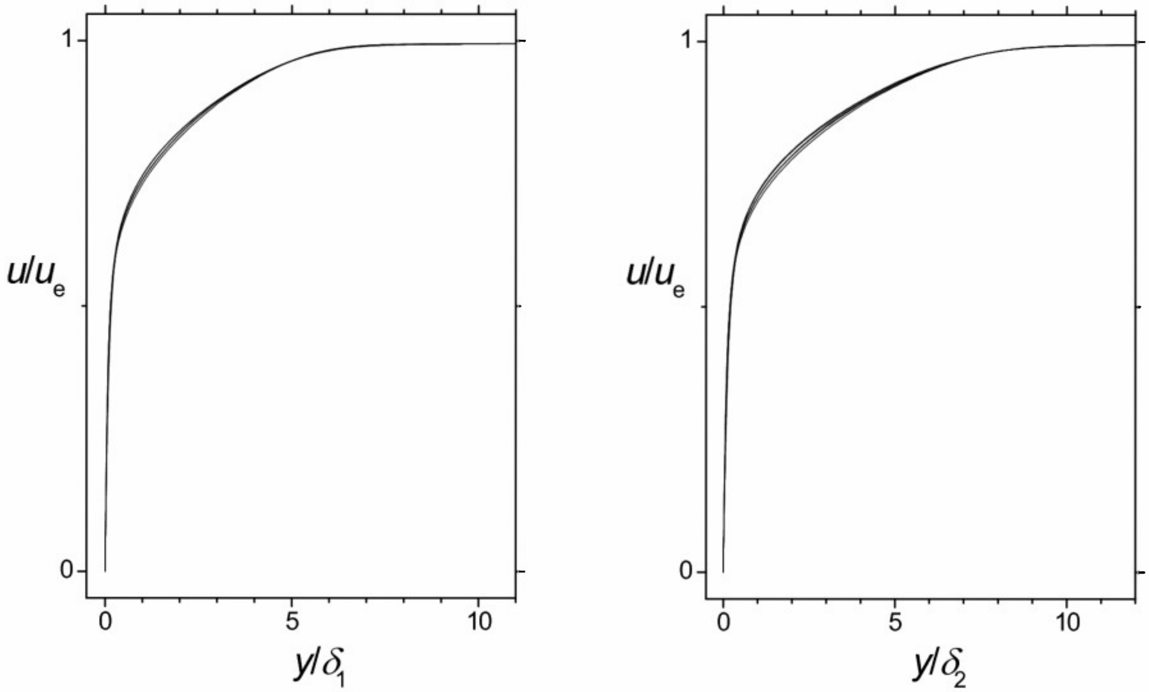

Khujadze and Oberlack [13] five Velocity Profiles for Re_θ = 1850, 2088, 2333, 2569, and 2807.

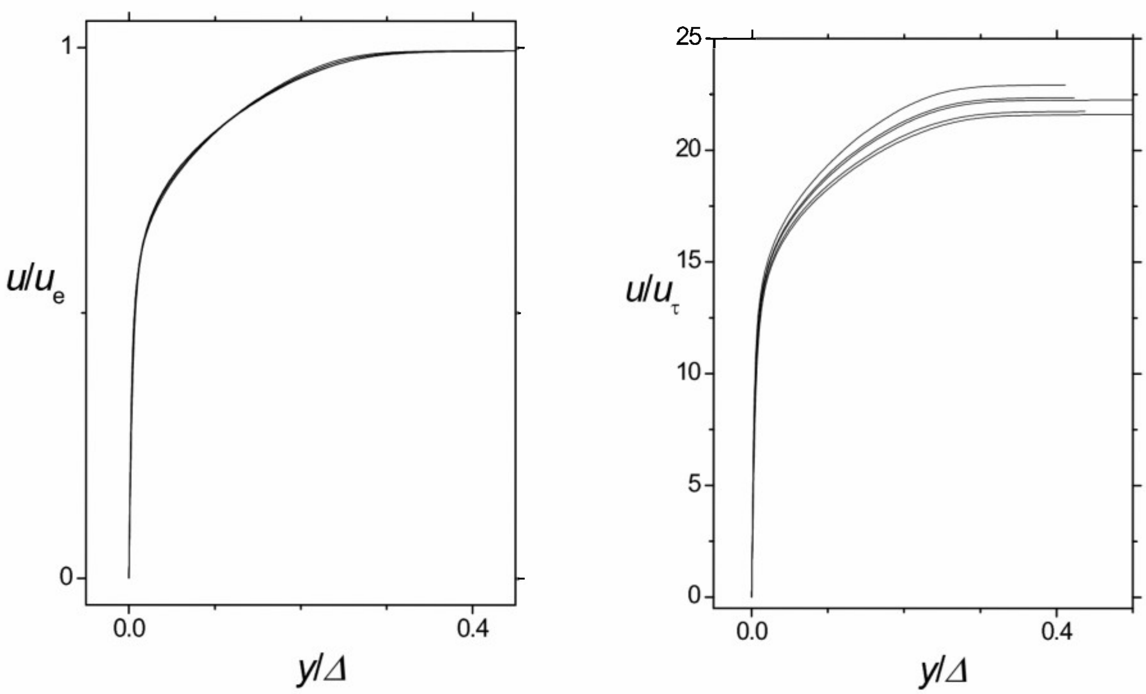

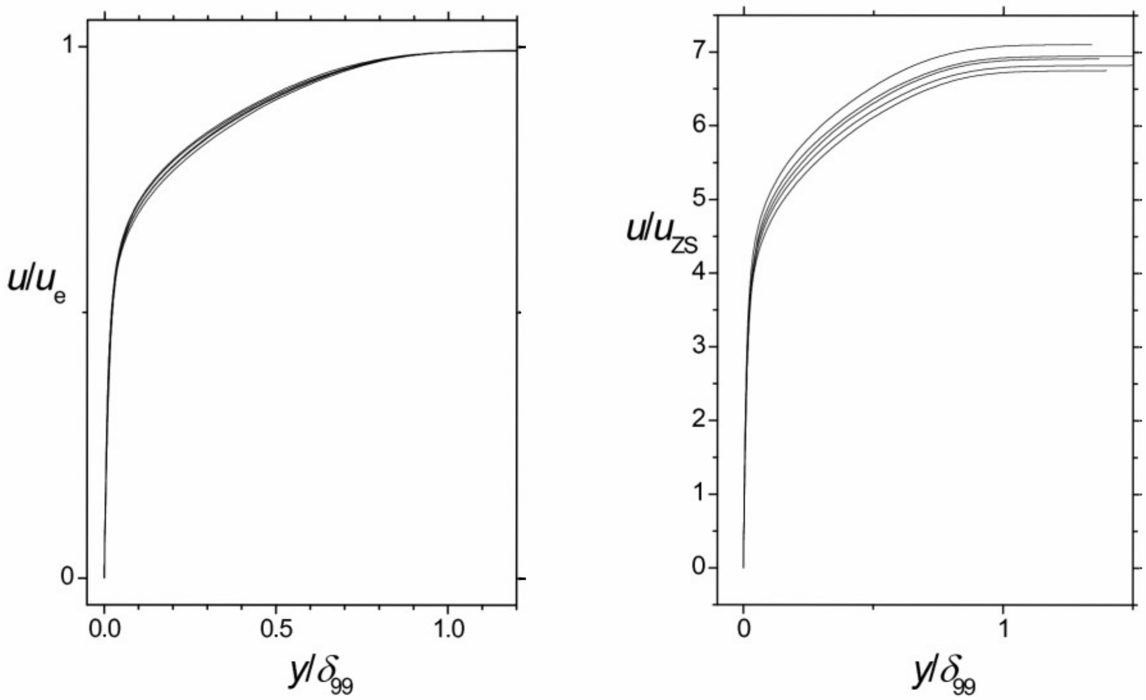

Khujadze and Oberlack [13] five Velocity Profiles for Re_θ = 1850, 2088, 2333, 2569, and 2807.

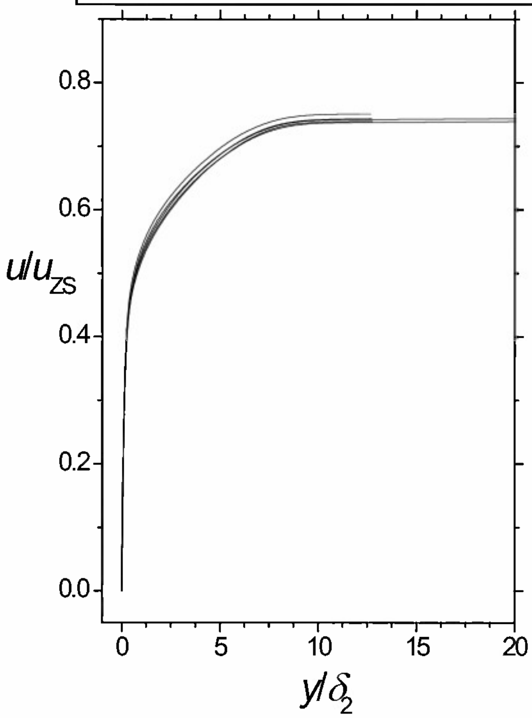

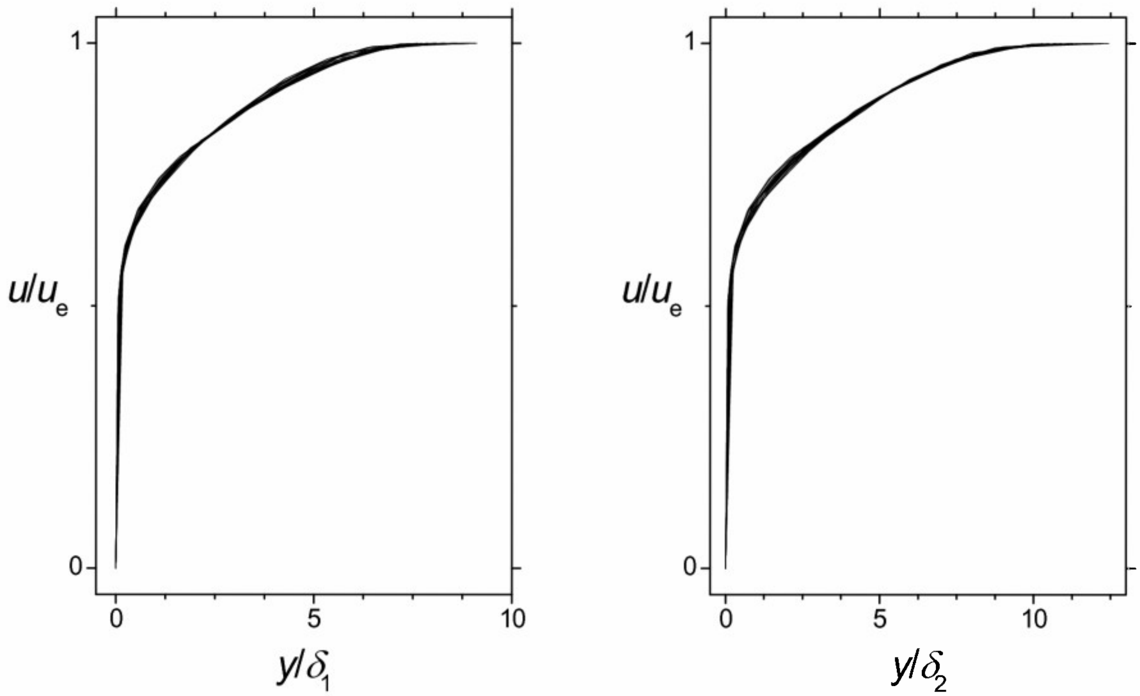

Wieghardt & Tillmann [14] data profiles for Re_θ = 4387, 4858, 5473, 6229, 7170, 8172, 8897, 9815, 10611, 11472, 12223,13043, 14024, 14703, and 15518.

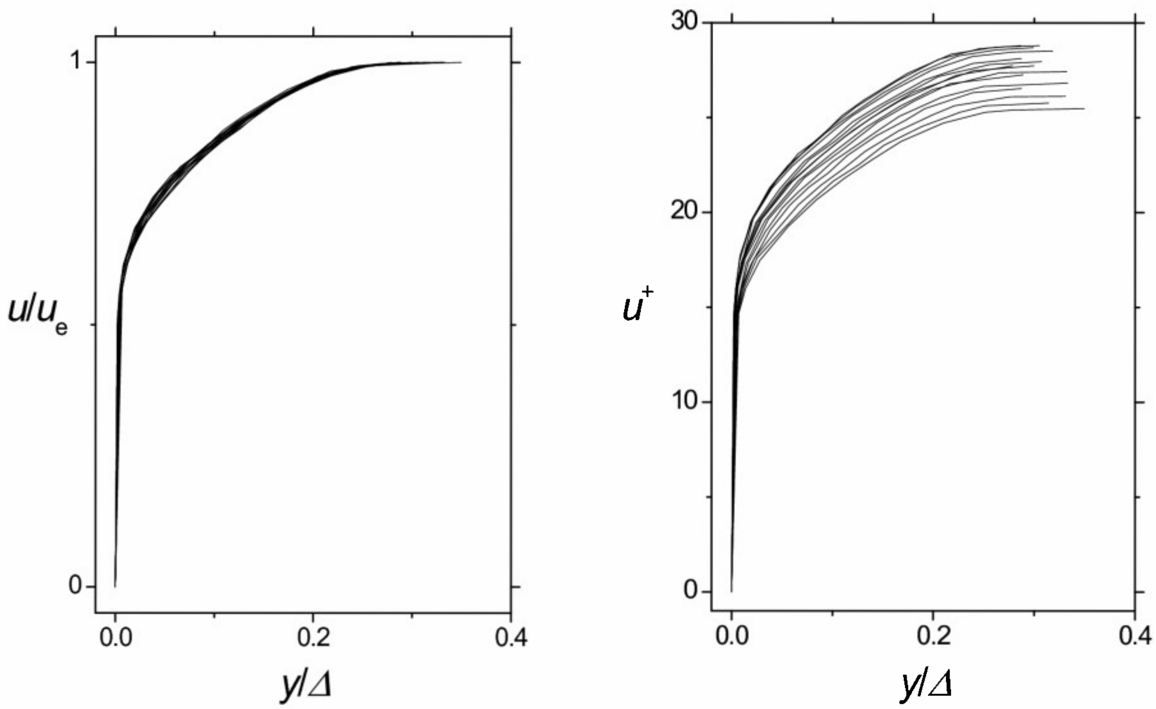

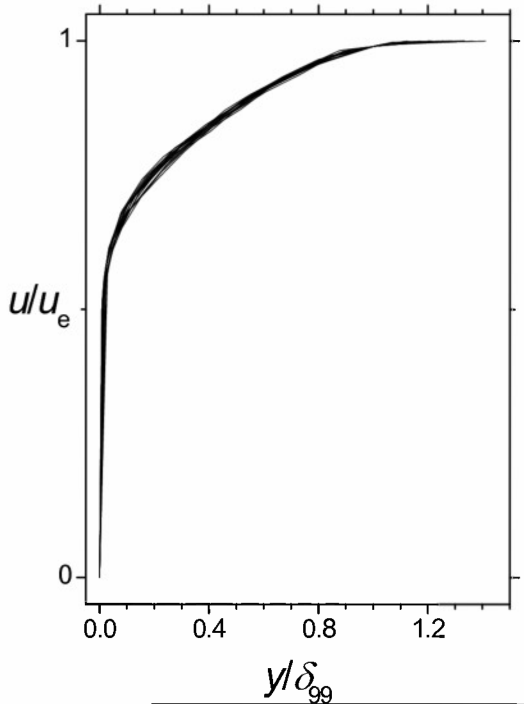

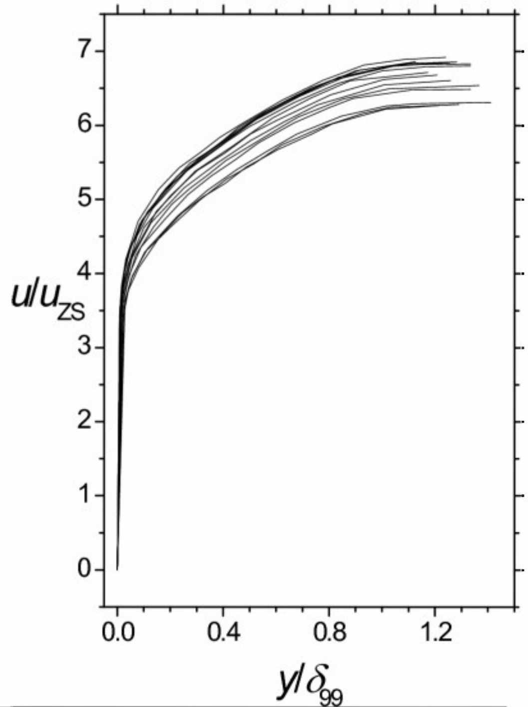

Wieghardt & Tillmann [14] data profiles for Re_θ = 4387, 4858, 5473, 6229, 7170, 8172, 8897, 9815, 10611, 11472, 12223,13043, 14024, 14703, and 15518.

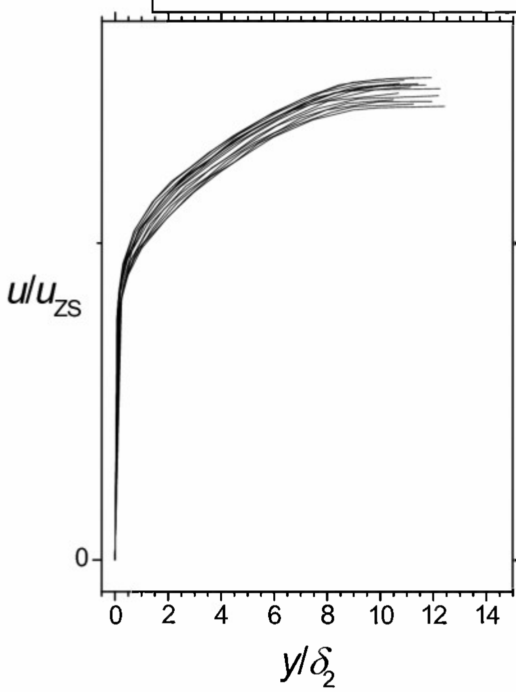

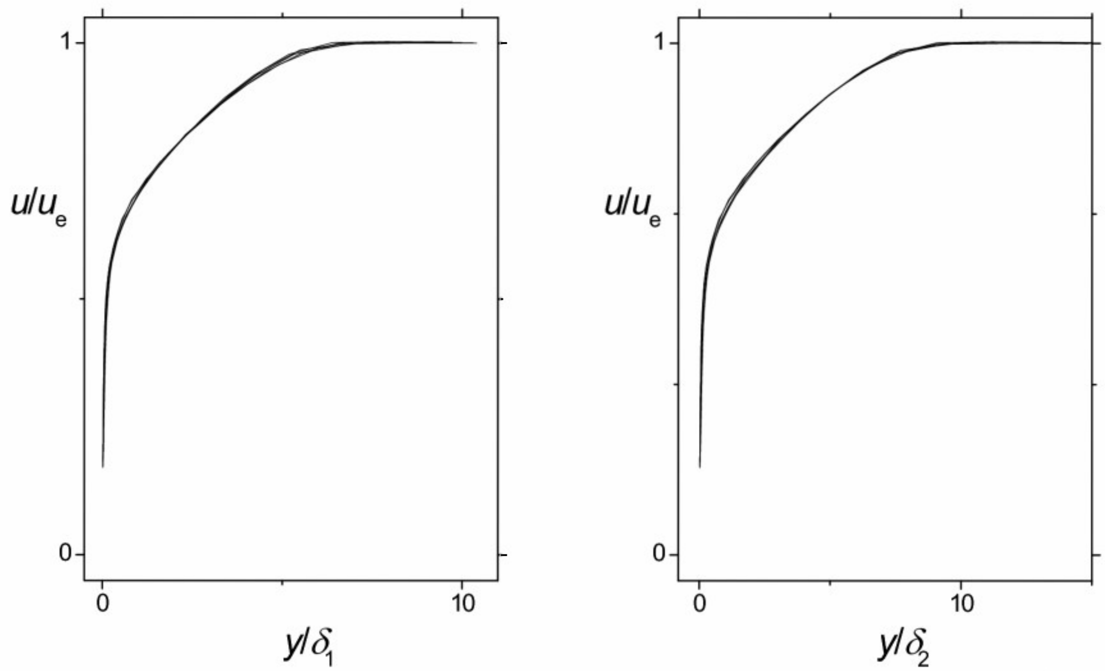

Österlund [16] velocity profiles for $u_e \cong 10.3$ m/s consisting of SW981129A, SW981128A, SW981127H, SW981126C, and SW981112A data sets.

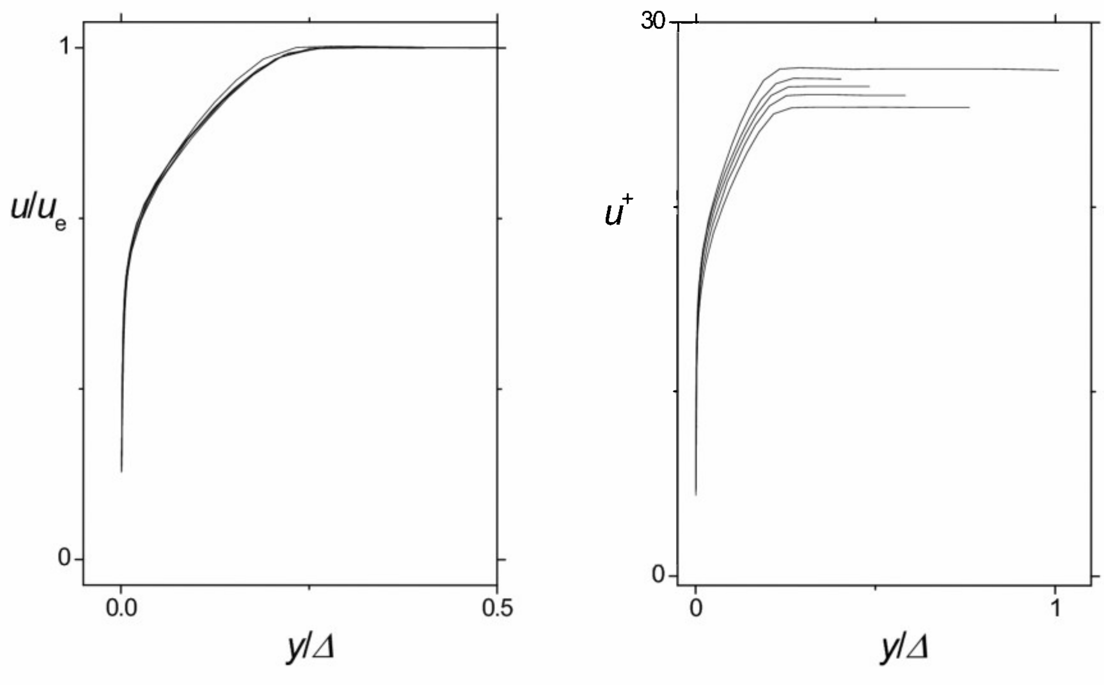

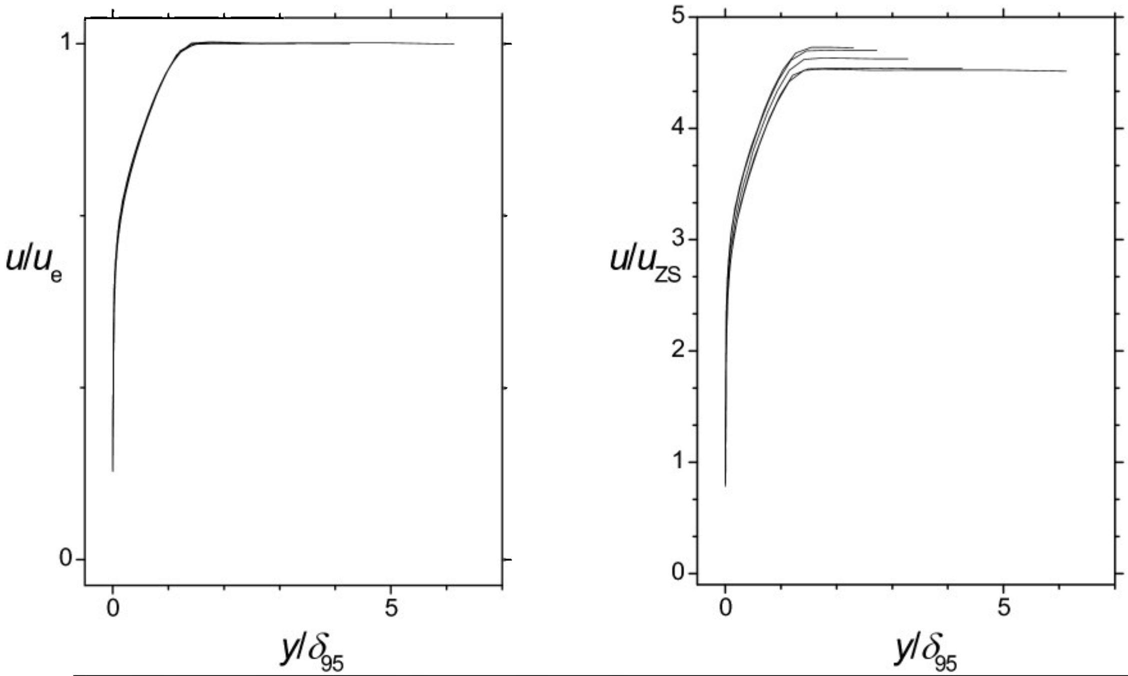

Österlund [16] velocity profiles for $u_e \cong 10.3$ m/s consisting of SW981129A, SW981128A, SW981127H, SW981126C, and SW981112A data sets.

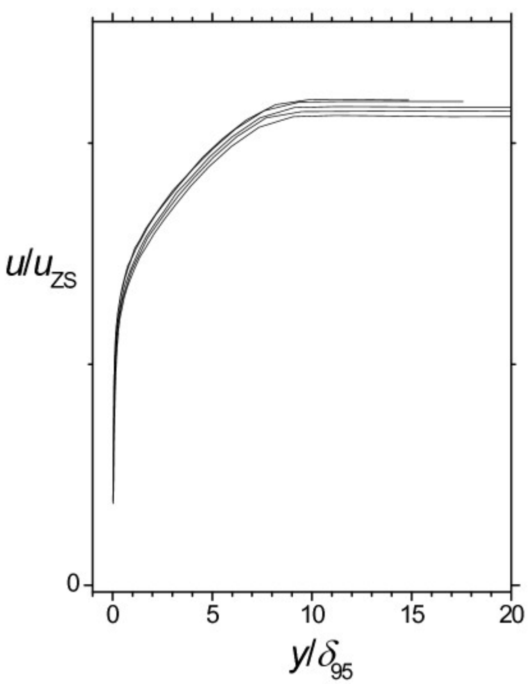

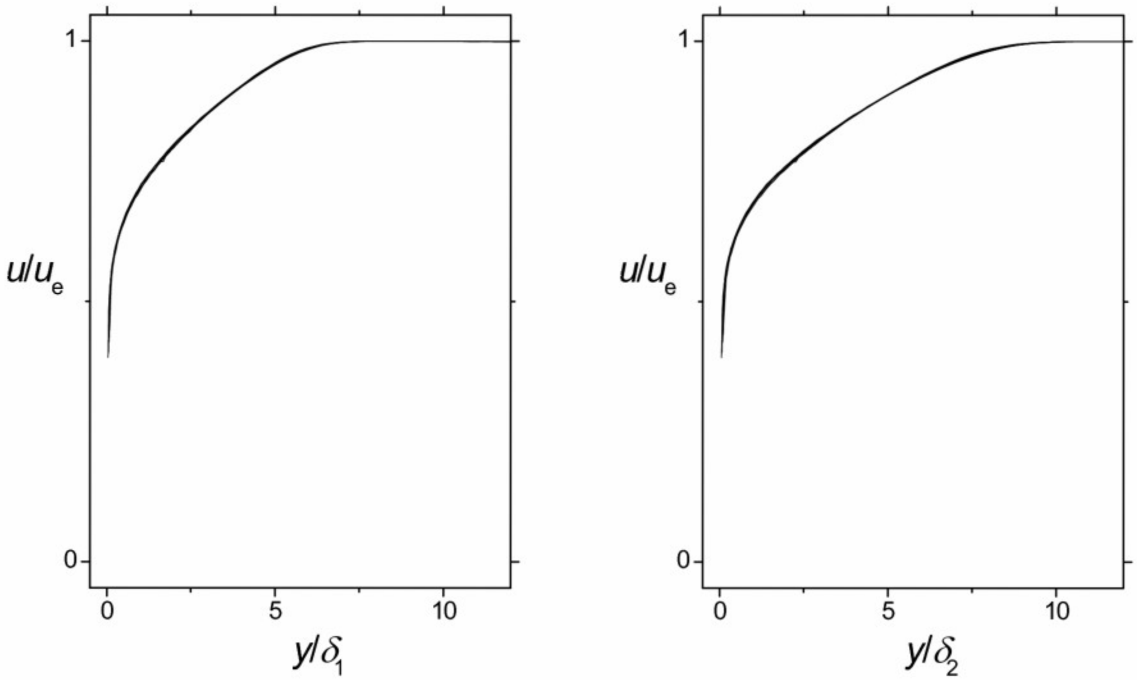

Smith [15] data fits for seven data sets consisting of Re_{θ} =4601, 4980, 5388, 5888, 6866, 7696, and 9148.

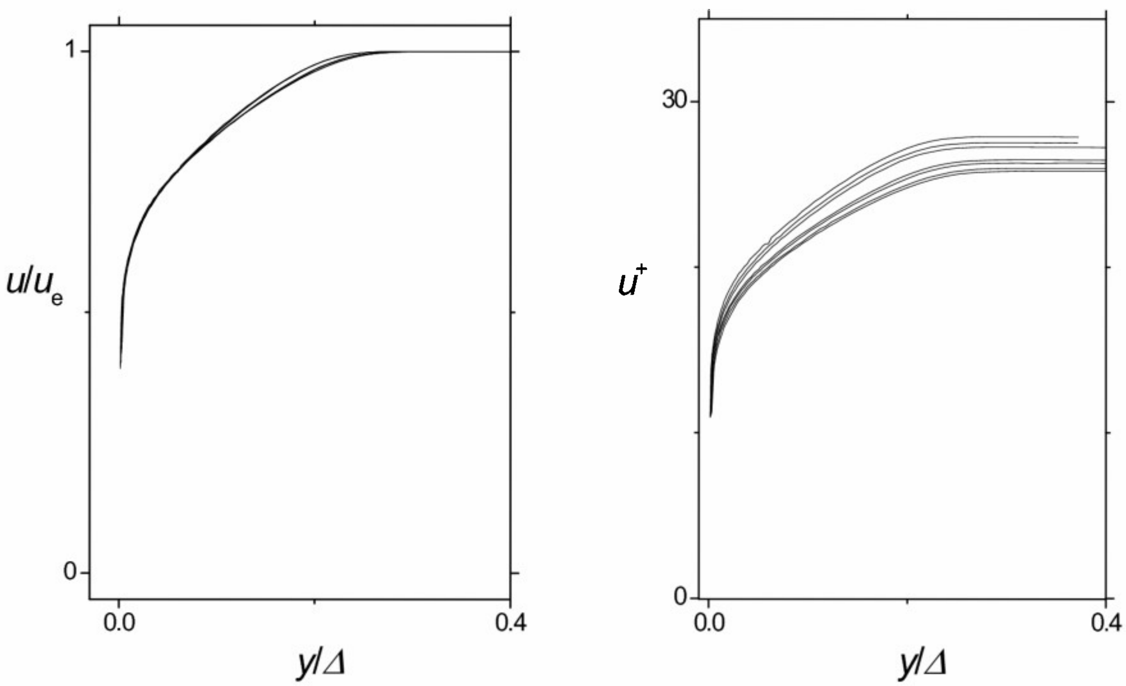

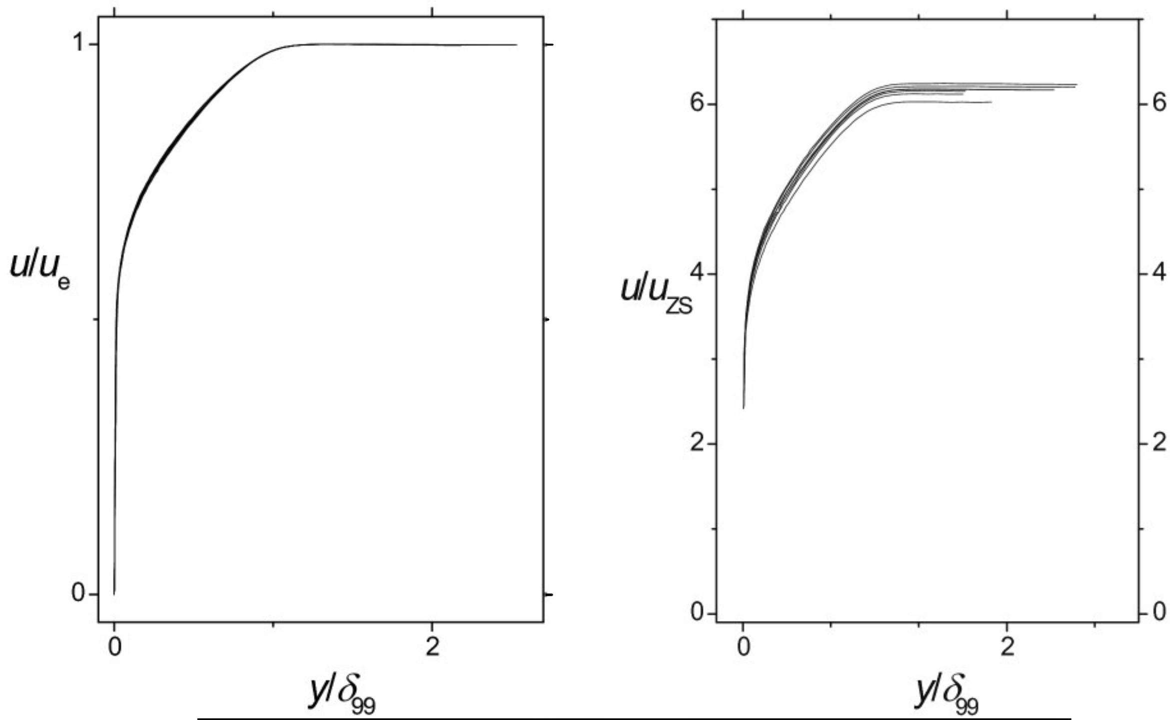

Smith [15] data fits for seven data sets consisting of Re_θ =4601, 4980, 5388, 5888, 6866, 7696, and 9148.

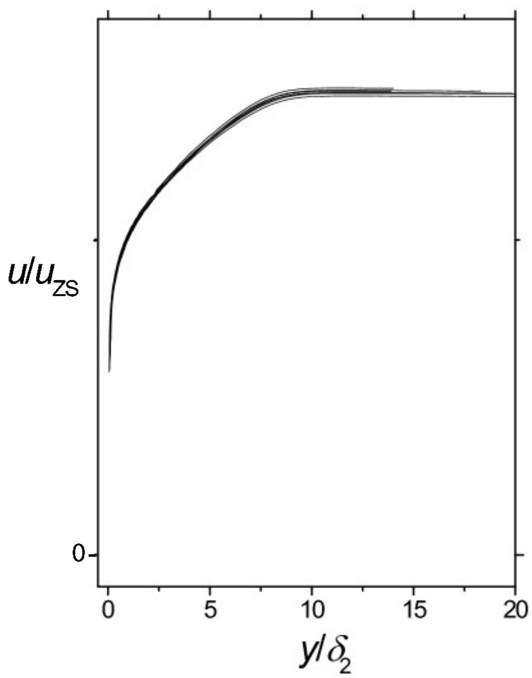

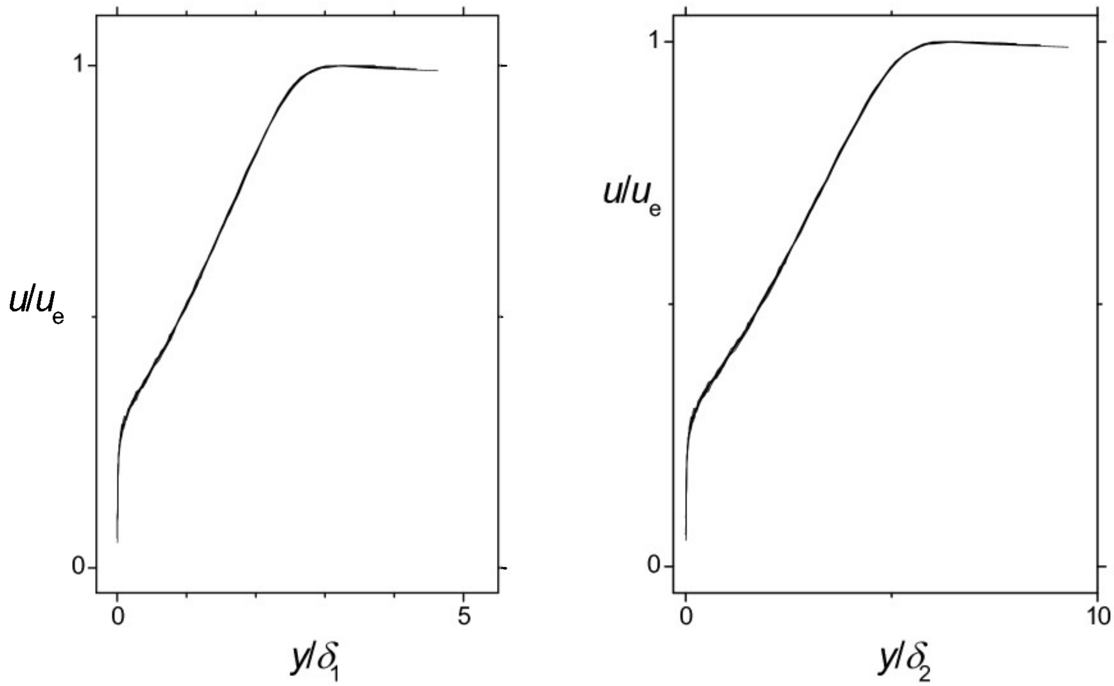

Skåre and Krogstad [12] seven Velocity Profile Plots taken at x=4.0, 4.2, 4.4, 4.6, 5.0, and 5.2 m.

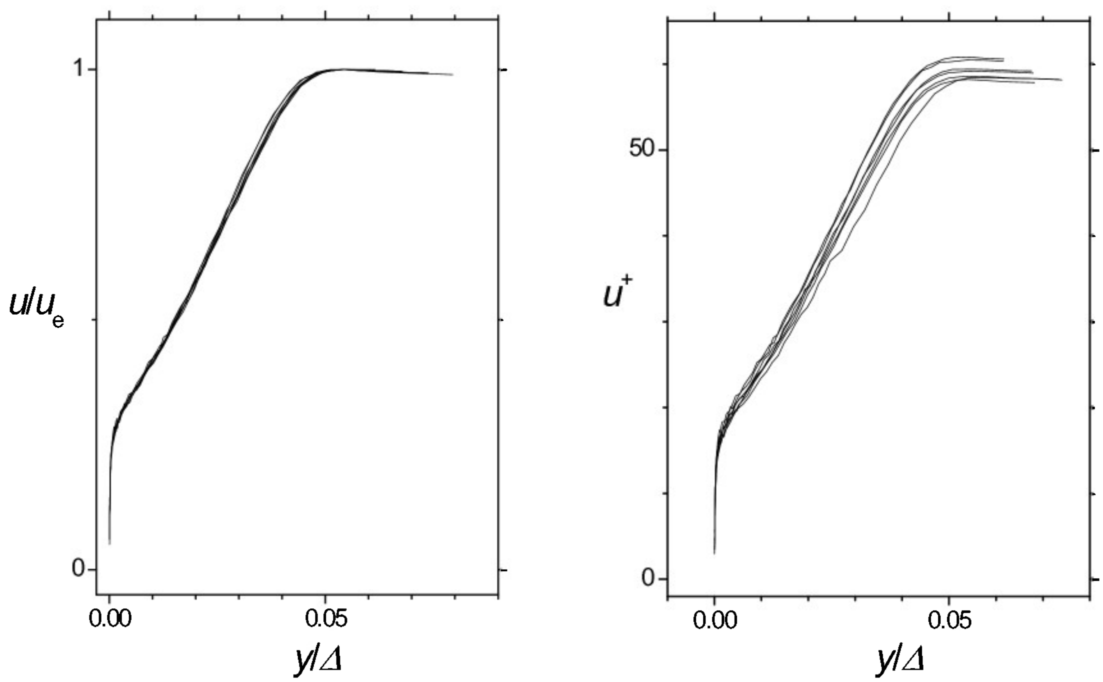

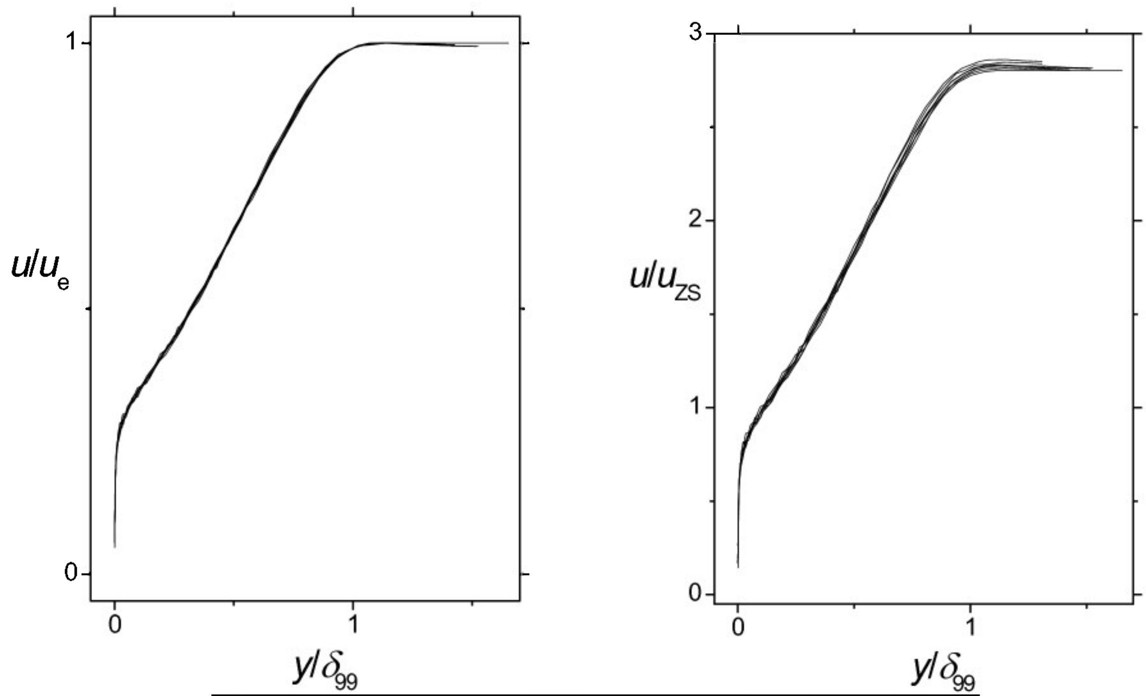

Skåre and Krogstad [12] seven Velocity Profile Plots taken at x=4.0, 4.2, 4.4, 4.6, 5.0, and 5.2 m.

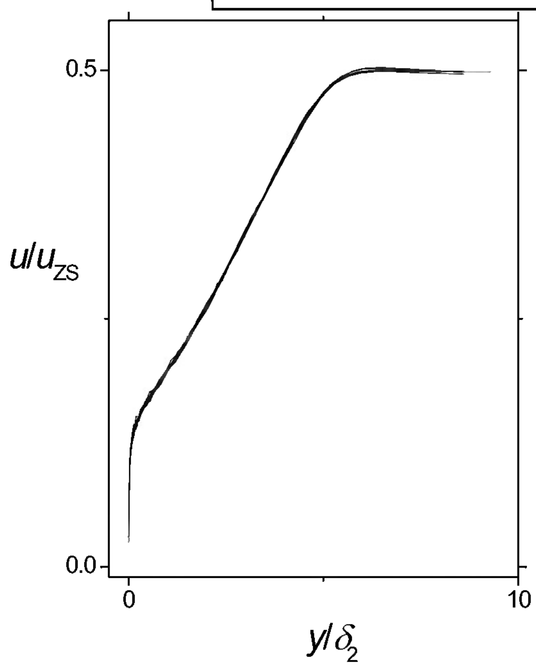

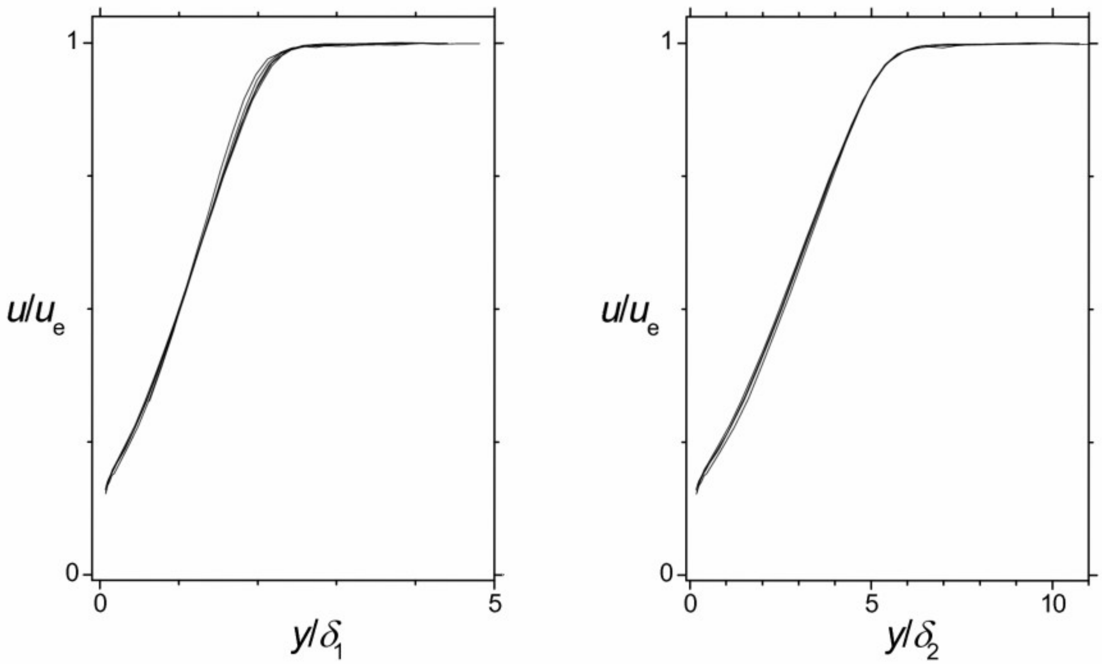

Elsberry, Loeffler, Zhou, & Wygnanski [11] five Velocity Profile Plots designated as Case A = 239, 264, 295, 325, and 362 by Elsberry, *et. al*.

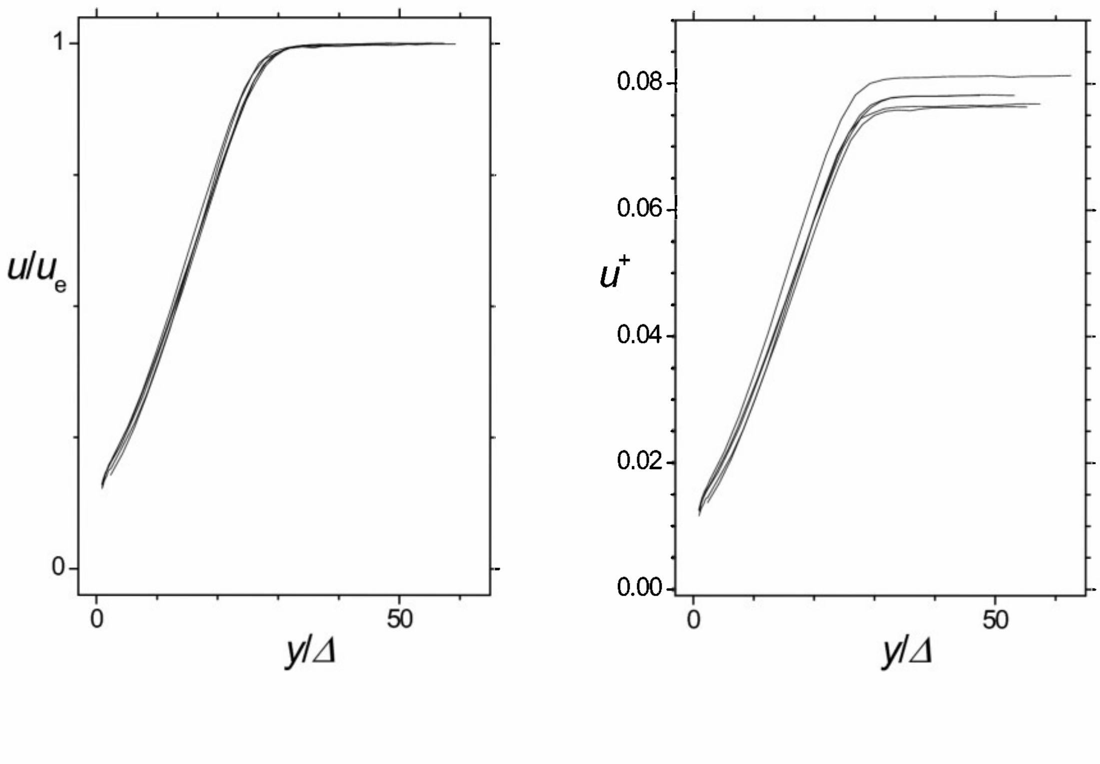

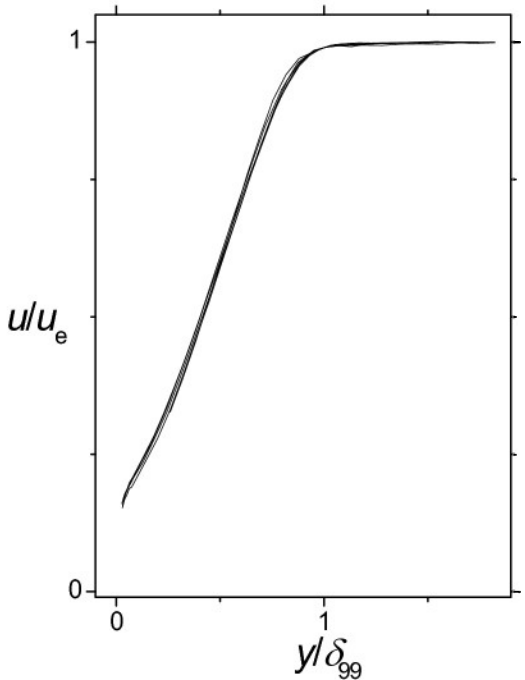

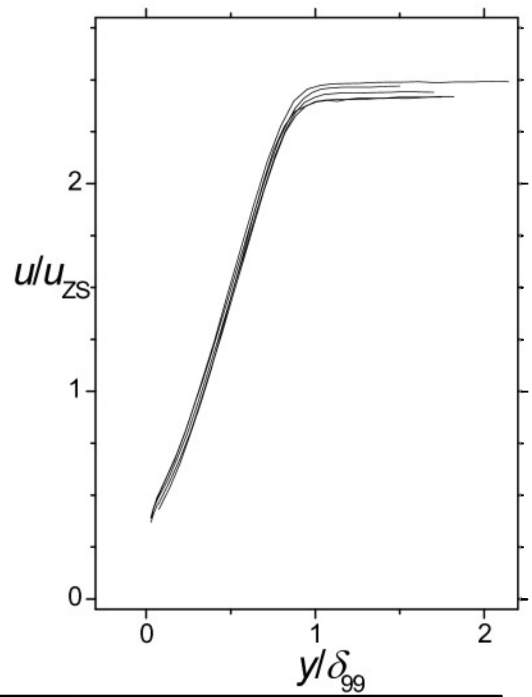

Elsberry, Loeffler, Zhou, & Wygnanski [11] five Velocity Profile Plots designated as Case A = 239, 264, 295, 325, and 362 by Elsberry, *et. al*.

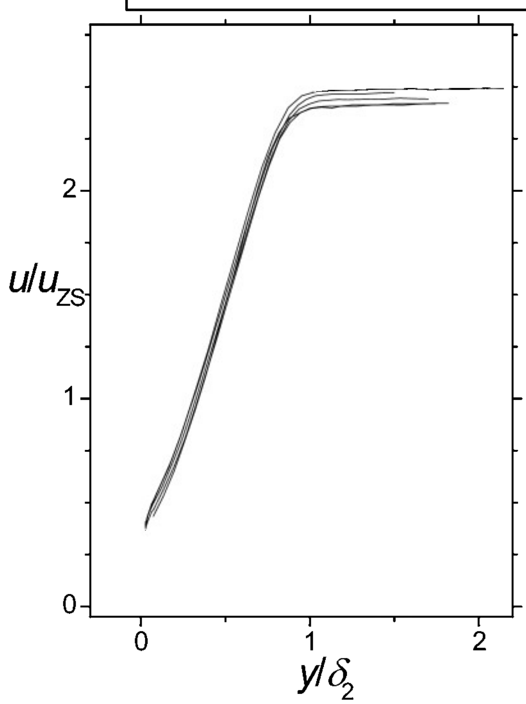

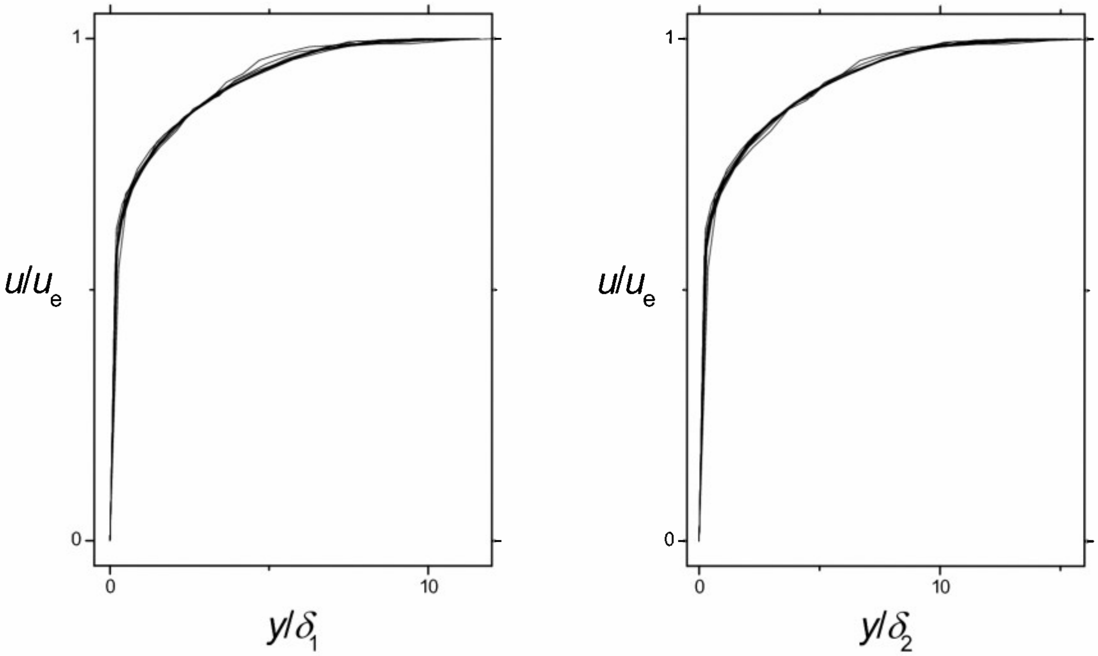

Ludwieg and Tillmann [17] twelve FPG profiles taken at x=0.782, 1.282, 1.782, 2.282, 2.782, 3.132, 3.332, 3.532, 3.732, 3.932, 4.132,

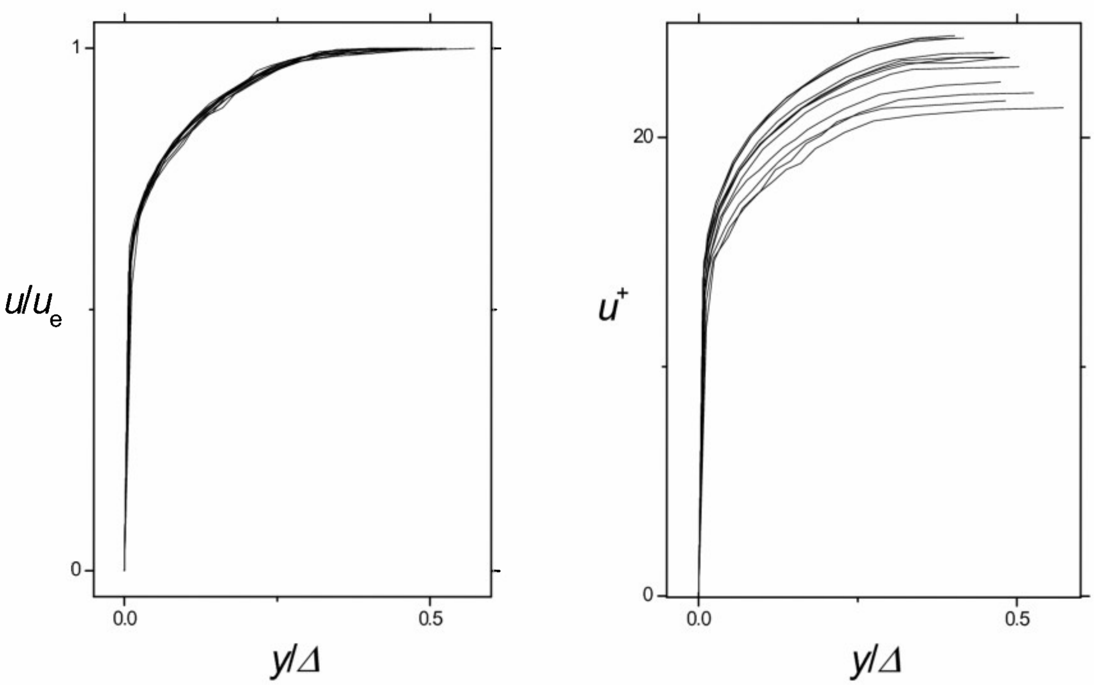

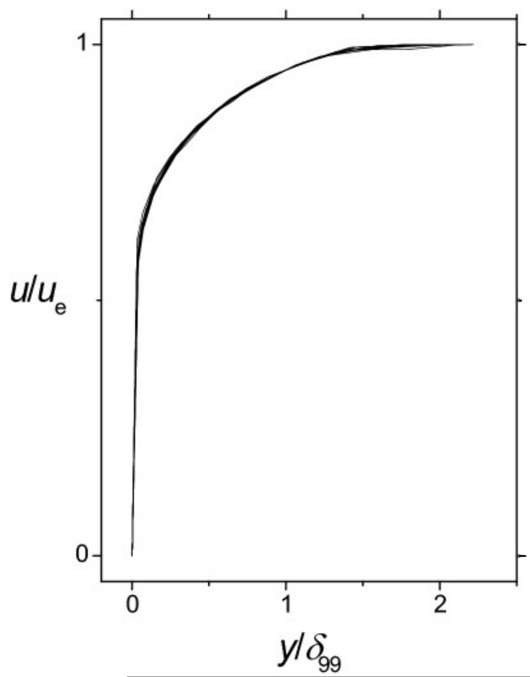

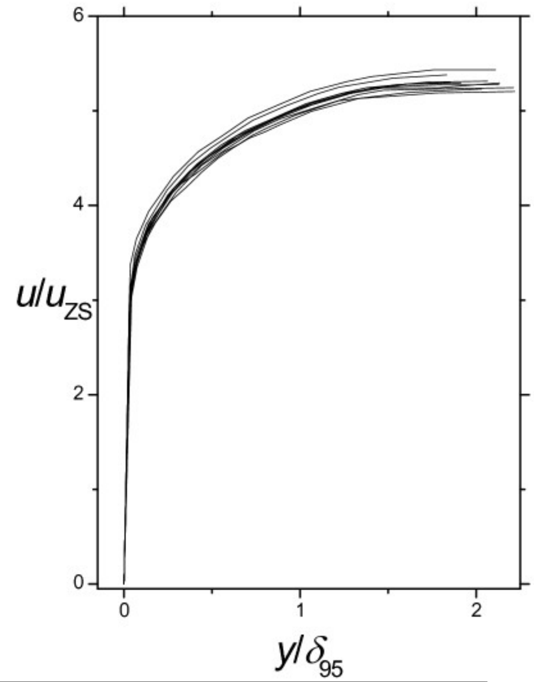

Ludwieg and Tillmann [17] twelve FPG profiles taken at x=0.782, 1.282, 1.782, 2.282, 2.782, 3.132, 3.332, 3.532, 3.732, 3.932, 4.132,

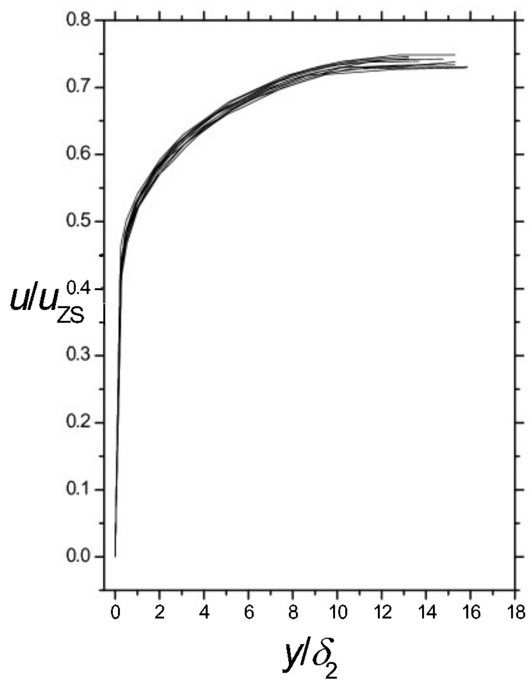

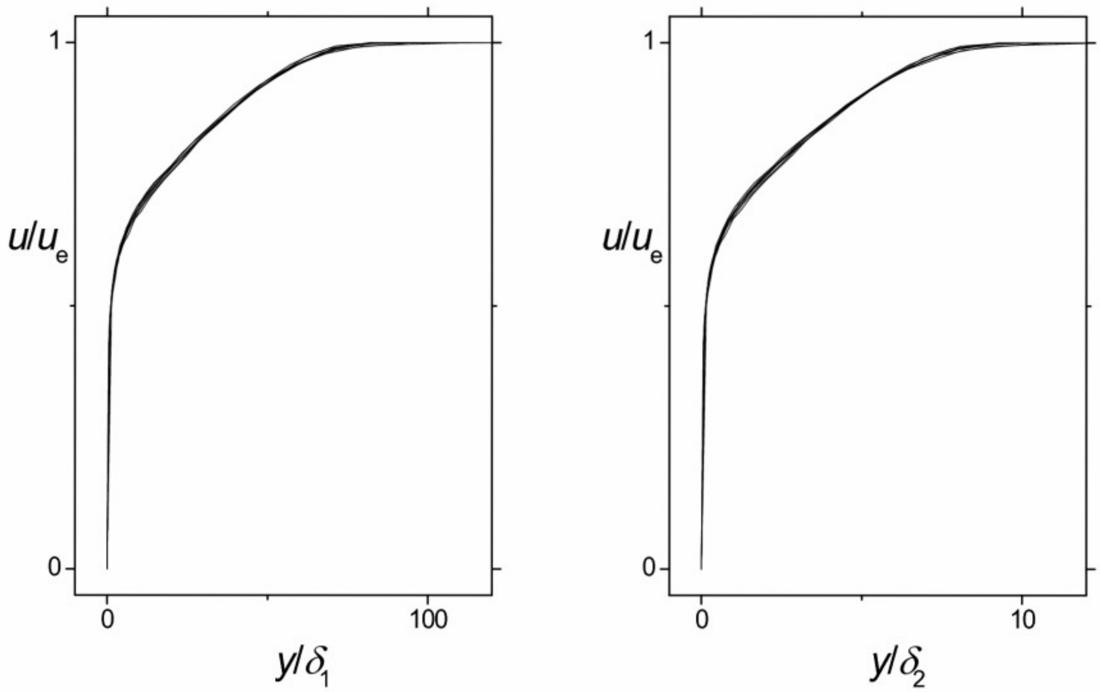

Samuel and Joubert [19] fits to seven profiles taken at x= 0.855, 1.16, 1.44, 1.76, 2.1, 2.26, and 2.4 m. Not shown are five other data sets not showing similarity.

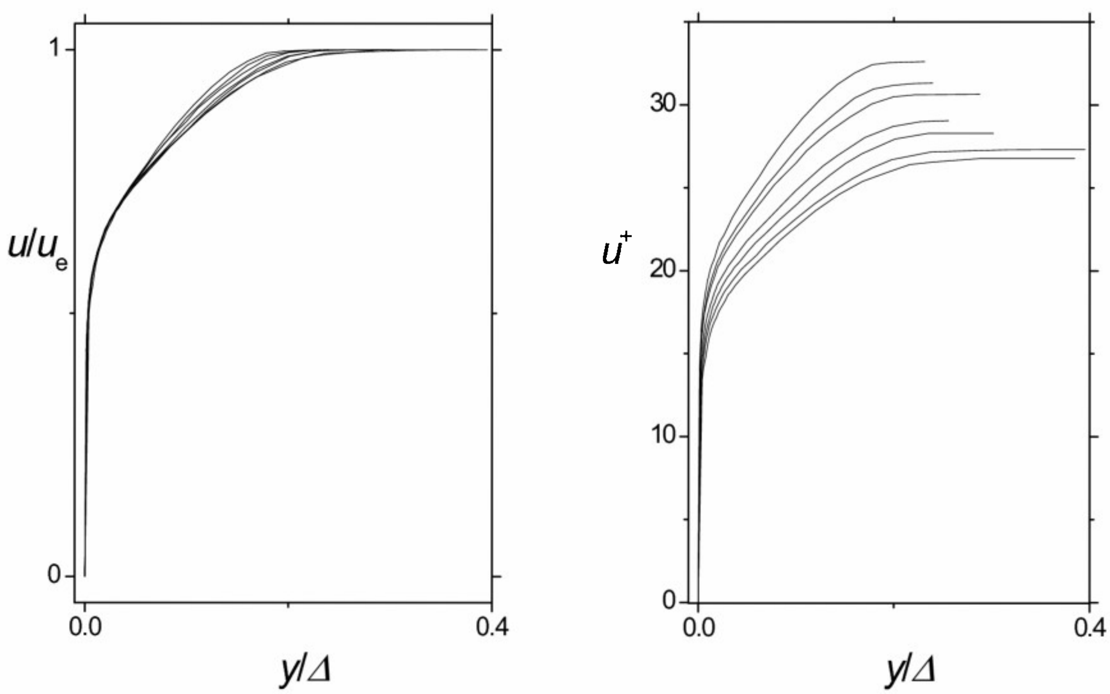

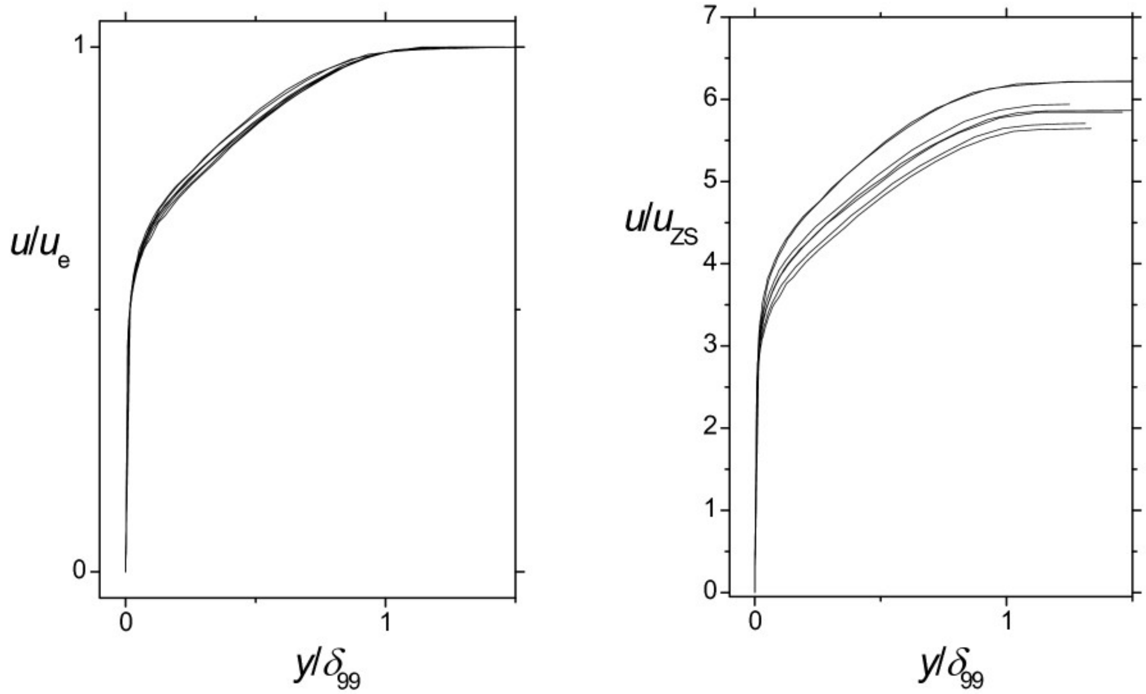

Samuel and Joubert [19] fits to seven profiles taken at x= 0.855, 1.16, 1.44, 1.76, 2.1, 2.26, and 2.4 m. Not shown are five other data sets not showing similarity.

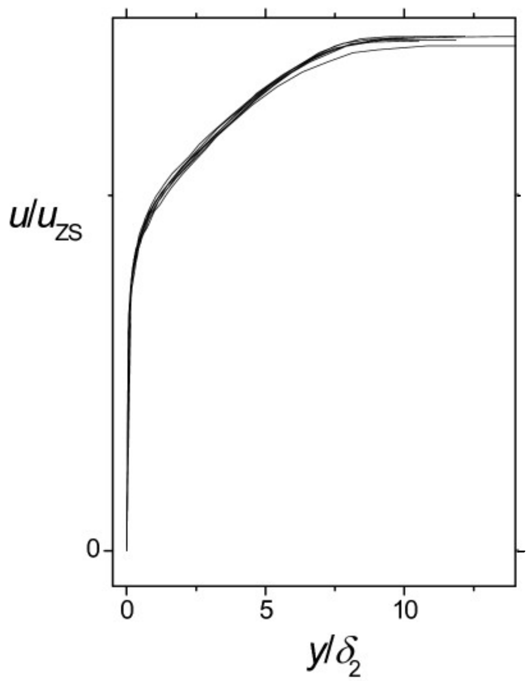

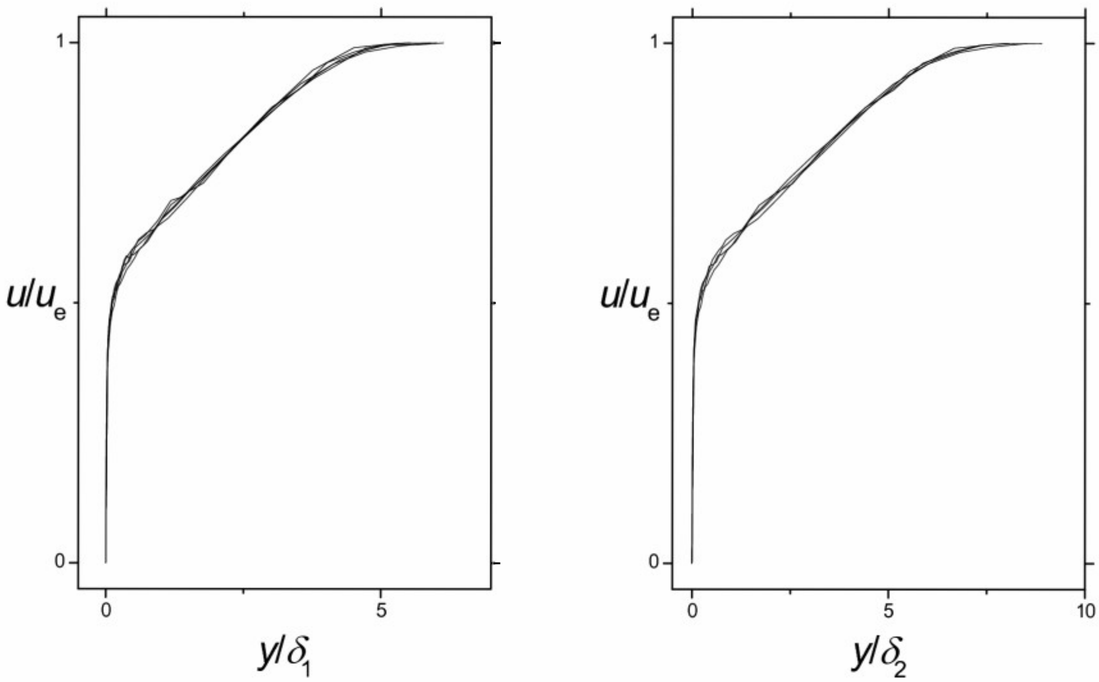

Clauser [1] five velocity profiles with Re_θ = 11453, 14007, 15515, 16182, and 17405.

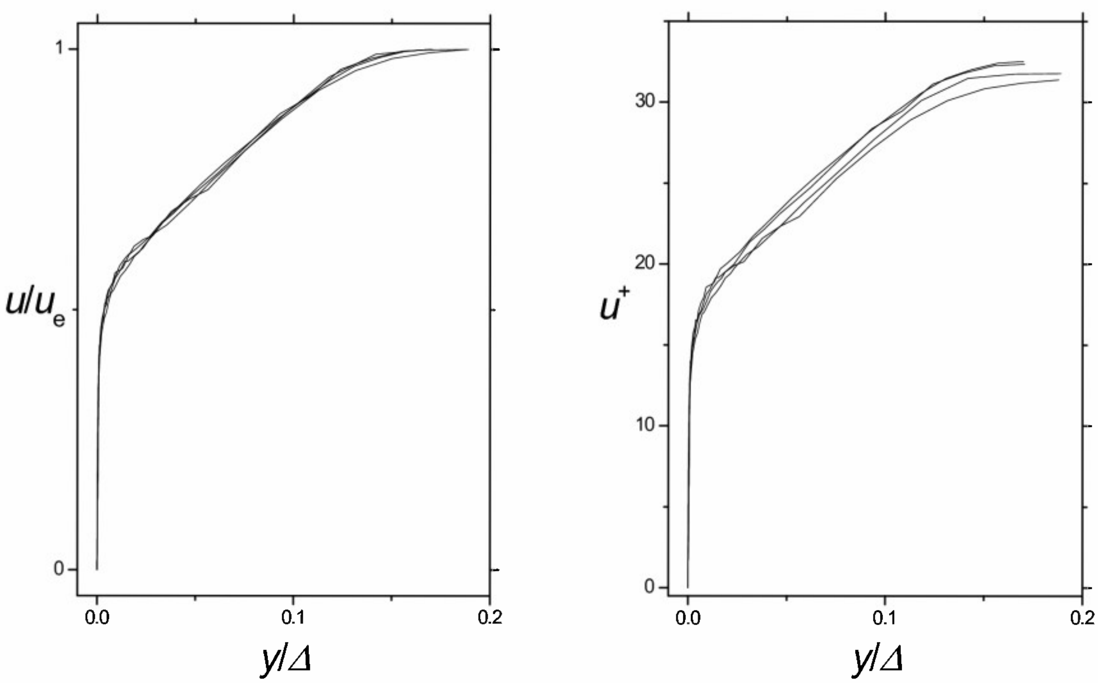

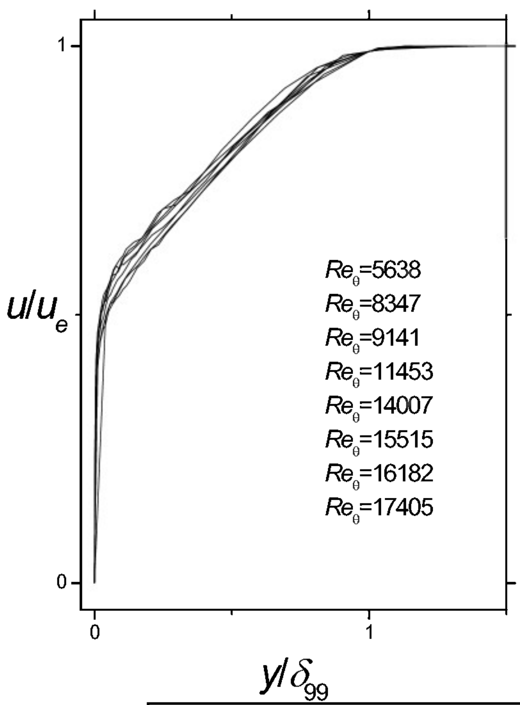

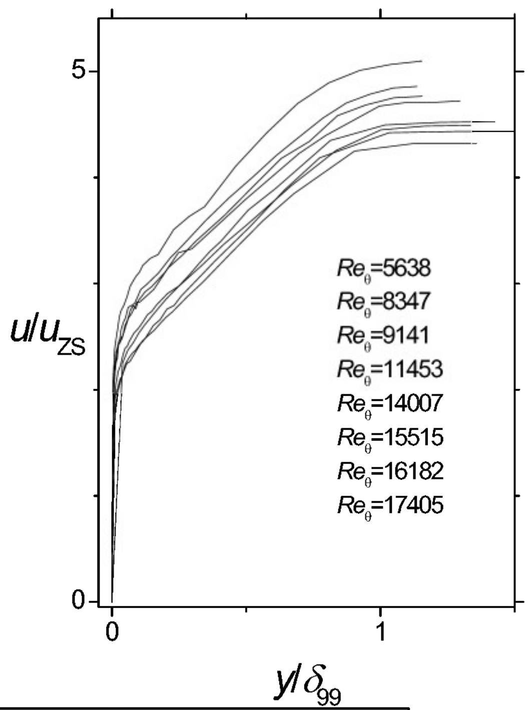

Clauser [1] five velocity profiles with Re_θ = 11453, 14007, 15515, 16182, and 17405.

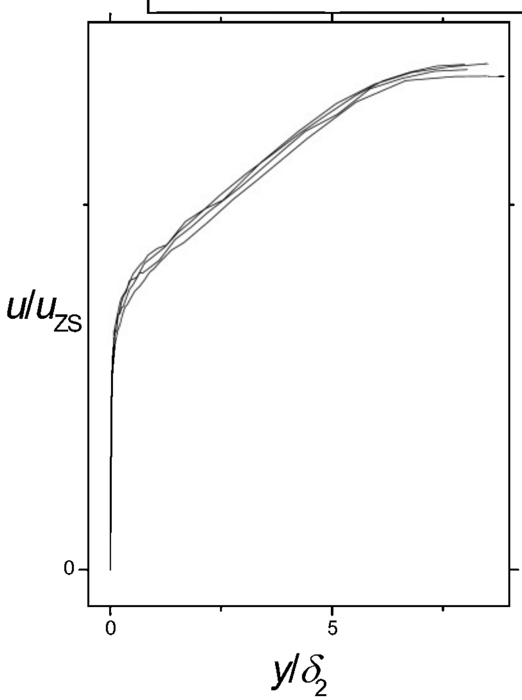

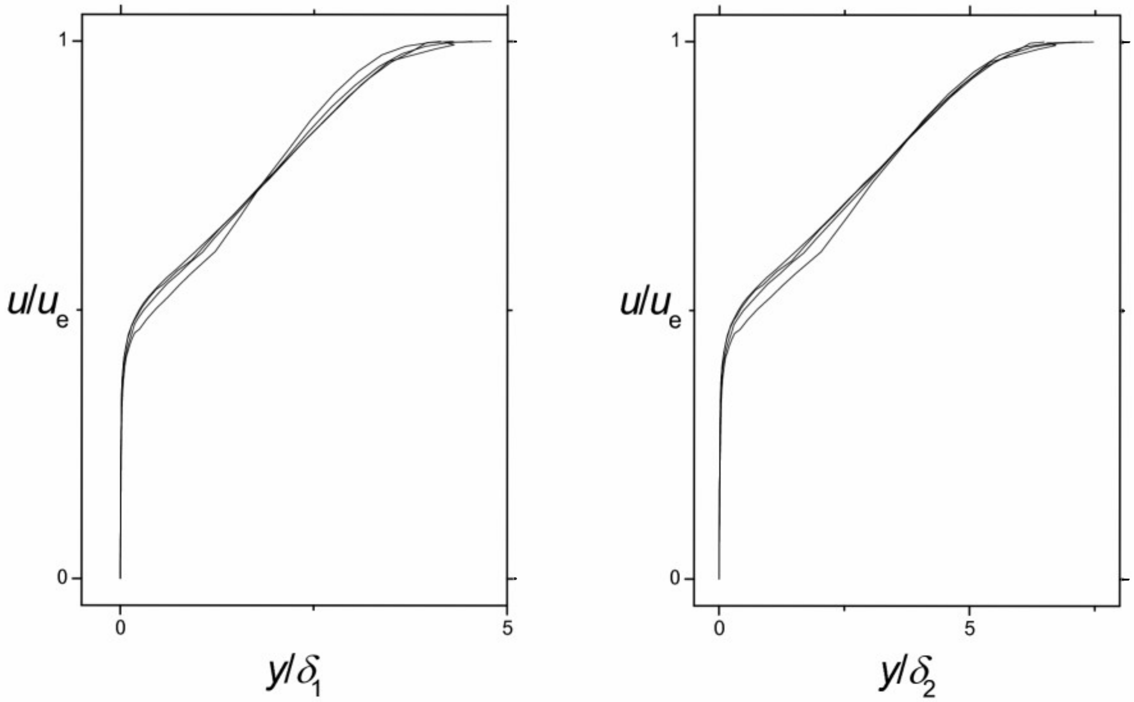

Bradshaw and Ferriss [18] four velocity profiles with x= 1.917, 3.917, 5.417, and 6.917.

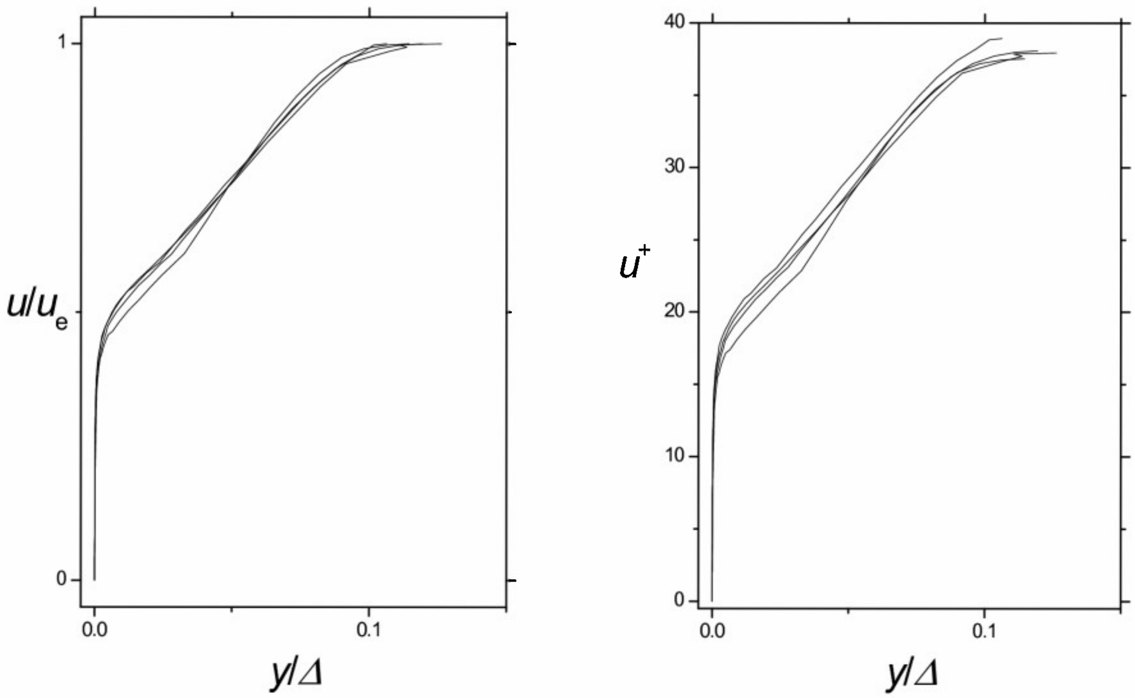

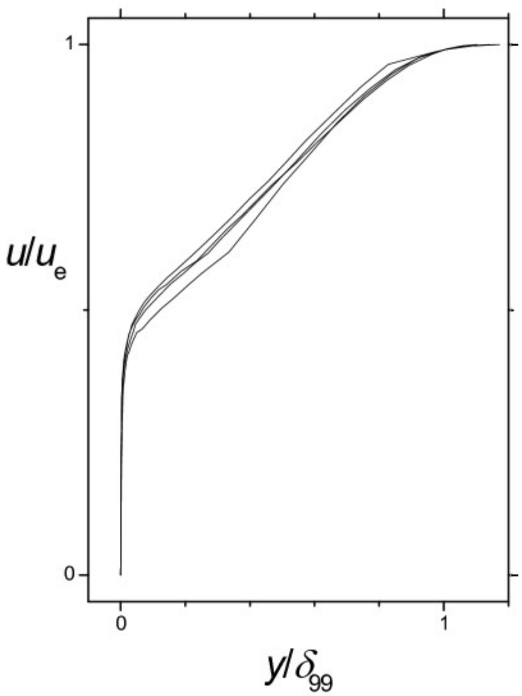

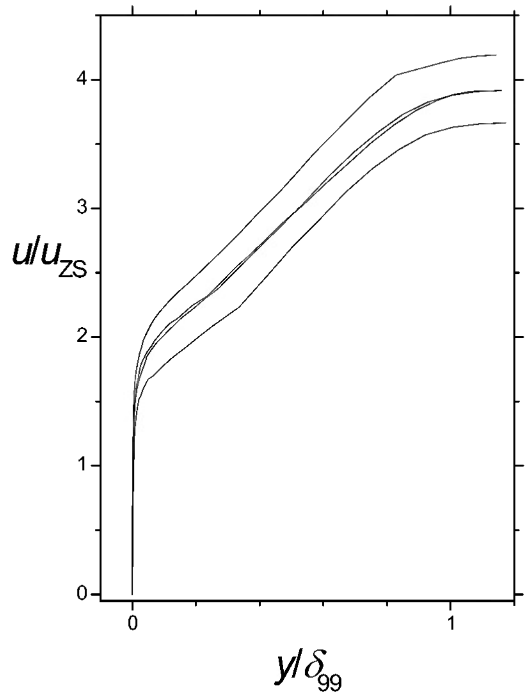

Bradshaw and Ferriss [18] four velocity profiles with x= 1.917, 3.917, 5.417, and 6.917.

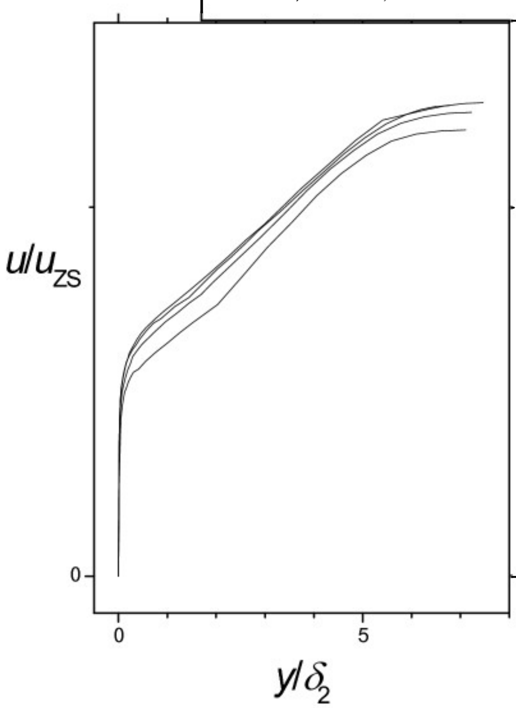

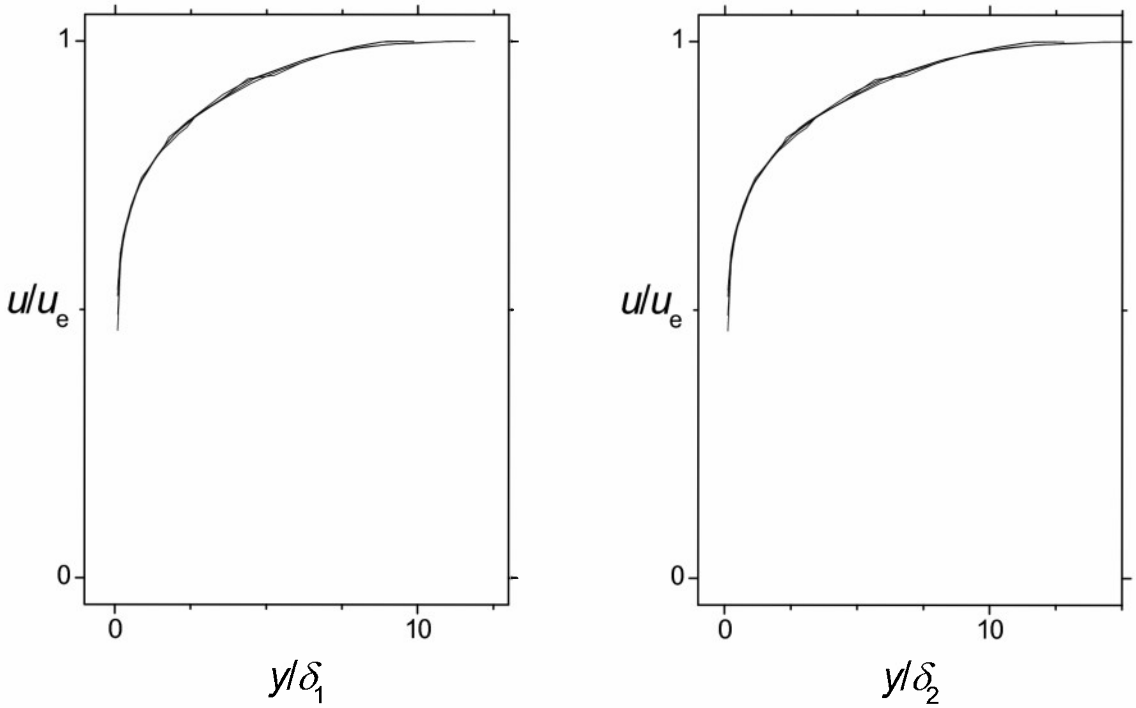

Herring and Norbury [10] data set; last four profiles of six designated Ident 2700.

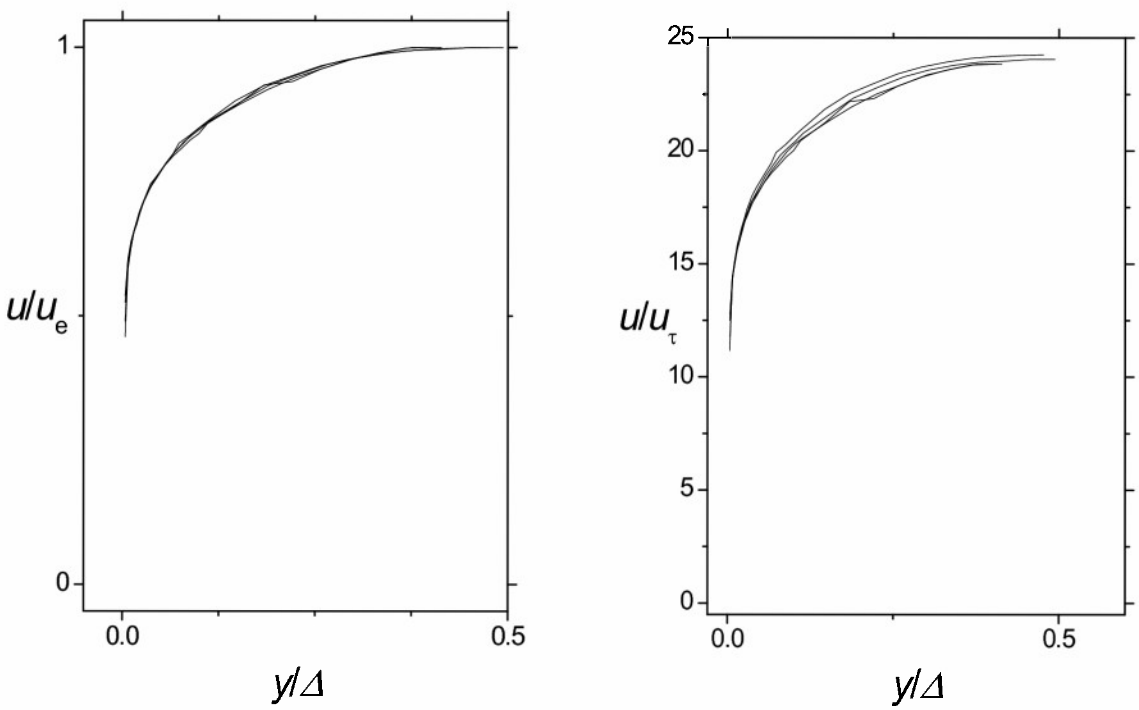

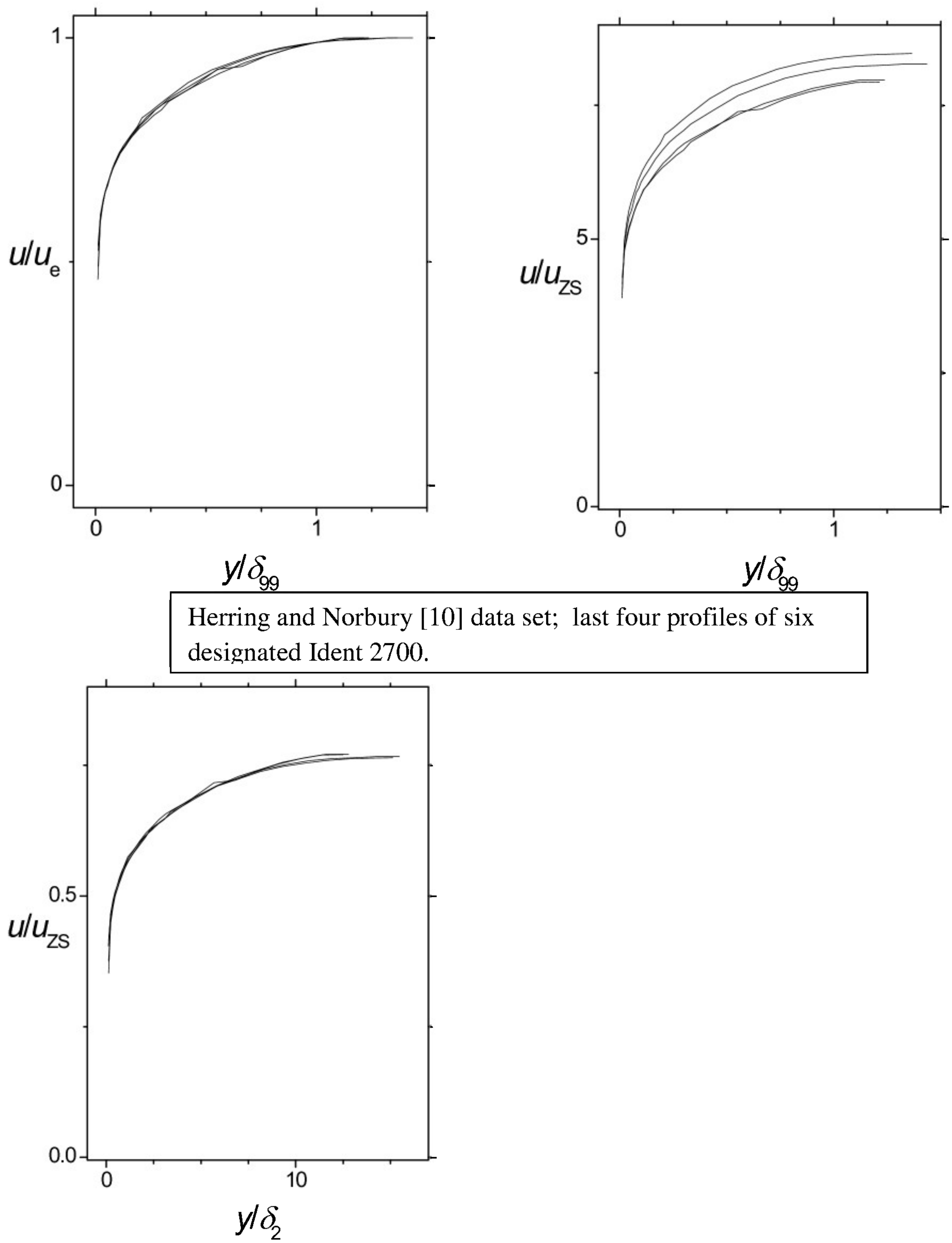

Herring and Norbury [10] data set; last four profiles of six designated Ident 2700.

Appendix C: Scale Comparisons for $\overline{\tilde{u}\tilde{v}}$

The following plots are support data for the Technical Report entitled "Similarity Scaling of the Outer Region of the Turbulent Boundary Layer", by David W. Weyburne. The plots are compiled to show the $\overline{\tilde{u}\tilde{v}}$ profiles plotted using the different length and velocity scales for the data sets considered for the report. The plots are provided for visual verification of the claims made in the main body of the Report. They are not identified with Figure numbers but rather as the ensemble of plots as Appendix C.

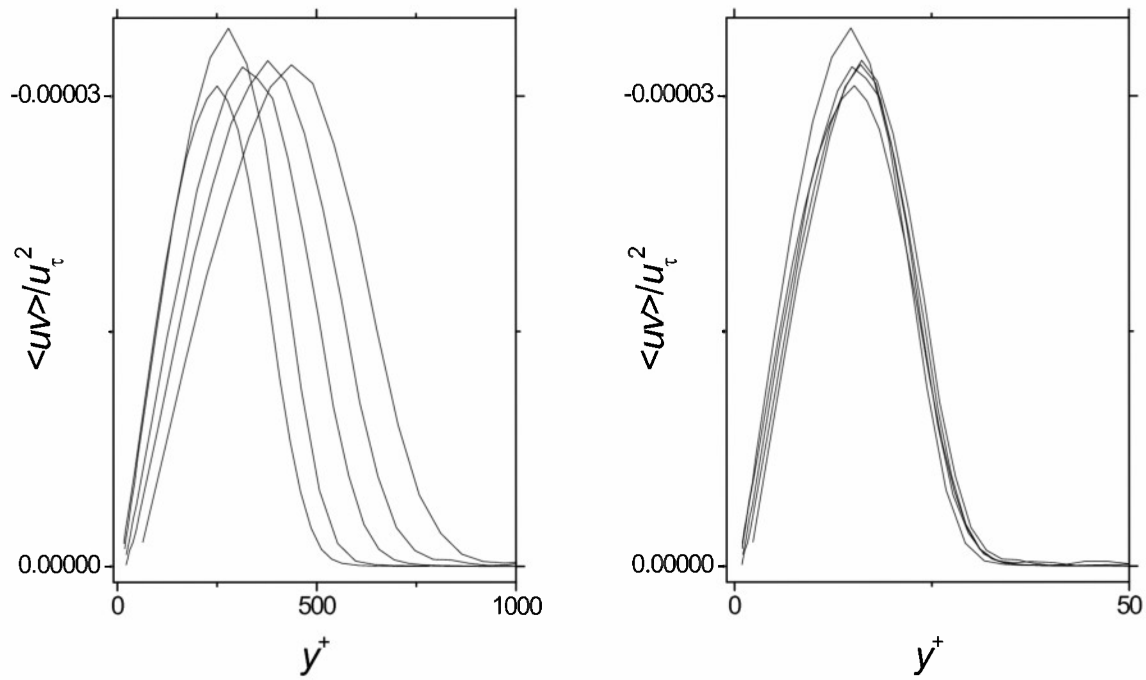

Elsberry, Loeffler, Zhou, & Wygnanski [11] five Reynolds Stress Profiles <uv> plots designated as Case A = 239, 264, 295, 325, and 362 by Elsberry, *et. al.* [11].

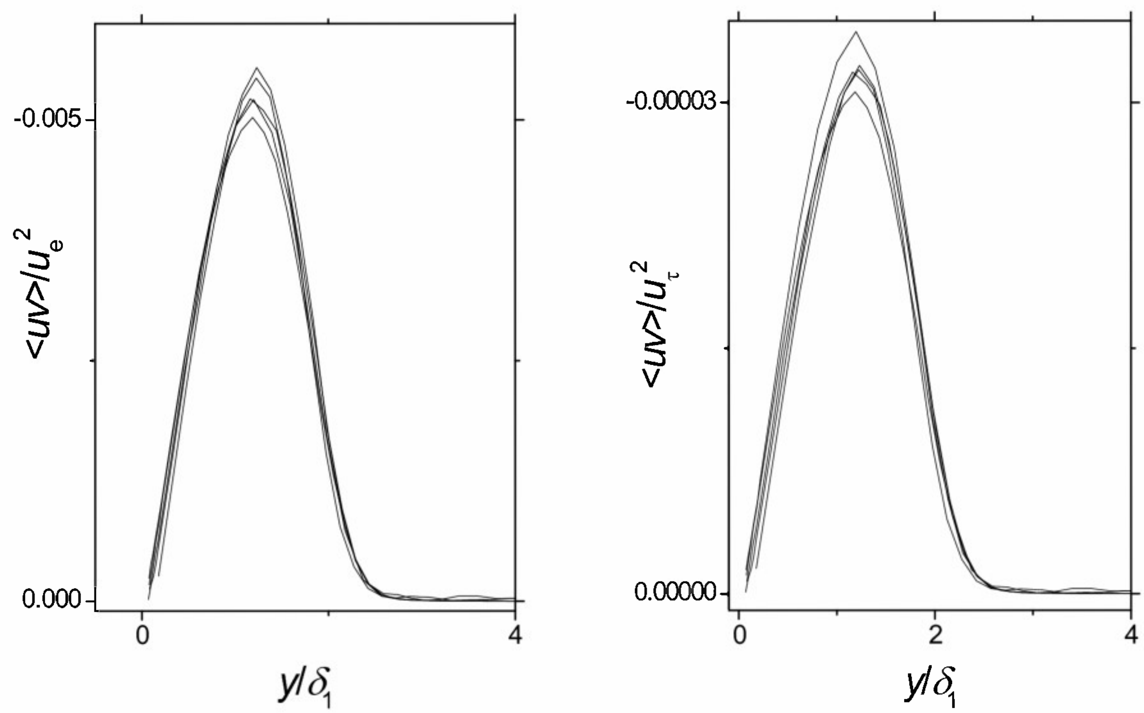

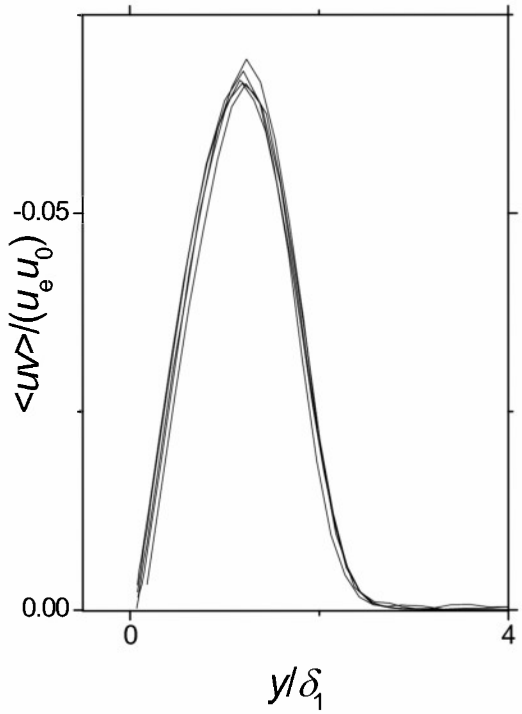

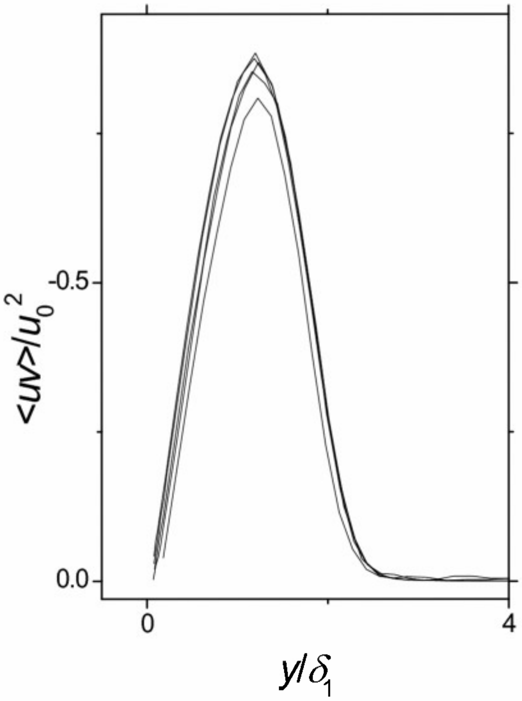

Elsberry, Loeffler, Zhou, & Wygnanski, (2000) five Reynolds Stress Profiles <uv> plots designated as Case A = 239, 264, 295, 325, and 362 by Elsberry, *et*. *al*. [11].

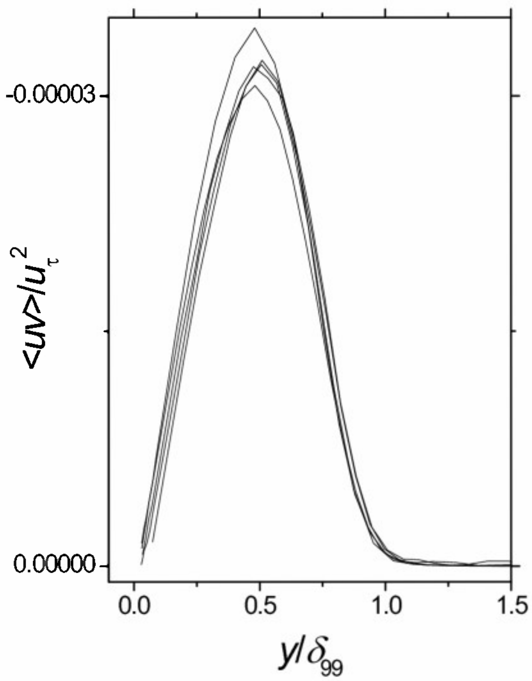

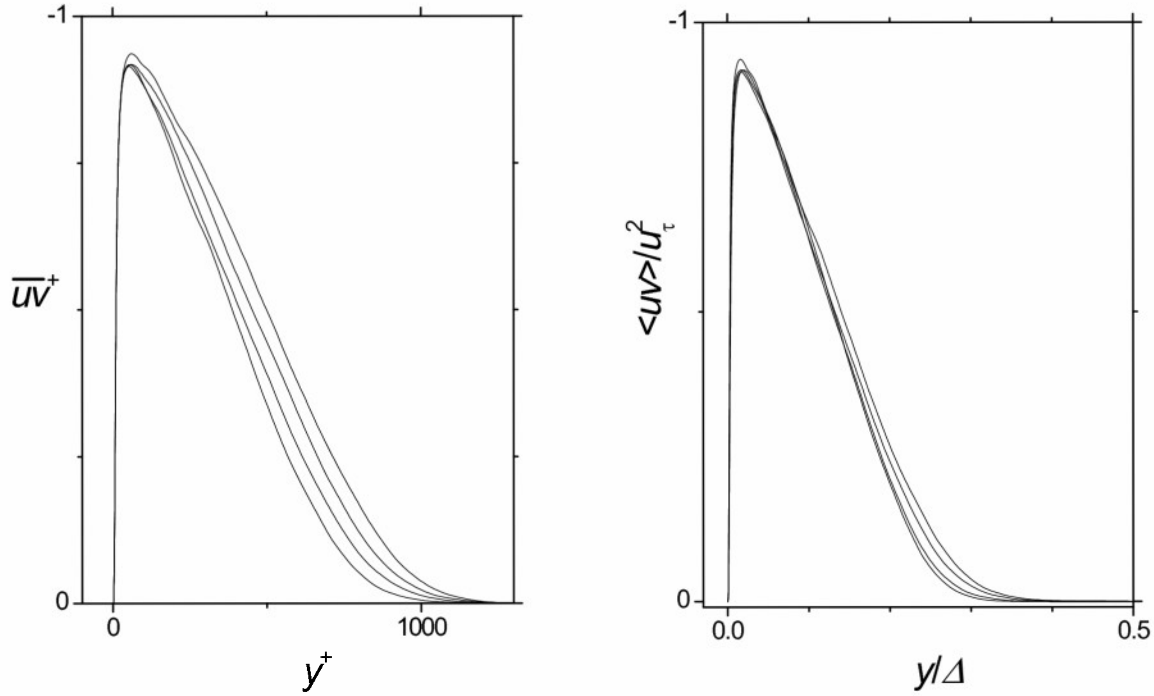

Khujadze and Oberlack [13] four Reynolds Stress Profiles <uv> for Re_θ = 2088, 2333, 2569, and 2807. Note for this case $u_e = u_0$.

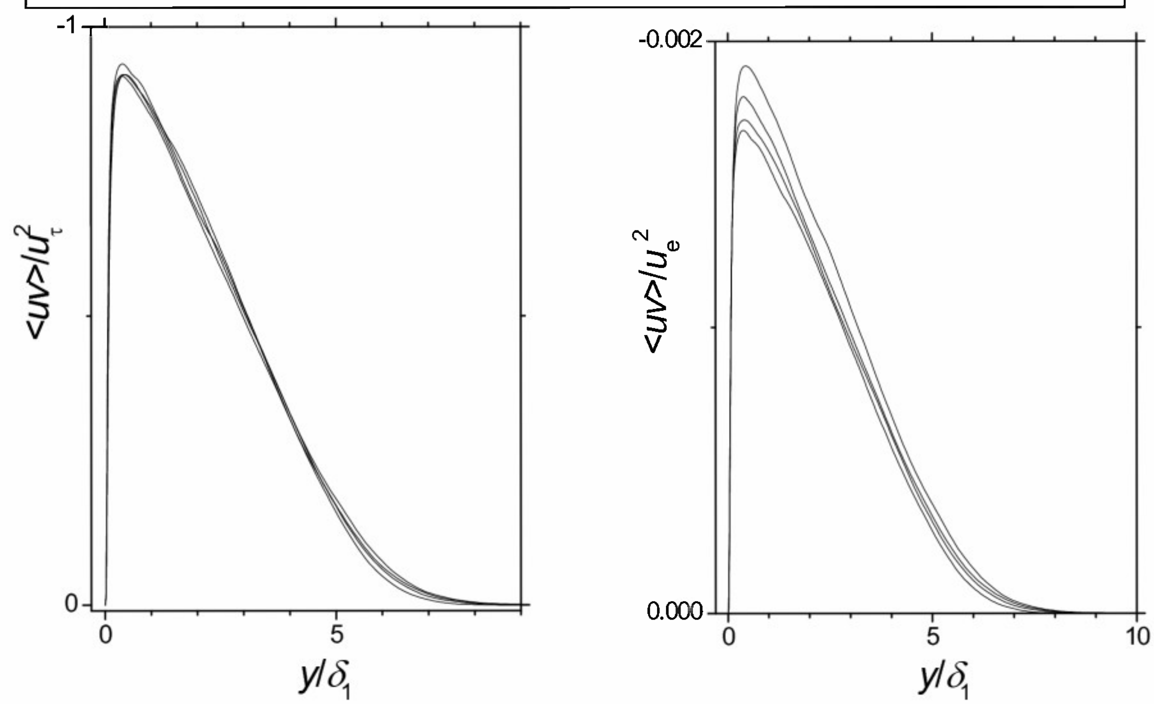

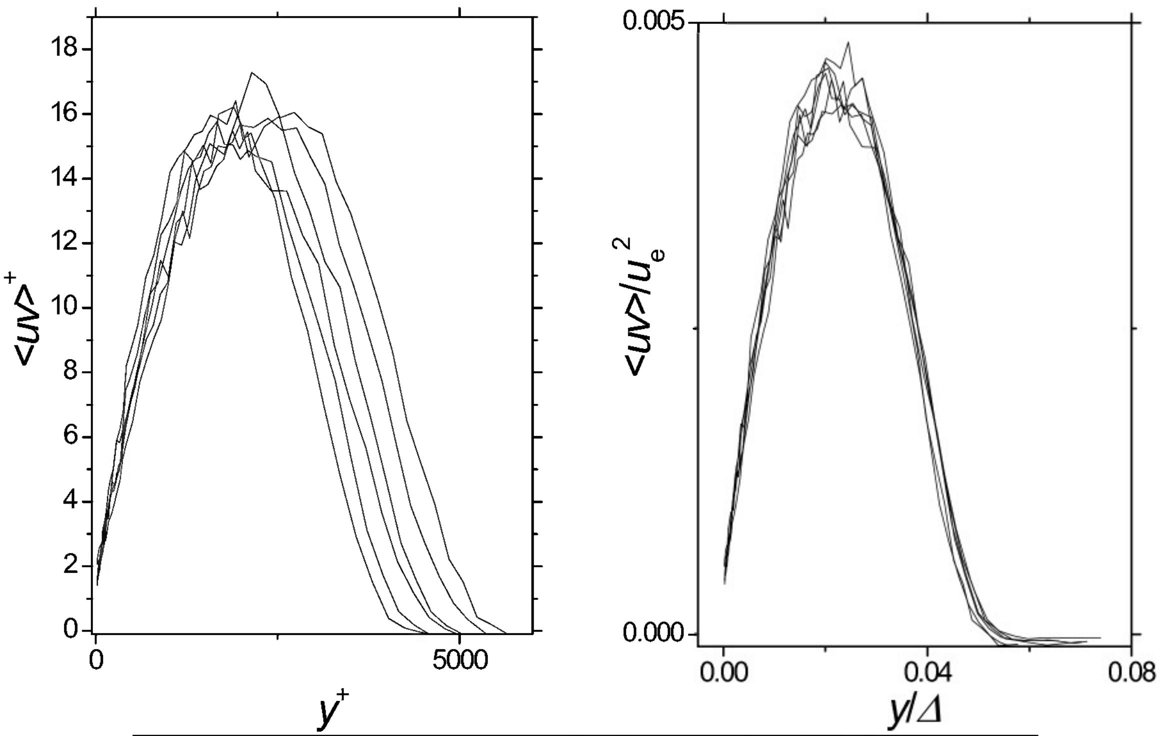

Skåre and Krogstad [12] six Reynolds Stress Profiles <uv> plots taken at x=4.0, 4.2, 4.4, 4.6, 5.0, and 5.2 m.

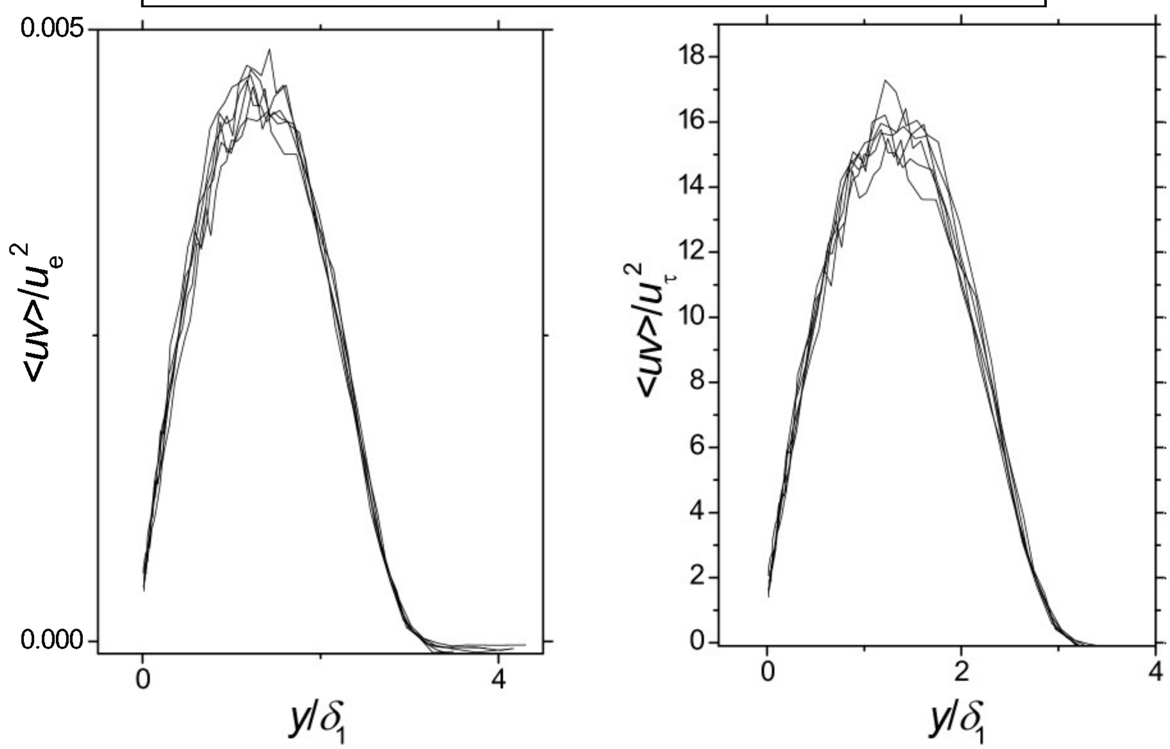

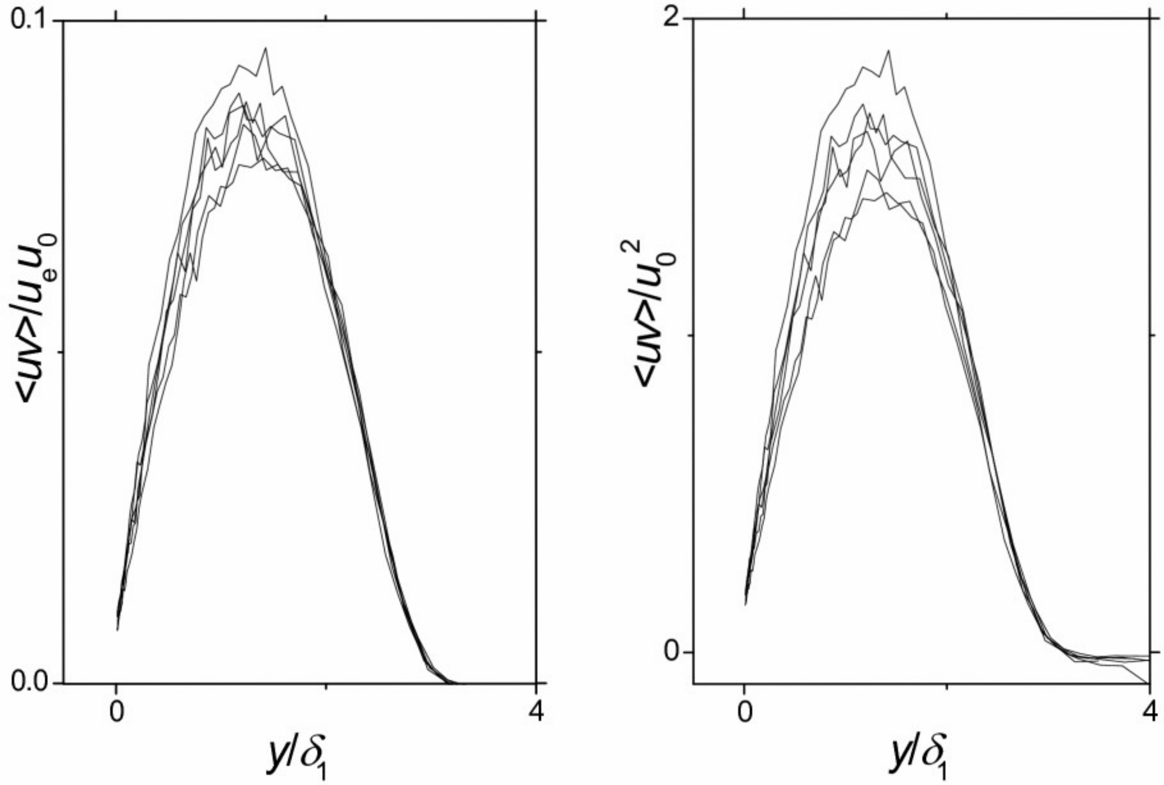

Skåre and Krogstad [12] six Reynolds Stress Profiles <uv> plots taken at x=4.0, 4.2, 4.4, 4.6, 5.0, and 5.2 m.

Appendix D: Scale Comparisons for $\overline{\tilde{u}\tilde{u}}$

The following plots are support data for the Technical Report entitled "Similarity Scaling of the Outer Region of the Turbulent Boundary Layer", by David W. Weyburne. The plots are compiled to show the $\overline{\tilde{u}\tilde{u}}$ profiles plotted using the different length and velocity scales for the data sets considered for the report. We include the DeGrraff and Eaton results even though this data is not taken at different x-locations. The plots are provided for visual verification of the claims made in the main body of the Report. They are not identified with Figure numbers but rather as the ensemble of plots as Appendix D.

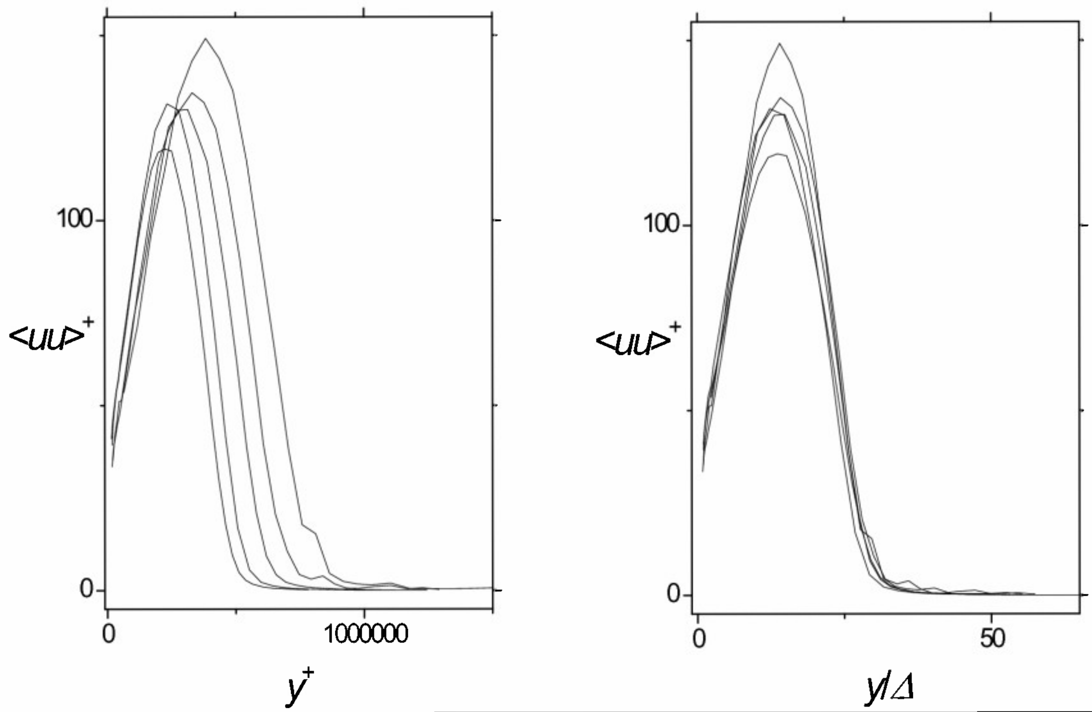

Elsberry, Loeffler, Zhou, & Wygnanski [11] five Reynolds Stress Profiles <uu> plots designated as Case A = 239, 264, 295, 325, and 362 by Elsberry, *et. al*. [11].

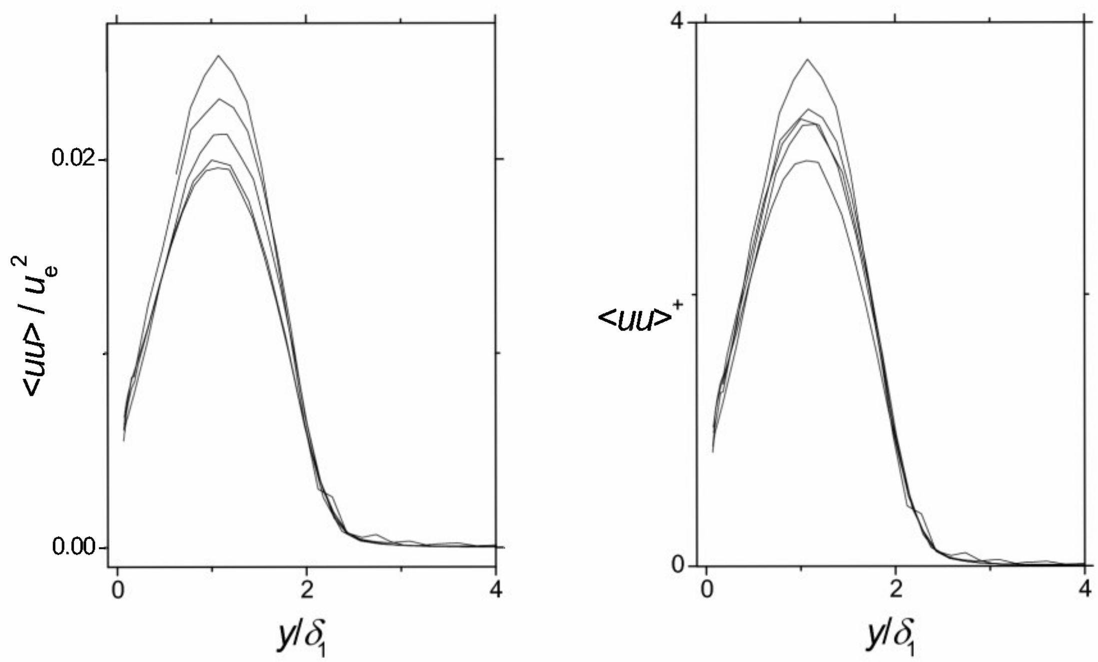

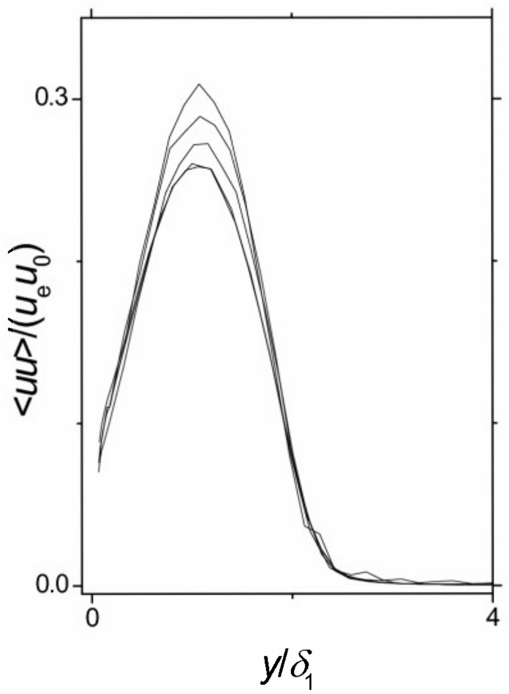

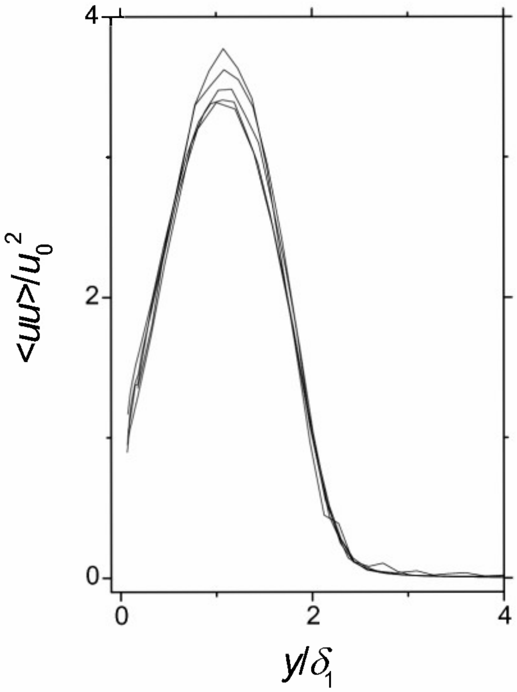

Elsberry, Loeffler, Zhou, & Wygnanski [11] five Reynolds Stress Profiles <uv> plots designated as Case A = 239, 264, 295, 325, and 362 by Elsberry, *et. al.* [11].

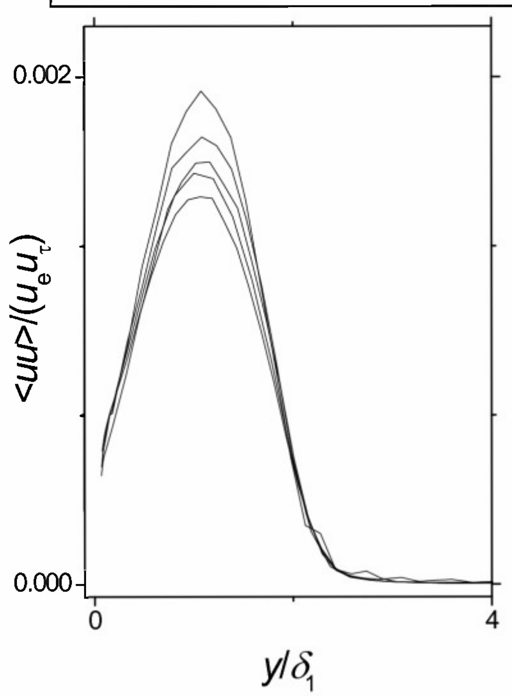

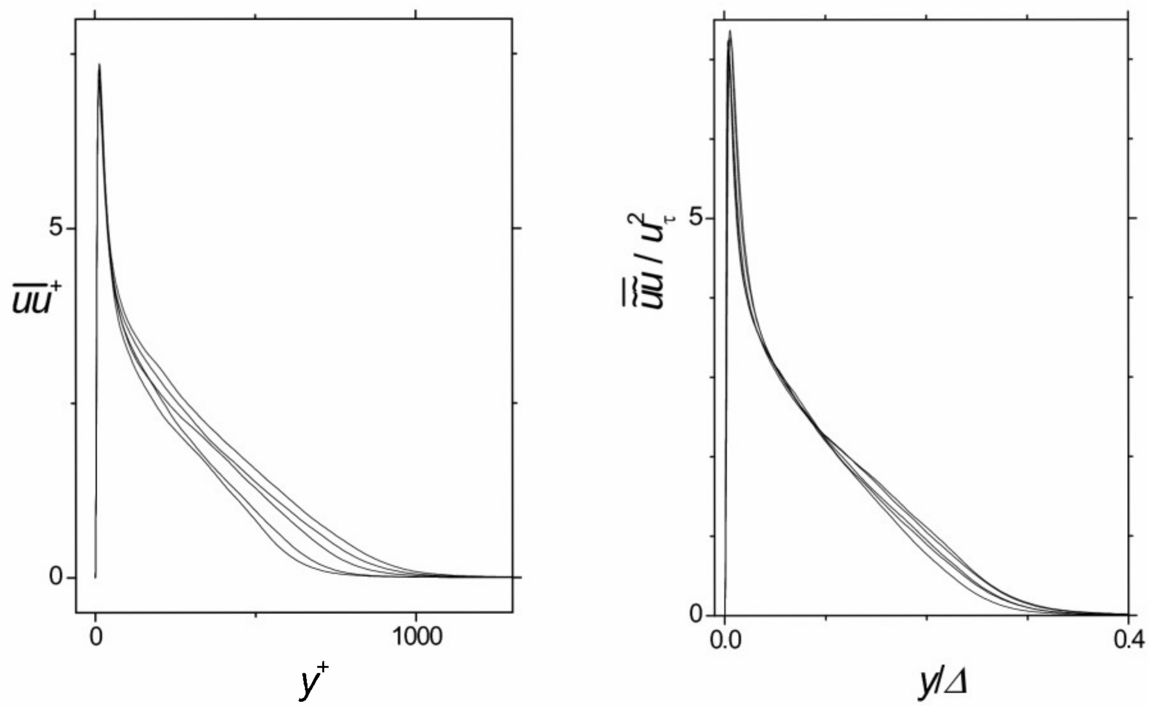

Khujadze and Oberlack [13] five Stress Profiles <uu> for $Re_\theta =$ 1850, 2088, 2333, 2569, and 2807.

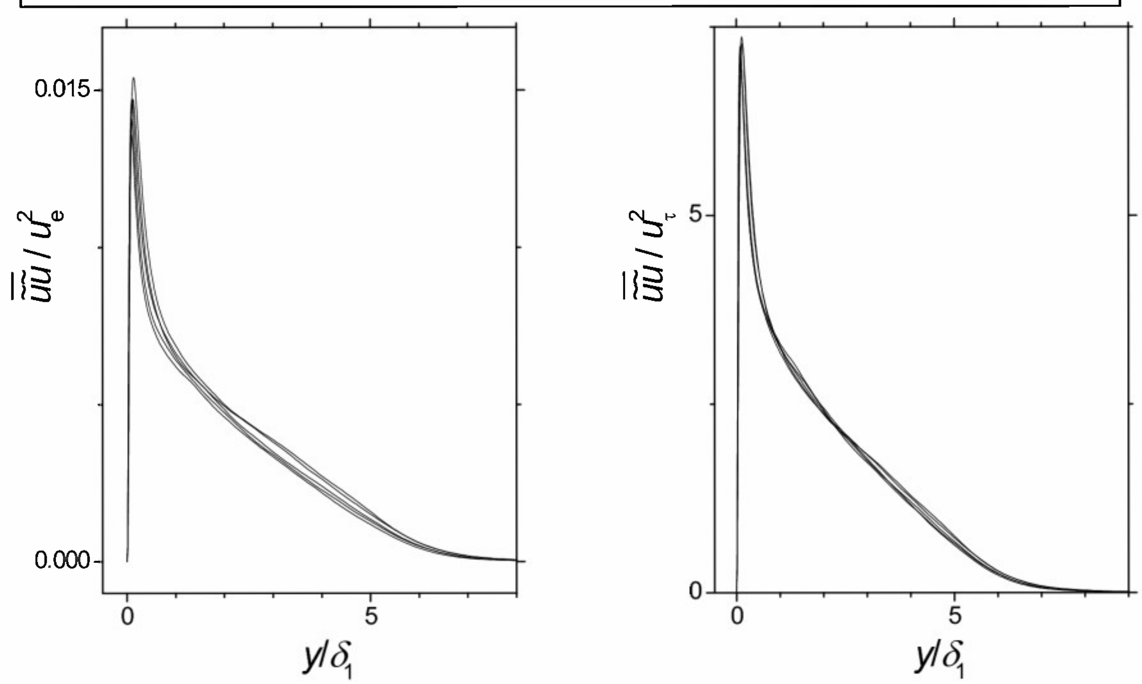

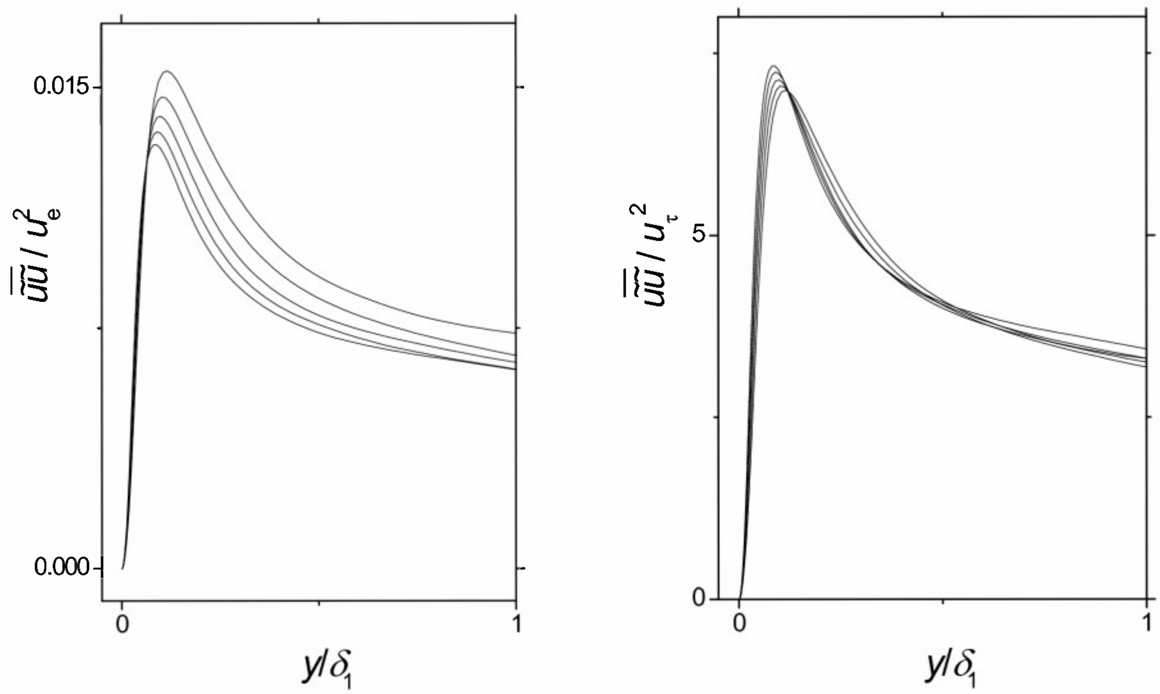

Khujadze and Oberlack [13] five Stress Profiles <uu> for Re_θ = 1850, 2088, 2333, 2569, and 2807.

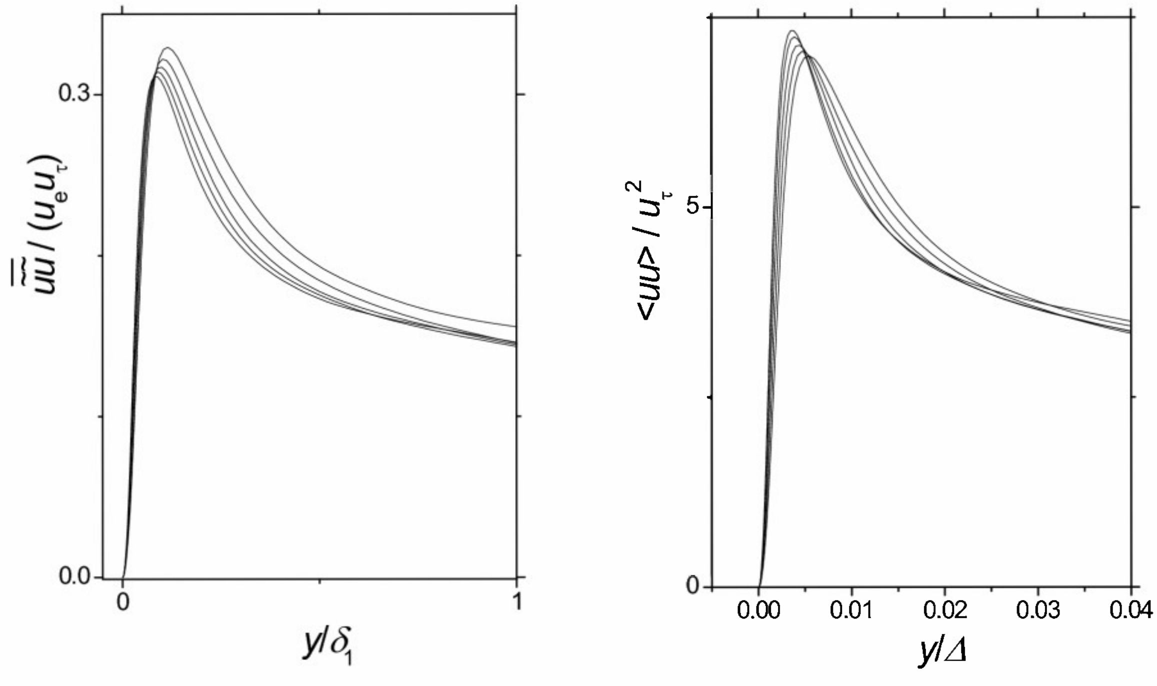

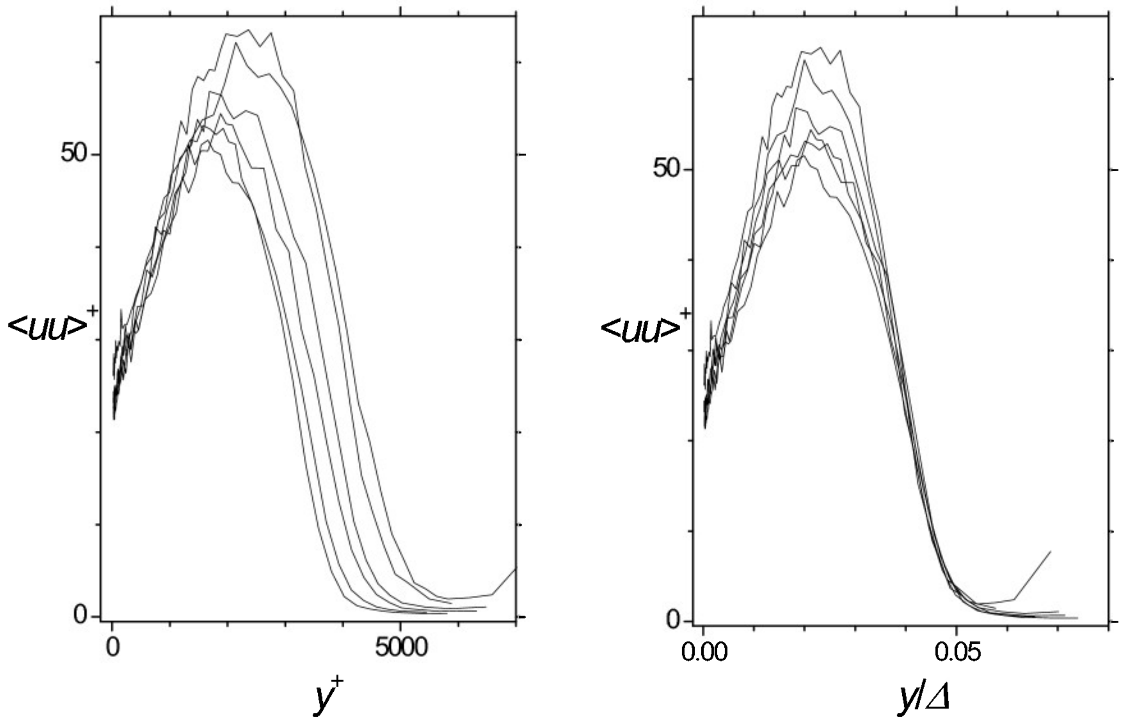

Skåre and Krogstad [12] six Stress Profiles plots <uu> taken at x=4.0, 4.2, 4.4, 4.6, 5.0, and 5.2 m.

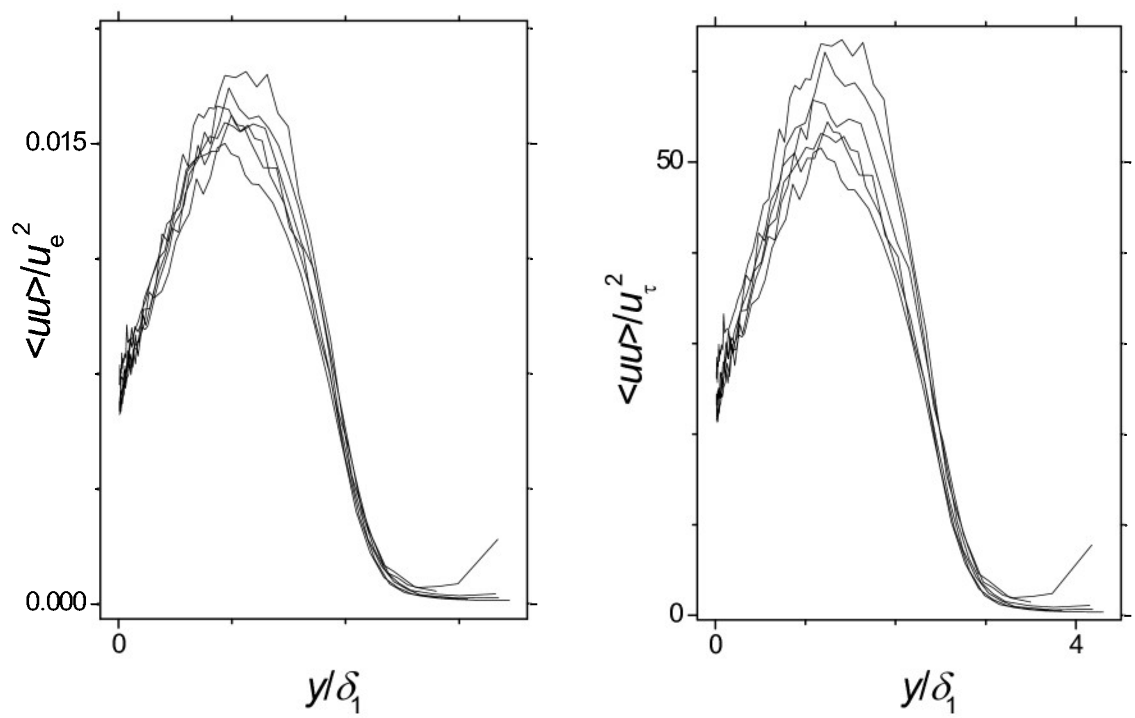

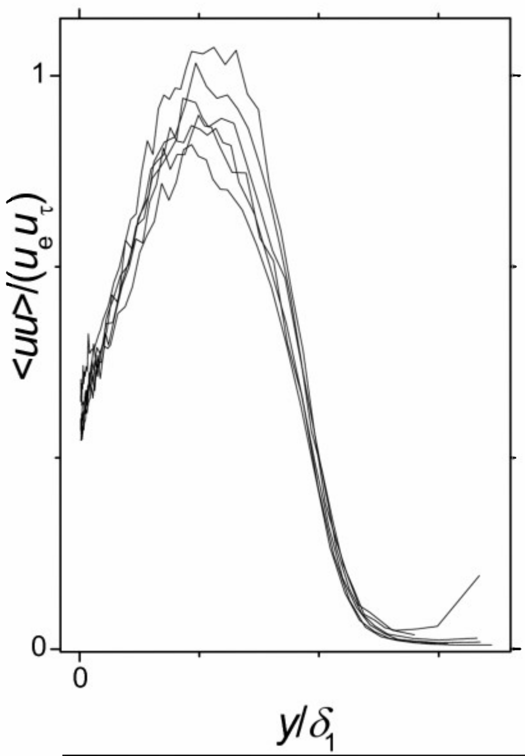

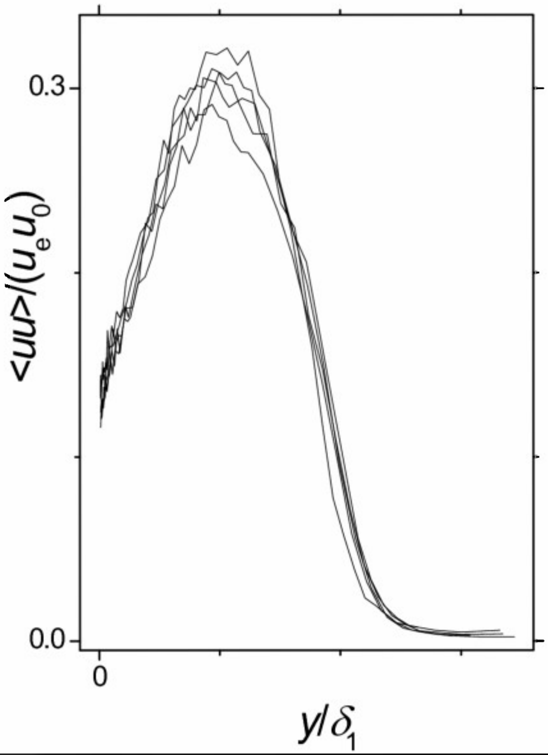

Skåre and Krogstad [12] six Stress Profiles plots <uu> taken at x=4.0, 4.2, 4.4, 4.6, 5.0, and 5.2 m.

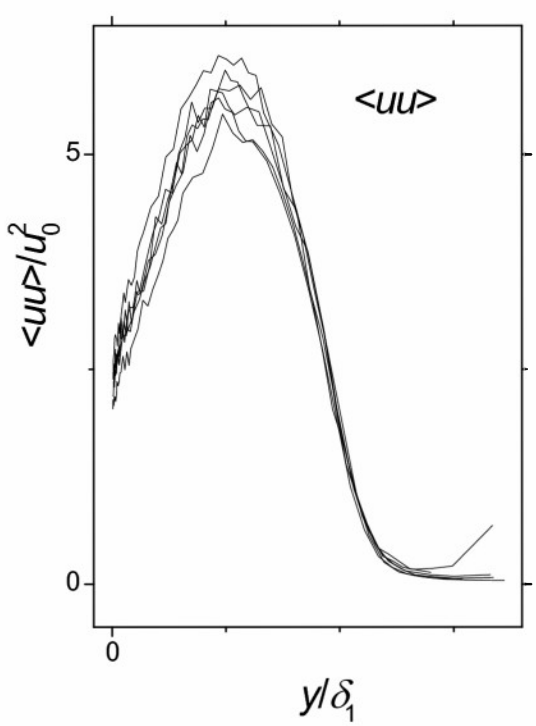

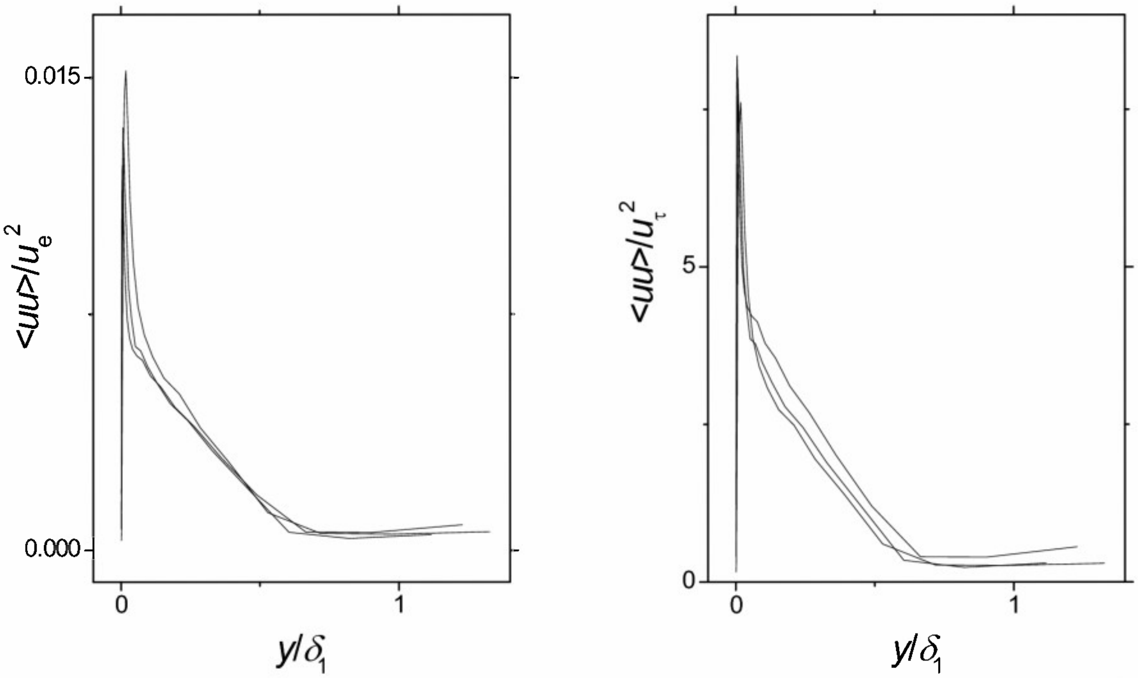

DeGraaff and Eaton [22] three Stress Profiles plots <uu> taken at Re_{θ} =1430, 2900, and 5200.

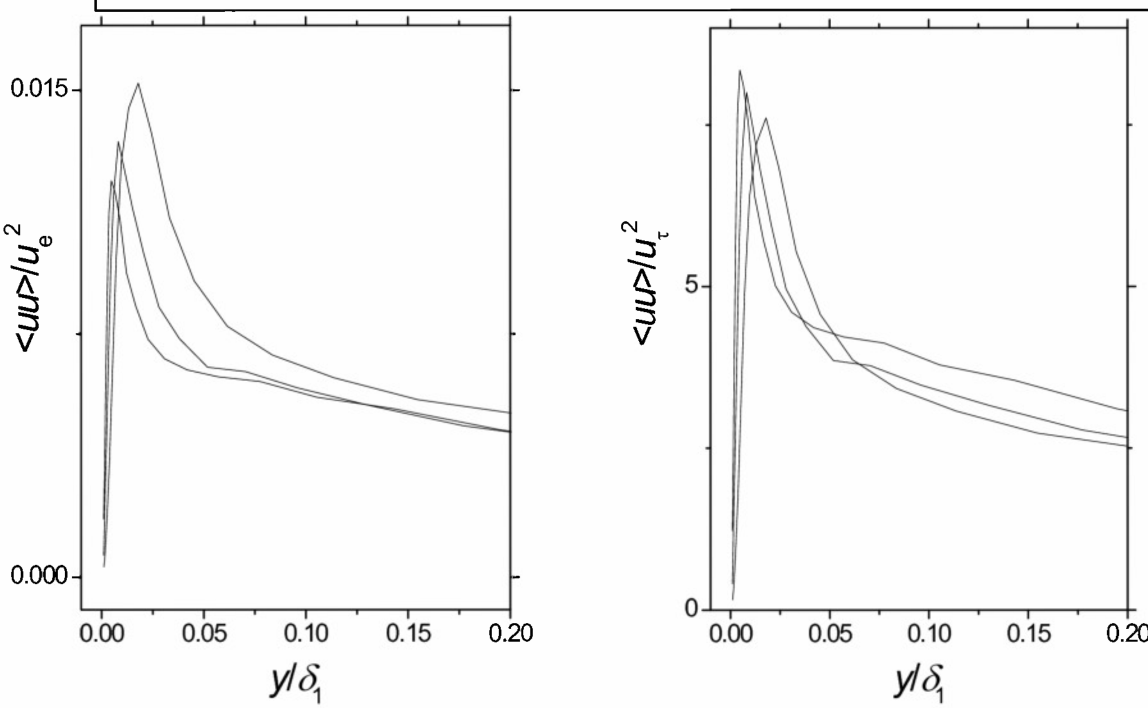

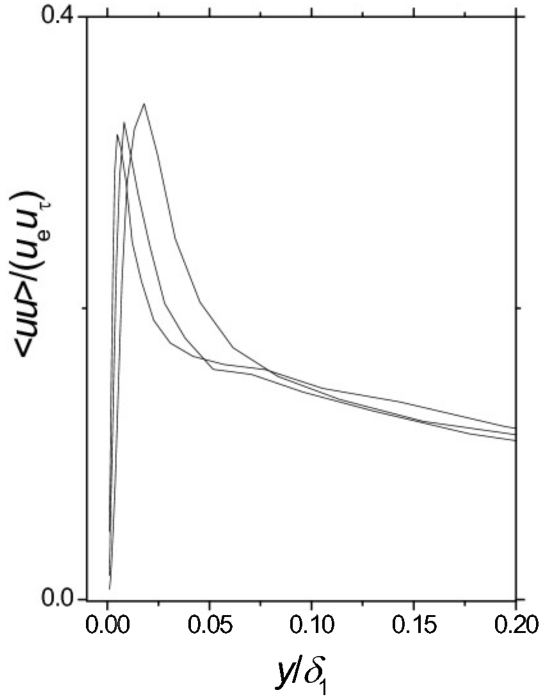

DeGraaff and Eaton [22] three Stress Profiles plots <uu> taken at Re_θ =1430, 2900, and 5200.